RESEARCH & DEVELOPMENT

AGGREGATE BASE COURSE MATERIAL TESTING AND RUTTING MODEL DEVELOPMENT

Liang Chern Chow

Debakanta Mishra, Ph.D.

Erol Tutumluer, Ph.D.

Department of Civil and Environmental Engineering

University of Illinois at Urbana-Champaign

NCDOT Project 2013-18

FHWA/NC/2013-18

December 2014

Technical Report Documentation Page

1. Report No. FHWA/NC/2013-18	2. Government Accession No.	3. Recipient's Catalog No.
4. Title and Subtitle Aggregate Base Course Material Testing and Rutting Model Development		5. Report Date December 2014
		6. Performing Organization Code
7. Author(s) Liang Chern Chow, Debakanta Mishra, Ph.D., and Erol Tutumluer, Ph.D.		8. Performing Organization Report No.
9. Performing Organization Name and Address Department of Civil and Environmental Engineering University of Illinois at Urbana-Champaign 205 North Mathews Ave, Urbana, Illinois 61801		10. Work Unit No. (TRAIS)
		11. Contract or Grant No.
12. Sponsoring Agency Name and Address North Carolina Department of Transportation Research and Analysis Group 1 South Wilmington Street Raleigh, North Carolina 27601		13. Type of Report and Period Covered Final Report November 1, 2012 – May 31, 2014
		14. Sponsoring Agency Code NCDOT Project 2013-18
Supplementary Notes:		

16. Abstract

Road pavements in North Carolina have a long history of good performances of unbound base courses often constructed with high quality crushed aggregate materials. The objective of this study was to evaluate rutting potentials of aggregate materials used in pavement base course in North Carolina and develop and calibrate rutting damage models primarily based on laboratory data to use them with mechanistic-empirical (ME) pavement design approaches such as the AASHTO's Pavement ME Design procedure. A complete suite of characterization tests were conducted on 16 aggregate materials with laboratory samples consistently prepared for a mid-range dense-graded base course gradation. The tests included imaging-based aggregate particle shape analyses, moisture-density, resilient modulus, shear strength, and permanent deformation. The concept of Shear Strength Ratio (SSR), defined as the ratio between applied stress levels and the material's shear strength (stress/strength), was introduced to examine effects of varying proportions of stress/strength on the permanent deformation behavior. Clearly, the permanent deformation responses of the aggregate materials correlated better to shear strength than the resilient modulus properties. The accumulated permanent strains were found to steadily increase with applied stress levels. When plastic fines existed in the aggregate gradation, the permanent deformation potential was drastically higher. Note that AASHTO's Pavement ME Design approach could not adequately distinguish between the performances of aggregate materials with similar resilient moduli but with different shear strength and thus the different permanent deformation characteristics. Accordingly, the experimental results were used to establish a consistent database to investigate the permanent deformation trends influenced by aggregate material properties, shear strength, applied stress states and stress/strength ratios, and to develop a new rutting model referred to as the CMT model. Case studies compared the CMT model predictions with those from the Pavement ME Design procedure and evaluated the adequacy of the proposed model. Based on the findings, a practical design approach is recommended for better prediction of aggregate base rutting potentials.

17. Key Words Unbound Aggregate, Pavement Base Course, Permanent Deformation, Rutting, Shear Strength, Shear Stress Ratio, Triaxial Testing	18. Distribution Statement

19. Security Classif. (of this report) Unclassified	20. Security Classif. (of this page) Unclassified	21. No. of Pages 116	22. Price

Form DOT F 1700.7 (8-72) **Reproduction of completed page authorized**

DISCLAIMER

The contents of this report reflect the views of the authors and not necessarily the views of the University. The authors are responsible for the facts and the accuracy of the data presented herein. The contents do not necessarily reflect the official views or policies of either the North Carolina Department of Transportation or the Federal Highway Administration at the time of publication. This report does not constitute a standard, specification, or regulation.

Trademark or manufacturers' names appear in this report only because they are considered essential to the object of this document and do not constitute an endorsement of product by the Illinois Center for Transportation and the North Carolina Department of Transportation.

ACKNOWLEDGEMENTS

This publication is a deliverable of the Contract/Agreement #2013-18/UI Grant #AA990 between North Carolina Department of Transportation and the University of Illinois. The research described in this publication was conducted at the Illinois Center for Transportation (ICT) with financial support provided by the North Carolina Department of Transportation (NCDOT).

Research team members want to thank ICT staff, particularly, Aaron Coenen, Marc Killion, James Meister, and James Pforr, for their assistance with laboratory efforts at the Advanced Transportation Research and Engineering Laboratory (ATREL). Research team members also want to thank Dr. Judith B. Corley-Lay, Chunkun Su and Suriyati Supaat from the NCDOT Material and Tests Unit, for their cooperation and providing test data for this research study. Finally, the authors would like to thank the members and visiting scholars of the UIUC Transportation Geotechnics Research Group, namely, Dr. In Tai Kim, Dr. Sedat Cetin, Hasan Kazmee, Maziar Moaveni, Yu Xie, Chao Fu, Meng Han, Caitlin O'Brien, Yuxuan Wang, and Ce Zhang, for their assistance and contributions to various parts of the project.

EXECUTIVE SUMMARY

This research study was aimed at evaluating rutting potentials of unbound aggregate materials commonly used in the state of North Carolina (NC) for pavement subbase/base construction. Shear strength and permanent deformation tests were conducted at the University of Illinois on sixteen different crushed aggregate materials to predict field rutting performances of base courses constructed with these materials. The original intent was to properly factor them into mechanistic-empirical (M-E) pavement design approaches such as the MEPDG or AASHTO's Pavement ME Design procedure through calibration of the rutting damage models. To accomplish the overall objective, the project specific goals linked to the proposed tasks were as follows: (1) identify and select local base course aggregates from quarries in NC, (2) conduct triaxial monotonic shear strength and repeated load permanent deformation tests, (3) investigate the effects of shear strength, applied stress states and material properties on plastic shakedown behavior of the aggregate materials to determine the most damaging field loading conditions through permanent deformation testing, (4) based on the newly established laboratory database, calibrate the rutting damage model used in the MEPDG or Pavement ME Design software, or propose new improved rutting prediction models, and finally, (5) prepare a set of recommendations for developing new performance-based specifications including strength criteria for these unbound aggregate layers.

The laboratory phase considered a target engineered gradation within the lower and upper limits of North Carolina Department of Transportation (NCDOT) dense-graded base course specification bands; laboratory-established compaction curves for the 16 aggregate materials were used to prepare specimens for shear strength and permanent deformation testing. The complete suite of laboratory characterization tests included imaging-based aggregate particle shape analyses, moisture-density tests, resilient modulus, shear strength, and permanent deformation tests. The concept Shear Strength Ratio (SSR), defined as of the ratio between applied stress levels and the material's shear strength (stress/strength), was introduced in Task 2 based on the shear strength test results, and used in Task 3 to properly examine the effects of varying proportions of stress/strength on the permanent deformation behavior of unbound materials. Clearly, the permanent deformation responses of the aggregate materials correlated better to shear strength than the resilient modulus properties. The accumulated permanent strains were found to steadily increase with applied stress levels in a linear fashion. When plastic fines existed in the aggregate gradation, the permanent deformation potential was drastically higher. Since all aggregate materials were quarry crushed, no clear trends were observed between the imaging based aggregate shape, texture and angularity properties and the permanent deformation behavior.

The experimental results established a consistent database to investigate the permanent deformation trends influenced by aggregate material properties, shear strength, applied stress states and stress/strength ratios, and to develop a new rutting model referred to as the CMT model. Case studies compared the model predictions with those from the MEPDG or Pavement ME Design procedure and evaluated the adequacy of the proposed model. Based on the findings, a practical design approach is recommended for better prediction of aggregate base rutting potentials.

TABLE OF CONTENTS

LIST OF TABLES

LIST OF FIGURES

CHAPTER 1: INTRODUCTION

1.1 OVERVIEW AND PROBLEM STATEMENT

Rutting or accumulation of permanent deformation is the primary damage/distress mechanism observed in unbound aggregate base/subbase layers in pavements. Accordingly, wheel path rutting resistance is a major performance measure for designing pavements with aggregate base/subbase layers. Aggregate base/subbase permanent deformation may contribute significantly to the overall flexible pavement surface ruts. For example, low quality/strength granular materials are generally more susceptible to higher permanent deformation accumulation. A properly compacted good quality aggregate base/subbase, on the other hand, adequately prevents settlement and any lateral movement in the layer through high shearing resistance and contributes significantly to dissipation of wheel load stresses. The NCHRP 4-23 study identified shear strength of unbound aggregates as one of the most significant mechanistic properties influencing pavement performance (Saeed et al. 2001). Moreover, shear strength property rather than resilient modulus (M_R) has been consistently shown to better correlate with unbound aggregate permanent deformation behavior for predicting field rutting performance (Thompson 1998; Tao et al. 2010).

The influence of stress state on the M_R of unbound materials is well known (Hicks and Monismith 1971; Rada and Witczak 1981; Thompson and Elliott 1985; Uzan 1985). Increased confining stress levels can substantially increase the resilient modulus of unbound pavement materials, particularly for coarse grained granular base materials, while increased shear stress levels can substantially decrease the resilient modulus, particularly for fine grained subgrade soils. Although the influence of stress state on unbound resilient modulus is relatively well understood, its influence on the actual performance—rutting, cracking, roughness—of flexible pavements is less clearly known in practice. The incorporation of stress state influences on the resilient modulus of unbound granular base and subbase layers has been explicitly included in the AASHTO's empirical pavement design procedure since 1986. This issue has taken on more significance with the recent release of the Pavement ME Design implementation of the mechanistic-empirical (M-E) pavement design procedure. Whereas the earlier implementation of the M-E pavement design procedure in the public domain MEDPG software explicitly included stress dependence of unbound resilient moduli as Level 1 inputs, this capability has been removed from the Pavement ME Design software implementation. Until today, the latest M-E pavement design approach MEPDG or Pavement ME Design procedure does not consider stress dependency in rutting performance.

1.2 RESEARCH OBJECTIVES

The overall objective of this research study was to evaluate and modify the approach currently used in the AASHTO's M-E pavement design method (Pavement ME Design) for predicting the rut accumulation in unbound aggregate base/subbase layers. The researchers aimed at accomplishing this objective by completing an extensive suite of shear strength and permanent deformation tests on sixteen (16) selected granular materials commonly used in the state of North Carolina (NC) for base/subbase applications. In addition to applied stress and shear strength, extensive evaluation of selected aggregate properties, such as gradation, angularity, fines content, plasticity index (PI), and moisture, on unbound aggregate base rutting performance were carried out under the scope of this research study. The ultimate goal was to prepare a set of recommendations for developing new performance based rutting evaluations including strength criteria for these unbound aggregate layers.

1.3 RESEARCH METHODOLOGY

The proposed research scope for this project comprised five (5) different tasks aimed at achieving specific goals for accomplishing the overall research objective:

<u>Task 1: Selecting Granular Materials Used for Unbound Base and Subbase</u>

The selection of aggregate materials was primarily based on the types, sources and properties of crushed stone materials locally available in the state of North Carolina. Widely spread geological features of different quarry sources and crushing methods inevitably introduced varying mineralogical compositions (i.e. granite, basalt, limestone etc.) and gradation to the different aggregate materials. Accordingly, this task required assistance from and working closely with the NCDOT State Pavement Management Unit and aggregate industry. A total of sixteen (16) aggregate materials were selected and shipped to the Illinois Center for Transportation (ICT) facility located in Rantoul, Illinois for studying the strength and permanent deformation behaviors. Details on the sources of these aggregate materials are provided in Chapter 3.

<u>Task 2: Development of Granular Material Property Database for Laboratory Testing</u>

The main objective of this task was to determine the engineering properties of the selected aggregate materials based on the NCDOT standard material specifications. For each aggregate material satisfying the dense-graded base course requirements for field construction, the following engineering properties were evaluated and examined: (1) grain size distribution; (2) compaction characteristics (i.e. optimum moisture content and maximum dry density); (3) percent of the maximum density the base course is commonly compacted in the field; (4) resilient modulus (M_R) test data conducted on the granular material at field placement density and moisture content, and, if applicable, (5) any strength, modulus and deformation data available for dry and/or wet side of optimum moisture content conditions. The laboratory characterization procedures and methodologies (i.e. specimen preparation) were carefully examined and standardized to produce comparable test results from both the laboratories of NCDOT Material and Tests Unit and the University of Illinois.

Task 3: Laboratory Shear Strength and Permanent Deformation Testing

Under this task, cylindrical triaxial tests were conducted on the aggregate samples to determine: (1) shear strength properties from monotonic displacement-controlled loading tests, and (2) permanent deformation accumulation trends under repeated loading at different applied load (stress) levels in relation to strength property. The primary purpose of conducting shear strength tests was to determine granular material strength properties, namely friction angle (ϕ) and cohesion intercept (c). Based on the concept of Shear Stress Ratio or SSR (introduced in Chapter 3), the second part of this task comprised a series of repeated load triaxial tests conducted at specified target stress levels to study the aggregate permanent deformation behavior.

Task 4: Development of New Rutting Damage Models

Based on the laboratory test data on aggregate material permanent deformation accumulation trends, this task primarily focused on the development and calibration of new and existing rutting models, respectively, for unbound aggregate base/subbase. The predictions from rutting models used in MEPDG and Pavement ME Design programs were scrutinized and compared with permanent deformation models incorporating the effects of material shear strength and applied stress levels. A new rutting model, referred to as the "Chow-Mishra-Tutumluer (CMT) Rutting Model," was proposed to incorporate the effects of material shear strength and applied stress states during unbound aggregate layer rutting predictions. This involved several tasks to validate the proposed model: (1) performing regression analyses to determine specified model parameters for each of the 16 granular materials; (2) implementation of finite element analysis and/or layered elastic programs to estimate in-situ stress states at the mid-depth of unbound aggregate layers based on typical North Carolina low, moderate and high volume pavement sections; (3) optimizing the proposed permanent deformation model parameters using statistical and scientific approaches; (4) comparing the model predictions for the unbound aggregate layer permanent deformations with the results from the existing MEPDG pavement design program. The ultimate objective of this task was intended for Pavement ME Design rutting model calibrations or proposing a new rutting model to be implemented in M-E pavement design.

Task 5: Final Report and Implementation

A final report was prepared based on all research findings that include laboratory test results, developed permanent deformation models, and model calibration parameters for all studied granular materials. Recommendations for developing new performance-based specifications including strength criteria for these aggregate materials are also presented in this report to aid NCDOT engineers in the design of flexible pavement systems incorporating the use of unbound aggregate base/subbase layers.

1.4 REPORT ORGANIZATION

Chapter 2 of this report provides a brief review of pavement rutting mechanisms and material properties affecting the performances of flexible pavements constructed with unbound aggregate base/subbase layers. Existing permanent deformation models developed from repeated load triaxial testing and the relevant mechanistic-empirical (M-E) design rutting damage models are also discussed. Chapter 3 describes the research approach adopted in this project to develop an extensive laboratory test matrix for studying the effects of different variables, such as the shear strength and applied stress levels, on the permanent deformation accumulations in various aggregate materials. Relevant technical features of the laboratory equipment used to test the aggregate specimens are discussed first followed by the descriptions and details of the sample preparation and testing procedures. The results of the laboratory tests, namely, imaging-based aggregate shape, texture and angularity, and shear strength and repeated load triaxial tests are presented in Chapter 4. Based on the laboratory test results, an evaluation framework is established in Chapter 5 and a new rutting model is proposed based on the concept of controlling applied stress as a fraction of the strength property under the same confining pressure conditions. Major findings of the research study are summarized in Chapter 6. Finally, a practical approach is recommended for designing unbound aggregate base layers considering the effects of aggregate shear strength and applied stress levels into the rutting prediction algorithm.

CHAPTER 2: BACKGROUND AND LITERATURE REVIEW

2.1 INTRODUCTION

This chapter presents a review of the literature on available models developed for predicting permanent deformation behavior of unbound granular materials. Each prediction model comes with certain model parameters and the level of difficulty in obtaining these model parameters is discussed in detail. In addition, the rutting damage model utilized in the current MEPDG or Pavement ME design program is also described for its completeness and/or deficiencies to justify the needs of this research study.

2.2 RUTTING MECHANISMS

Past studies (i.e. Barksdale 1972; Thom and Brown 1988; Brown and Chan 1996; Lekarp et al. 2000) list several factors: (1) degree of saturation and/or moisture content, (2) dry density, (3) fines content/plasticity, (4) mineralogy, (5) grain-size distribution, (6) principal stress orientation, and (7) stress history etc., to contribute significantly to the permanent deformation behavior of granular materials. However, the true nature of the rutting mechanism of unbound materials is not yet completely understood. It has been observed that deformation under repeated loading is the result of the following mechanisms:

- Densification/dilation
- Distortion
- Attrition

The densification/dilation mechanism is the process of volume change through reorientation and rearrangement of particles, as a result, compressibility of soil structure. A dense-graded unbound aggregate base material is expected to behave similar to densely packed soils or dense sand when subjected to shear. Dilative behavior like shear induced excess pore water pressure of a saturated Minnesota DOT Class V unbound granular material was measured in an unpublished study by Chow and Labuz (2010). Distortion is characterized by the motions of bending, sliding and rolling of individual particles. Particle bending is governed by the particle shape properties such as flatness and elongation, whereas sliding and rolling are characterized by interparticle friction resistance. For example, round and smooth gravel are more susceptible to deformation. Attrition mechanism is the crushing and breakdown of particles when applied contact load exceeds strength limit of the single particles. Particle crushing is governed by particle shape, size, mineralogy, strength of individual aggregate particles and effective pressure. Moreover, the deformation of granular materials can be volumetric, shear, or both that are resulting from various combinations of the above three mechanisms. Volumetric strains are mainly associated with densification/dilation and attrition, whereas shear strains are mainly contributed through distortion.

2.3 PROPERTIES AFFECTING GRANULAR MATERIAL BEHAVIOR

The shear behavior of granular soils is fundamentally determined by density, effective stress and soil structure. Porosity, void ratio and moisture content reflect density for various types of soil. For a given granular soil, increase in density or decrease in porosity, generally implies an increase in interparticle contact area, hence, shearing resistance. Barksdale (1972) found that decreasing the degree of compaction from 100% to 95% of maximum dry density increased permanent axial strain by 185% on average. Increase in compaction effort from the standard Proctor to the modified Proctor increased maximum density and decreased permanent deformations by 80% for crushed limestone and 20% for gravel, respectively (Allen 1973). Furthermore, van Niekerk (2002) reported that increasing the degree of compaction from 97% to 103% increased the axial stresses required to cause a similar magnitude of permanent axial strain for the tested specimens.

Friction angle decreases as the effective normal stress increases. This behavior is a consequence of the reduction in the rate of increase of contact area as the effective normal stress increases. In granular soils such as rockfill or crushed aggregates, this is primarily caused by the crushing of particle contacts and polishing of particle surfaces (Terzaghi et al. 1996). Change in effective stress is also the result of increasing moisture content. Thompson and Robnett (1979) and Dempsey (1982) found that open-graded aggregates did not develop pore water pressure and the resilient modulus decreased. Thom and Brown (1987) observed that no noticeable pore water pressure developed below 85% saturation and that most of the reduction in resilient modulus was due to the lubricating effect of water. Therefore, moisture can have a positive effect on unbound granular materials as long as the moisture increases the capillary suction between particles. Once the saturation reaches a point where it reduces the capillary suction, the moisture assumes a detrimental role preventing residual deformation and causing a lubricating effect. At even higher saturation levels, where excess pore water pressure can develop, effective stress is reduced, hence resulting in reducing rutting resistance (Thom and Brown 1987).

The shearing resistance or strength of granular soils is the result of resistance to movement at interparticle contacts. This interparticle contact is related to mineralogical compositions of granular particles because interparticle sliding frictional resistance between two surfaces is derived from primary valence bonding at contact points, which are related to crystal structure of the minerals as well as intercrystalline bonding (Terzaghi et al. 1996). The mineralogical and geological properties of the rock formation and the crushing process define the shape of the crushed particles. For example, basalt rockill and granitic schist rockfill were found to have friction angle of 47º and 37º, respectively (Terzaghi et al. 1996).

On a macroscopic level, the strength of granular materials could be reasoned by the degree of surface roughness, texture and angularity of aggregate particles. Allen (1973) and Barksdale and Itani (1989) investigated the effects of the surface characteristics of unbound granular materials and found that angular particles resisted permanent deformation better than rounded particles because of the improved particle interlock and higher angle of shear resistance between particles. Barksdale and Itani (1989) also concluded that blade-shaped crushed particles are slightly more susceptible to rutting than other types of crushed aggregate and that cube-shaped, rounded river gravel with smooth surfaces is more susceptible than crushed aggregates. More recently, Rao et al. (2002) studied the impact of imaging based aggregate angularity index variations on the friction angle of different aggregate types and reported an increase in aggregate shear strength when the percentage of crushed particles was increased. An increase in crushed materials beyond 50% substantially increased friction angle obtained from triaxial shear strength tests including a higher resistance to permanent deformation accumulation. Later on, Pan et al. (2004) found that increased surface texture and particle angularity as quantified from imaging increased the resilient modulus of asphalt concrete indicating that surface characteristics directly related to permanent deformation resistance.

2.4 EXISTING PREDICTIVE MODELS FOR RUTTING ACCUMULATION

Modeling of permanent deformations is less widely studied compared to resilient response of unbound granular materials for a number of reasons: (1) the experimental study of permanent deformation behavior is time consuming and requires large number of load cycles (i.e. 10^3 or more); (2) permanent deformation test results are considerably much more scattered than resilient modulus test results; and (3) laboratory derived permanent deformation models are less applicable to pavement layered structural analysis and subjected to external conditions (i.e. temperature, moisture, different wheel loads). Consequently, most existing permanent deformation models have been derived based on three following aspects:

- Empirical relation between permanent deformations (or strains) and number of load cycles at a particular state of stress;
- Empirical relation between permanent deformation (or strain) and state of stress at a given load cycle; and,
- Incremental models, which are generally based on the theory of elasto-plasticity.

In this section, existing predictive models proposed by different researchers are summarized. "ϵ_p" and "N" are axial deformation strain and the number of load cycles, respectively.

2.4.1 Barksdale (1972)

Barksdale (1972) proposed one of the first predictive models of permanent deformation accumulation in unbound granular materials. Barksdale (1972) performed repeated load triaxial tests on crushed stone materials and soil-aggregate mixtures with 100,000 load cycles using a constant confining pressure and triangle stress pulse, and proposed a linear relationship between permanent axial strain and the logarithm of number of load cycles given below:

$$\epsilon_p = a + b \log N \tag{2.1}$$

where a and b are regression model parameters determined through analyses of experimental data.

2.4.2 Monismith et al. (1975)

Monismith et al. (1975) proposed the log-log relationship between permanent strain and number of load cycles at a given stress level as shown below. This model is also known as phenomenological model.

$$\epsilon_p = AN^b \tag{2.2a}$$

$$\log \epsilon_p = A + b \log N \tag{2.2b}$$

The log(ϵ_p)-log(N) appeared to be an appropriate, versatile and practical approach to capture permanent deformation accumulation. Monismith et al. (1975) and Maree (1978) suggested that for soils and granular materials the model parameter b was generally within the range of 0.12 to 0.2 for stress conditions under "failure" strength. The lower limits are for subgrade soils. However, a limitation of this model is that reciprocal of parameter b exhibits numerical instability of this model as permanent deformations approach infinity (∞) and zero at first load cycle (N = 1) and large value of N, respectively. This also implies that parameter A represents asymptote of permanent deformation at large number of load cycle. Therefore, this model only predicts permanent deformation behavior below the plastic shakedown limit, which is the asymptotic permanent deformation response defined in the Shakedown theory (Werkmeister 2003). Studies have shown that parameter b varies between 0.1-0.2, and A term varies and is strongly dependent on repeated stress state and material strength (Khedr 1985; Garg 1997).

2.4.3 Pappin (1979)

Pappin (1979) recommended a simple relationship to account for the effect of stress in predicting permanent shear strain:

$$\gamma_p = (\text{fn } N) L \left(\frac{q}{p}\right)_{max}^{2.8} \tag{2.3}$$

where γ_p is permanent shear strain; (fn N) is the shape function, which depends on number of load cycles; p is mean normal stress; p is mean normal stress = $(\sigma_1 + \sigma_2 + \sigma_3)/3$; q is deviator stress = $(\sigma_1 - \sigma_3)$; L is length of stress path = $(p^2 + q^2)^{1/2}$; and $(q/p)_{max}$ is maximum stress ratio.

This model considers ϵ_p is proportional to the stress path length, L and ratio of deviator stress to mean stress at a power of 2.8.

2.4.4 El-Mitiny (1980) and Khedr (1985)

El-Mitiny (1980) and Khedr (1985) proposed the strain rate model based on log-log relationship of permanent deformation and number of load cycles. El-Mitiny (1980) studied rutting and fatigue performances of various asphalt mixtures and concluded that aggregate type and asphalt content significantly controlled the rutting parameter. Khedr (1985) later conducted variable confining pressure (VCP) triaxial tests on crushed limestone at different stress states, moisture contents and densities. The results suggested a power relationship existed between permanent strain rate and number of load cycles, as shown in Equation (2.4). A major difference in this model is that permanent strain rate is inversely proportional to the number of load cycles.

$$\frac{\epsilon_p}{N} = aN^{-b} \tag{2.4}$$

where a and b are model parameters. Parameter a, which represents rutting susceptibility, was found to be highly dependent on stress state and resilient modulus.

2.4.5 Tseng and Lytton (1989)

The model by Tseng and Lytton (1989) was based on 16 repeated load triaxial tests. This laboratory test database included several different granular base materials, each with different density and moisture content, subjected to various loading conditions. Granular materials studied were granite, limestone and gravelly sand. From these data, Tseng and Lytton (1989) demonstrated the importance of unbound granular material characterization in predicting rutting in flexible pavements and introduced a predictive model by incorporating three material parameters.

$$\epsilon_p = \epsilon_0 e^{-\left(\frac{\rho}{N}\right)^{\beta}} \tag{2.5}$$

where ϵ_0, β and ρ are different material parameters, depending on material physical properties, moisture content and bulk stress of laboratory testing.

2.4.6 Wolff (1992)

Wolff (1992) used full-scale accelerated pavement testing database compiled in South Africa to predict permanent deformation accumulation in unbound aggregate base and subbase layers. The granular materials used in the database included crushed stone, natural gravel and gravel-soil with different density and fines plasticity. This model is presented in Equation (2.6):

$$\epsilon_p = (mN + a)(1 - e^{-bN}) \tag{2.6}$$

where a, b and m are model parameters, in which m has physical interpretation of permanent deformation accumulation indicating plastic shakedown (m = 0) and plastic creep response (m > 0). In another study, Wolff and Visser (1994) compared the quality of granular materials and concluded that asymptotic rate of permanent deformation is smaller in higher quality materials.

2.4.7 Thompson and Nauman (1993)

Much analogous to Equation (2.3), Thompson and Nauman (1993) practically used rut depths obtained from selected AASHTO Road Test data to correlate with rutting rate and number of load cycles:

$$RR = \frac{RD}{N} = A/N^B \tag{2.7}$$

RR and RD in the above equation are rutting rate and rut depth in inches, respectively. A and B terms are developed from field calibration testing data. Low A terms are noted for lower stress ratios and high A terms are for high stress ratios. This model essentially indicates that the rate of permanent deformation decreases with the increase of the number of load cycle.

2.4.8 van Niekerk and Huurman (1995)

van Niekerk and Huurman (1995) proposed a predictive model based on the phenomenological model with the addition of stress state components, as presented below:

$$\epsilon_p = a_1 \left(\frac{\sigma_1}{\sigma_{1,f}}\right)^{a_2} \left(\frac{N}{1000}\right)^{b_1 \left(\frac{\sigma_1}{\sigma_{1,f}}\right)^{b_2}} \tag{2.8}$$

where σ_1 is major principal stress; $\sigma_{1,f}$ is major principal stress at failure; and a_1, a_2, b_1 and b_2 are model parameters. The stress ratio ($\sigma_1 / \sigma_{1,f}$) is exclusive from the A and B parameters in Equation (2.2), causing a_1 and b_1 to be stress independent. This model was later expanded to the form given in Equation (2.10a).

2.4.9 Paute et al. (1996)

Paute et al. (1996) recommended a hyperbolic relationship between number of load cycles and permanent strain accumulation after 100 cycles, given in Equations (2.9a) and (2.9b):

$$\epsilon_p = \frac{A\sqrt{N}}{B+\sqrt{N}} \tag{2.9a}$$

$$\epsilon_{p,100} = A\left(1 - \left(\frac{N}{100}\right)^{-B}\right) \tag{2.9b}$$

where $\epsilon_{p,100}$ is permanent deformation for number of load cycles after 100 cycles; parameter A and B in above equations are regression model parameters. Note that Paute's model excluded the rapid rate accumulation of permanent deformation because of the difficulty in predicting permanent deformation development within the first 100 cycles. In both cases, A represents the asymptote of accumulation of permanent deformation at large number of cycles.

2.4.10 Huurman (1997)

Huurman (1997) investigated permanent deformation behavior of natural and crushed sands by applying up to one million load cycles in repeated load triaxial tests. All tests were conducted at a confining pressure of 12 kPa (1.74 psi) and different stress ratios ($\sigma_1 / \sigma_{1,f}$) ranged from 0.838 to 0.978. Based on their earlier study, Huurman (1997) improved Equation (2.8) to the following predictive model:

$$\epsilon_p = A\left(\frac{N}{1000}\right)^B + C\left(\exp\left(D\frac{N}{1000}\right) - 1\right) \tag{2.10a}$$

where A, B, C and D are stress dependent model parameters, and can be represented by X in the following equation:

$$X = x_1\left(\frac{\sigma_1}{\sigma_{1,f}}\right)^{x_2} \tag{2.10b}$$

where x_1 and x_2 are variables representing related coefficients a_1, b_1, c_1, d_1 and a_2, b_2, c_2, d_2, respectively.

2.4.11 Ullidtz (1997)

In the same year, Ullidtz (1997) used Discrete Element Method (DEM) to model deformation behavior of granular materials and proposed a relatively simple model that includes applied stress based on the phenomenological model. According to this model, parameter A is independent of the effects of applied stress:

$$\epsilon_p = A\left(\frac{\sigma_d}{p_0}\right)^B N^C \tag{2.11}$$

where σ_d is deviator stress; p_0 is the normalizing reference stress (i.e. p_0 = 1 psi or 1 kPa); and A, B and C are parameters obtained from multiple regression analysis.

2.4.12 Lekarp and Dawson (1998)

Lekarp and Dawson (1998) argued that failure in granular materials under repeated loading is a gradual process, rather than a sudden collapse. They studied the effects of states of stress on permanent deformation accumulation and incorporated stress path into a new model:

$$\frac{\epsilon_p(N_{\text{ref}})}{(L/\text{p}_0)} = A\left(\frac{q}{p}\right)_{\max}^{B} \tag{2.12}$$

where $\epsilon_p(N_{\text{ref}})$ is permanent strain at a given reference number of load cycles N_{ref}, where $N_{\text{ref}} > 100$; L is the length of stress path; p is mean normal stress equals to $(\sigma_1 + \sigma_2 + \sigma_3)/3$; q is deviator stress = $(\sigma_1 - \sigma_3)$; $(q/p)_{\max}$ is maximum stress ratio; p_0 is the normalizing reference stress; and A and B are model parameters. Although this model has inclusively considered several stress-related variables, yet, it does not fully capture the effects of principal stress rotations and stress path loading slopes, which was found to be significantly affecting permanent deformation behavior of unbound granular materials (i.e. Lekarp et al. 2000).

2.4.13 Gidel et al. (2001)

Gidel et al. (2001) proposed a stress dependent permanent deformation model based on the laboratory studies of two granular materials at the French LCPC:

$$\epsilon_p = \epsilon_{p,0}\left[1 - \left(\frac{N}{N_0}\right)^{-B}\right]\left(\frac{L_{max}}{p_a}\right)^{n}\left(\frac{1}{m + \frac{s}{p_{max}} - \frac{q_{max}}{p_{max}}}\right) \tag{2.13}$$

where $p_{\max}$ is maximum mean normal stress; $q_{\max}$ is maximum cyclic deviator stress; $L_{\max}$ is stress path length, or $(p_{\max}^2 + q_{\max}^2)^{½}$; p_a is atmospheric pressure = 100 kPa (1 tsf); N_0 is reference number of cycles; and $\epsilon_{p,0}$, B and n are model parameters; m and s are parameters of the stress path, $q = mp + s$. This model considers two components: number of load cycles as a power function and stress component as a hyperbolic function. The predicted ϵ_p approaches infinitely large strains when the stresses reach the failure state of material.

2.5 MECHANISTIC-EMPIRICAL PAVEMENT DESIGN PROGRAM RUTTING MODEL

The new AASHTO mechanistic-empirical (M-E) pavement design procedure, Pavement ME Design program does not credit the contribution of the unbound aggregate base sufficiently for it to be cost competitive. To properly account for granular material quality impacting performance of pavements with unbound aggregate bases, the first challenge is to be able to incorporate shear strength or rutting potential into materials characterization through the inputs required by M-E design procedures such as Pavement ME Design.

In Pavement ME Design, permanent deformation (δ) of an unbound aggregate base/subbase layer is estimated by Equation (2.14), as a function of traffic repetitions (N), layer thickness (h), and vertical resilient strain computed for sublayer (ϵ_v). The ratio ϵ_0/ϵ_r, β, ρ are material properties and model parameters in the equation, which need to be computed as a function of moisture content, resilient modulus (M_R) and states of stress according to the original Tseng and Lytton (1989) rutting model. Note that the Pavement ME Design eliminated the stress state dependence and therefore changed this equation of permanent deformation – a critical long-term performance parameter – to assess rutting potential during construction through field measurement of moisture only.

$$\delta(N) = \beta_1 \left(\frac{\epsilon_0}{\epsilon_r}\right) e^{-\left(\frac{\rho}{N}\right)^{\beta}} \epsilon_v h \tag{2.14}$$

where $\delta(N)$ is permanent deformation corresponding to N-load application; β_1 is field calibration parameter; ϵ_0, β, ρ are material parameters; ϵ_r is resilient strain imparted in the laboratory to determine material properties; ϵ_v is vertical resilient strain computed from sublayer; and h is thickness of sublayer. The above equation can be rearranged to the following form:

$$\frac{\epsilon_p(N)}{\epsilon_v} = \beta_1 \left(\frac{\epsilon_0}{\epsilon_r}\right) e^{-\left(\frac{\rho}{N}\right)^{\beta}} \tag{2.15}$$

where ϵ_p is the permanent strain in the unbound pavement layer corresponding to N-load applications of a typical equivalent standard axle. The material parameters included in Equations (2.14) and (2.15) are calculated using the following equations:

$$\log\beta = -0.61119 - 0.017638\,\mathrm{W}_c \tag{2.16}$$

$$\log\rho = 0.622685 + 0.541524\,\mathrm{W}_c \tag{2.17}$$

$$W_c = 51.712 \times CBR^{-0.3586\,GWT^{0.1192}} \tag{2.18}$$

$$CBR = \left(\frac{\mathrm{M_R}}{2555}\right)^{1/0.64} \tag{2.19}$$

where W_c is equilibrium water content; GWT is depth of ground water table; CBR is California Bearing Ratio of unbound layer; and $\mathrm{M_R}$ is resilient modulus of layer and/or sublayer.

A closer look at Equations (2.14) through (2.19) reveals that permanent deformation accumulation in unbound layers is currently predicted without giving any consideration to the applied stress states. This is the outcome of an oversimplification of the original equations proposed by Tseng and Lytton (1989). In the formulations proposed by Tseng and Lytton (1989), both parameters β and ρ were dependent on the applied stress states. However, this stress dependency was later removed from the equations as it was believed to result in erroneous trends in unbound layer rut predictions (Witczak and El-Basyouny 2004). In the current formulations, the β and ρ parameters are correlated only with W_c, which is ultimately determined from *CBR* or resilient modulus (M_R), as given in Equations (2.18) and (2.19).

Equations (2.14) through (2.19) clearly establish that the current version of the AASHTO mechanistic-empirical pavement design method (Pavement ME Design) primarily relies on resilient modulus values to predict the permanent strain [ϵ_p (N)] accumulation under loading. Note that granular material shear strength properties or applied stress states are not considered in the unbound pavement layer rutting models.

2.6 SUMMARY

Rutting mechanisms of base course unbound aggregate material properties and the permanent deformation models of the existing empirical and semi-empirical predictive methods were reviewed in this chapter. As this review of literature indicates, the majority of these methods were mainly developed based on laboratory characterization, especially with repeated load triaxial testing.

Current predictive model as implemented in the latest mechanistic-empirical (M-E) pavement design program (i.e. Pavement ME Design) is also discussed. In its current form, the Pavement ME Design software does not consider aggregate material's shear strength and applied wheel load stress states while predicting the surface ruts contributed by unbound aggregate pavement base/subbase layers. To adequately characterize and predict the performance of unbound aggregate base/subbase pavement layers under repeated traffic loading, it is important for ME pavement design approaches to consider the effects of applied stress levels on unbound aggregate layer rutting.

CHAPTER 3: MATERIALS AND LABORATORY TESTS

3.1 INTRODUCTION

The majority of available predictive models presented in Chapter 2 indicate that the permanent deformation accumulation in unbound aggregate materials can be expressed as a function of load cycle, material properties and stress state. These variables are inclusively listed as the primary factors that contribute to the permanent deformation behavior of granular materials (Lekarp et al. 2000). Considering these factors, this chapter describes the scientific approach adopted in this research study to develop a laboratory test matrix for studying rutting performances of different unbound aggregate materials used in pavement base/subbase layers. Relevant technical features of the laboratory equipment used to test the aggregate specimens are discussed first, followed by the descriptions and details of the sample preparation and testing procedures.

3.2 MATERIALS RECEIVED

Totally, sixteen (16) different crushed aggregate materials, commonly used for unbound base/subbase applications in the state of North Carolina, were received from different quarries to be tested and evaluated in this study. The corresponding quarry, county and supplier of each material are alphabetically listed in Table 3.1. As received gradations of the individual materials are provided in Appendix A. Index properties, such as Atterberg limits for the fraction passing No. 40 sieve (0.425 mm), as well as moisture-density relationships are provided in Section 3.4.

3.3 DEVELOPMENT OF THE LABORATORY TEST MATRIX

Several investigators (Barksdale 1972; Thom and Brown 1988; Lekarp et al. 2000) conducted extensive laboratory studies on the repeated loading behavior of granular materials, and observed the following factors to have significant influence on the permanent deformation response of granular materials under repeated loading: (1) degree of saturation and/or moisture content, (2) dry density, (3) fines (often defined as material finer than 0.075 mm, or passing No. 200 sieve) content, (4) mineralogy, (5) grain-size distribution, (6) stress level (confining and deviator stress), (7) stress duration or loading frequency, and (8) specimen size. Accordingly, it is important to consider these factors when studying the repeated load deformation behavior of granular materials.

Table 3.1 List of Sixteen Crushed Stone Materials Studied

Quarry	County	Supplier
Arrowood	Mecklenburg	Martin Marietta
Belgrade	Onslow	Martin Marietta
Fountain	Pitt	Martin Marietta
Franklin	Macon	Harrison Construction Co.
Goldhill	Cabarrus	Vulcan Materials
Hendersonville	Henderson	Vulcan Materials
Jamestown	Guilford	Martin Marietta
Lemon Spring	Lee	Martin Marietta
Moncure	Lee	Wake Stone Corp.
Nash County	Nash	Wake Stone Corp.
North Wilkesboro	Wilkes	Vulcan Materials
Princeton	Johnston	Hanson Aggregates
Raleigh	Wake	Hanson Aggregates
Rockingham	Richmond	Vulcan Materials
Rocky Point	Pender	Martin Marietta
Rougemont	Durham	Hanson Aggregates

As previously mentioned, one of the main objectives of this research study was to incorporate the effects of applied stress states in permanent deformation predictive model development. Particularly, the effect of stress history is important in capturing the permanent deformation accumulation (Brown and Hyde 1975; Kim 2005). Permanent deformation accumulation resulting from immediate high stress level is found to be larger than deformation accumulation from successive smaller increases in stress level applications. When repetitive loads are applied, the gradual densification or stiffening of granular material results in less deformation accumulation compared to instantaneous applications of high stress levels. Subsequently, to study the effects of stress levels and to eliminate the effects of stress history on unbound aggregate permanent deformation behavior, it was decided to test the laboratory specimens at three distinct stress levels, labeled as: low, intermediate and high stress levels. These stress levels, also known as Shear Stress Ratios (SSRs), are discussed in Section 3.7. Permanent deformation testing at each e stress level comprised the application of 10,000 load cycles at a defined target deviator stress level while maintaining a constant confining pressure level. Note that the application of only 10,000 load pulses per SSR level may represent a limitation of the current test protocol, as it may not capture the transition from plastic creep (Range B) to incremental collapse (Range C) under very high number of load applications as defined by Werkmeister (2003). The selection of 10,000 load applications per stress level in this study was primarily due to time constraints associated with conducting tests at higher number of load applications (e.g. 100,000 cycles or more per stress level). Accordingly, single-stage loading tests correspond to 10,000 load applications at a specific stress level; multi-stage loading tests comprise three different single-stage loading tests conducted in sequence on a single specimen. Accordingly, multi-stage loading tests comprise the application of a total of 30,000 load cycles (3 stages x 10,000 load cycles per stage). Results from multi-stage and single-stage tests are included in Appendix D and E, respectively.

All laboratory tests were conducted at the Illinois Center for Transportation (ICT) facility located in Rantoul, Illinois. In accordance with the developed laboratory test matrix, Table 3.2 lists in detail the number of tests performed on all the granular materials. It should be noted that a minimum of three shear strength tests at different confining pressures were conducted to allow interpretation of strength properties, i.e. friction angle and cohesion intercept, by using a linear regression analysis method.

Table 3.2 Particle Shape, Shear Strength, and Permanent Deformation Test Matrix

Test Description		Number of Tests
I.	Enhanced University of Aggregate Image Analyzer (E-UIAIA) Shape Characterization A. Angularity B. Surface Texture/Roughness C. Flatness and Elongation	3[a]
II.	Shear Strength	3 or more
III.	Permanent Deformation A. Single-stage loading (at three individual stress levels) B. Multi-stage loading (at three consecutive stress levels)	 3[b] 1[b]

[a] Replicate tests performed.
[b] Tests performed at single constant confining pressure.

3.3.1 Grain Size Distribution

The contribution of gradation or grain size distribution is widely known to influence the mechanical properties and response of unbound aggregates. Different gradations essentially lead to significant alterations of granular soil behavior. This is because grain size distribution controls the packing configurations and particle-to-particle contacts of granular soil particles. A densely-packed configuration enhances particle-to-particle contact, therefore, increasing shearing resistance and lowering compressibility of soil aggregates. In pavement unbound aggregate base course materials, the grain size distribution is often preferred to be well-graded to provide adequate shearing resistance when subjected to traffic loading.

For the purpose of this study, the gradations of all 16 different granular materials had to be kept consistent. This would enable the control of grain size distributions and attribute any change in behavior to the induced changes in the granular material properties such as fines content (material finer than 0.075 mm, or passing No. 200 sieve), plasticity of fines and moisture content. Prior to sieve separation (Section 3.3.2), all materials were oven-dried and sampled by following procedures as described in ASTM C702 for sieve analyses. For each aggregate material, sieve analysis was conducted following ASTM C136 to check the as-received gradation for the requirement of NCDOT specifications. As received grain size distribution curves for all the aggregate materials can be found in Appendix A. The NCDOT unbound base course material specification is detailed in Table 3.3 and Figure 3.1.

Previous research studies (Thom and Brown 1988; Dawson et al. 1996; Tutumluer and Seyhan 2000; Mishra and Tutumluer 2012) highlighted the importance of using engineered gradations for laboratory testing of unbound granular materials. Particles corresponding to each size fraction were subsequently blended to achieve one constant gradation across all specimens. The mid-range of NCDOT unbound base course material specification band was selected as the target gradation for blending the specimens for laboratory testing, given in Table 3.3. Gradations were engineered to target 8% fines content (material finer than 0.075 mm, or passing No. 200 sieve), which has been established by researchers as an optimum configuration where the fines increase the overall stability of aggregate matrix (Mishra and Tutumluer 2012). The resulting grain size distribution curve is shown in Figure 3.1. Accordingly, the coefficients of uniformity (C_u) and curvature (C_c) were about 100 and 1.23, respectively, with this gradation. The target gradation is, subsequent*l*y, categorized as a well-graded material, or termed as GW-GM as specified in the Unified Soil Classification System (ASTM D2487).

Table 3.3 Engineered Gradation – Mid-band of NCDOT Lower and Upper Limits

Sieve Size		Average Cumulative Percent Passing (%)		
in. / No.	(mm)	NCDOT Specification Upper Limit	NCDOT Specification Lower Limit	Target Engineered Gradation
1.5 in.	36.1	100	100	100
1.0 in.	25.4	75	97	92
0.5 in.	12.7	55	80	68
No. 4	4.75	35	55	45
No. 10	2.00	25	45	35
No. 40	0.425	14	30	22
No. 200	0.075	4	12	8

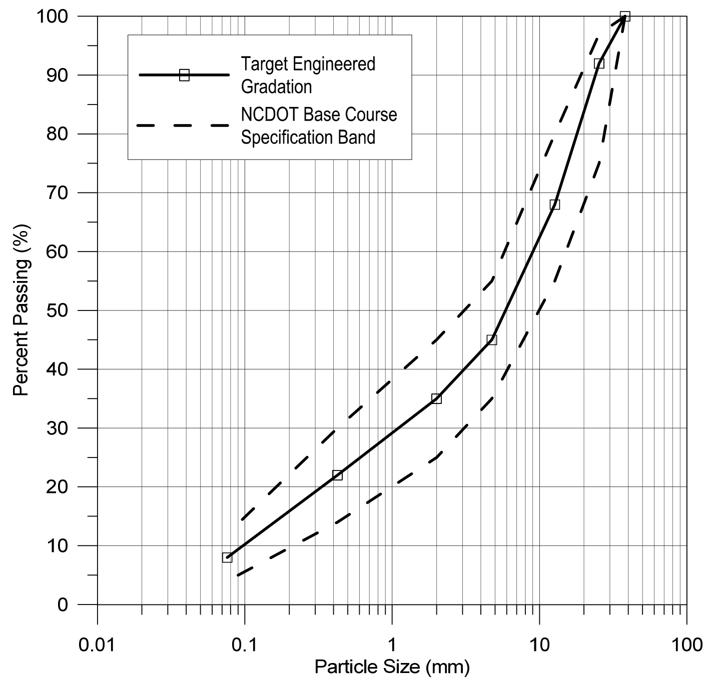

Figure 3.1 Engineered Gradation

3.3.2 Sieving and Size Separation

To control the gradation of an individual aggregate sample, sieving and separation of the aggregate materials by size was deemed to be a priority task. The stockpiles of all 16 materials received from different quarries were processed through a set of sieves following the practice of ASTM C136. The material retained on each sieve size was stored in seven separated buckets with individual particle sizes as indicated in Table 3.3. The sieving procedure was performed at the Advanced Transportation Research and Engineering Laboratory (ATREL) facility, which houses the Illinois Center for Transportation (ICT), based on dry sieving method of the aggregate stockpiles. Shown in Figure 3.2 are sieve shakers and buckets containing different particle sizes, respectively. Coarse-grained aggregate sizes from 1.0-in. (25.4-mm) to No. 4 (4.75-mm) sieve size were separated on Gilson Testing Screen following the best practices for quality control and manufacturer's recommendations. The materials passing No. 4 sieve (sizes corresponding to. No. 10, No. 40, No. 200 sieves and fines retained on pan) were separated on the DuraShake™ sieve shaker. Any oversize granular particle (i.e. larger than 1.5-in.) was discarded from the sieve operation and not used in this study.

(a)

(b)

(c)

Figure 3.2 Sieving and Size Separation Task: (a) TS-1 Gilson Testing Screen Used for Granular Particles Retained on No. 4 Sieve; (b) DuraShake™ Sieve Shaker Used for Granular Particles Passing No. 4 Sieve; and (c) Buckets for Storing Different Sizes of Granular Materials

3.4 MOISTURE-DENSITY RELATIONSHIPS AND ATTERBERG LIMITS

The compaction characteristics of all 16 granular materials were provided by NCDOT Material and Tests Unit. The compaction method was reported to follow procedures similar to modified compaction test (AASHTO T-180) but with additional 30 blows (total of 86 blows) applied to each layer with a 10-lb. (4.54-kg) rammer and 18-in. (457-mm) drop height.

Aggregate specimens were prepared at different moisture contents, and compacted in a 6-in. (152-mm) × 7-in. (178-mm) CBR mold in five (5) equal layers at 86 blows per layer. The resulting weights of aggregates per unit volume at different moisture contents were plotted against moisture content, giving a relationship for the dry densities obtained at various moisture contents. As a minimum, four tests (often more) were performed and used to draw a curve to establish the maximum dry density (MDD) and optimum moisture content (OMC) values. Table 3.4 summarizes the MDD and OMC values for all sixteen aggregate materials, listed alphabetically. Results from Atterberg limit tests (Liquid Limit and Plastic Limit) conducted on the fraction finer than 0.425 mm (passing No. 40 sieve) are also presented in Table 3.4.

Table 3.4 Moisture-Density and Index Properties of Aggregate Materials

Quarry	Maximum Dry Density (pcf)	Optimum Moisture Content (%)	Plasticity Index (%)	Liquid Limit (%)
Arrowood	153.5	4.2	NP[a]	18
Belgrade	131.3	7.4	NP	16
Fountain	141.2	6.1	NP	19
Franklin	151.5	4.7	NP	19
Goldhill	142.2	6.4	6	23
Hendersonville	139.3	5.5	NP	21
Jamestown	141.6	5.8	NP	23
Lemon Spring	140.9	5.5	NP	17
Moncure	148.2	5.2	NP	17
Nash County	142.3	5.7	NP	18
N. Wilkesboro	142.5	5.0	NP	24
Princeton	141.3	5.1	NP	18
Raleigh	139.6	6.1	NP	22
Rockingham	141.4	6.1	NP	22
Rocky Point	134.7	5.9	NP	17
Rougemont	144.1	6.1	NP	18

[a] NP: Nonplastic

As listed in Table 3.4, materials from Arrowood, Franklin, Moncure, and Rougemont quarries have the highest densities. In contrast, Belgrade and Rocky Point materials, which consisted of limestone aggregates, have the lowest densities. Generally, higher maximum dry density associates with denser packing. This relationship is alternatively plotted with friction angles in Figure 4.4. Note that all aggregate materials have nonplastic (NP) fines except Goldhill, which has a Plasticity Index (PI) of 6. Specifications commonly accept PI values less than or equal to 6 in pavement unbound aggregate base courses, though nonplastic fines is preferred. Note that the as-received Goldhill material had only 2.5% passing No. 200 (0.075 mm) sieve, which was much less than the others, although all the materials were eventually engineered to the same target gradation.

3.5 PARTICLE SHAPE, TEXTURE AND ANGULARITY

As discussed in Chapter 2, aggregate particle shape, texture and angularity have been recognized to influence the engineering behavior of unbound aggregates. The Enhanced University of Illinois Aggregate Image Analyzer (E-UIAIA), used in this study, is an improvement over the older version of UIAIA. This enhanced device is equipped with three high resolution (1292 × 964 pixels) Charge Coupled Device (CCD) progressive scan color cameras to capture three orthogonal views (front, top and side) of particles. Figure 3.3 shows the E-UIAIA used for establishing the morphological indices of aggregate particles during the current study. More details on the features of the E-UIAIA can be found elsewhere (Moaveni et al. 2013).

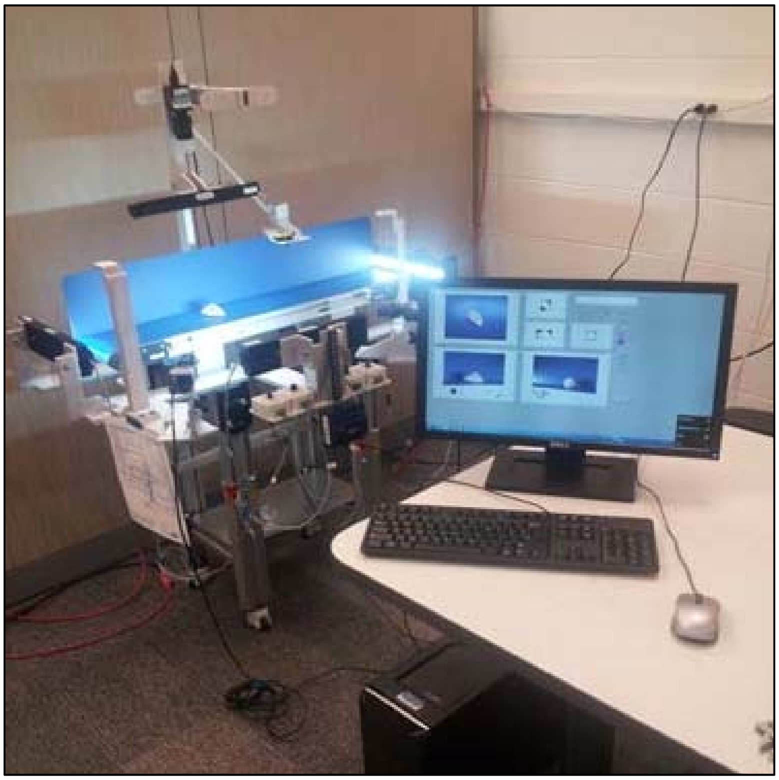

Figure 3.3 Enhanced University of Illinois Aggregate Image Analyzer (E-UIAIA)

In addition to capturing color images, E-UIAIA is capable of quantifying the following shape properties of aggregate particles as imaging based indices (Tutumluer et al. 2000; Rao et al. 2001; Rao et al. 2002; Pan and Tutumluer 2007; Moaveni et al. 2013):

- **Angularity Index (AI)**: A physical index to describe sharp versus smooth in aggregate particle, and has the degree unit. The final AI value is an area weighted average value of the individual AI values determined from three orthogonal views.

- **Surface Texture Index (STI)**: Surface roughness or irregularities of aggregate particle. Contrasts of texture are smooth river gravel with polished surface as compared to crushed limestone or granite with very rough textured surface. The final STI value is an area weighted average value of the individual STI values determined from three orthogonal views.

- **Flat and Elongated Ratio (FER)**: Ratio of the longest to shortest dimensions characterized from three views of an aggregate particle. The FER values are taken average after a suitable number of particles are tested.

These imaging based shape indices have been validated by successfully measuring aggregate properties and linking results to corresponding laboratory strength data and field rutting performances (Rao et al. 2002; Pan et al. 2004).

In this study, fifty (50) particles corresponding to two particle sizes, 1-in. (25.4-mm) and 0.5-in. (12.5-mm), were randomly collected from each of the sixteen aggregate materials, and scanned using the E-UIAIA through three replicate tests. Results from the E-UIAIA image analyses are presented and discussed in Chapter 4. All the collected aggregate particles were washed thoroughly using clean water and oven-dried before the image analysis.

3.6 RESILIENT MODULUS TESTING

In addition to the compaction characteristics, resilient modulus (M_R) test results for all sixteen aggregate materials were also provided by the NCDOT Material and Tests Unit. As already described in Section 2.5, the elimination of stress dependency from the original Tseng and Lytton (1989) equation has resulted in permanent deformation predictions of unbound granular layers to be solely predicted from the moisture content and resilient modulus values. Accordingly, the stress dependent resilient modulus is a primary input parameter for the design of unbound aggregate base/subbase layers in pavement structures. For the purpose of this study, it is therefore, necessary to obtain resilient modulus related resilient or recoverable strain during the model calibration process (Task 4) for comparison and performance evaluation.

The resilient modulus testing followed the procedure as listed in AASHTO T307-99. Each material was weighed according to its maximum dry density and optimum moisture content values as listed in Table 3.4, then was compacted in six (6) equal layers in a 6-in. (152-mm) diameter and 12-in. (305-mm) high mold with a 10-lb (4.54-kg) hammer from 18-in. (457-mm) drop height. It was assumed that target density was achieved when weighed materials were all compacted to a predetermined layer height. Therefore, there was no specified blow count for each layer during compaction. Test sequences for base/subbase materials started with 1,000 cycles for conditioning phase.

3.7 TRIAXIAL SHEAR STRENGTH TESTING

One of the main objectives of this study was to incorporate the effects of shear strength and applied stress levels into unbound aggregate permanent deformation predictive models. Accordingly, Task 3 highlights the importance of shear strength properties of aggregate materials prior to developing a specified stress/strength ratio for the next stage of testing. The stress/strength ratio, or Shear Stress Ratio (SSR), will be discussed later. In this study, the shear strength test procedure followed the conventional triaxial shear strength test using a 1% strain per minute loading rate on 12-in. (305-mm) high cylindrical specimens. Although rapid shear strength tests, with a loading rate of 12.5% strain per second, have been reported to better simulate actual pavement condition under slow-moving vehicle wheel load, the mobilized peak strengths were only slightly higher than conventional triaxial tests utilized in this study.

Three specimens were initially tested at confining pressure levels of 5 psi (34.5 kPa), 10 psi (68.9 kPa), and 15 psi (103.4 kPa) to establish the aggregate shear strength properties (friction angle and cohesion intercept). Depending on the quality of test results, additional tests were conducted at similar and other confining pressures to adequately establish the Mohr-Coulomb failure envelope. Peak stresses, or deviator stresses at failure, were carefully examined and compared to evaluate the strength properties of different granular materials. The friction angle (ϕ) and cohesion intercept (c) values of all granular materials were determined using regression analysis-based linear interpolation, and are summarized in Section 4.4.

3.7.1 Shear Strength Test Specimen Preparation

All triaxial shear strength tests were conducted at the ATREL facility. Test specimens were prepared in the same manner as resilient modulus test samples described in Section 3.6. Test specimen dimensions were 6-in. (152-mm) in diameter and 12-in. (305-mm) in nominal height. For each aggregate material tested, specimens were proportioned to achieve the mid-specification gradation as emphasized in Figure 3.1, followed by batch-mixing with target moisture contents.

An aluminum split-mold lined with a 31-mil (0.79-mm) neoprene membrane was assembled on the triaxial cell base plate. A 10-lb (4.54-kg) drop hammer was used to compact six (6) successive lifts at the target density level (selected in the current study to be equal to the maximum dry density). Following compaction, concentricity was checked on the top lift with a bull's eye-type surface level before the load cell was placed on top of the specimen. Prior to removal of segmented specimen mold, an internal vacuum was attached to the specimen. The specimen was supported by the internal vacuum upon removal for the aluminum split-mold. Because the neoprene membrane used during the compaction was frequently punctured, a second 25-mil (0.64-mm) thick membrane was externally placed on the specimen. Two rubber O-rings were used to tighten the membrane, at both the cap and base of specimen. Finally, the triaxial chamber and top plate was placed on the base plate. The specimen was then carefully placed in the loading frame.

Prior to applying confining pressure, the axial load piston was brought into contact with the specimen cap to ensure proper seating and alignment of the piston with the cap. During this procedure, extra attention was paid to ensure that the magnitude of the contact (or seating) load did not exceed a corresponding pressure level of 1-2 psi (6.89-13.8 kPa). Next, the confining pressure was applied manually through an air valve. After the air pressure was stabilized, the gage reading was recorded to the nearest 0.5 psi (3.4 kPa). Subsequently, the vacuum was removed from the drainage port of the triaxial cell. All shear strength tests were conducted using an actuator displacement rate of at 0.002-in./sec (0.0051-mm/sec) or 1% axial strain/min after the data acquisition system was readily configured. Figure 3.4 shows the complete setup of triaxial shear strength apparatus with confining pressure of 5 psi (34.5 kPa) applied prior to shearing phase. After the completion of each test, the specimen was weighed and oven-dried for moisture content measurement.

3.7.2 The Concept of Shear Stress Ratio (SSR)

The Shear Stress Ratio (SSR or τ_f / τ_{max}), defined as the ratio between induced shear stress to the shear strength of a particular aggregate material, was used in the current study to establish the stress levels to be used during repeated load permanent deformation testing of the aggregate materials. For an individual stress state, a limiting value of SSR is believed to control the permanent deformation response of unbound aggregate materials (Seyhan and Tutumluer 2002). The fundamental state of stress used in this study was based on Mohr-Coulomb yield criteria. Accordingly, the representation of τ_f / τ_{max} originates from the Mohr-Coulomb failure envelope as illustrated in Figure 3.5. For a certain combination of confining pressure (σ_3) and deviator stress (σ_d) applied during triaxial testing, the mobilized normal pressure and shearing resistance (represented by σ_f and τ_f, respectively) on the potential failure surface (oriented at an angle of 45°+ ϕ /2 with the horizontal) can be computed.

Figure 3.4 Shear Strength Test Setup in Triaxial Cell prior to Shearing Phase

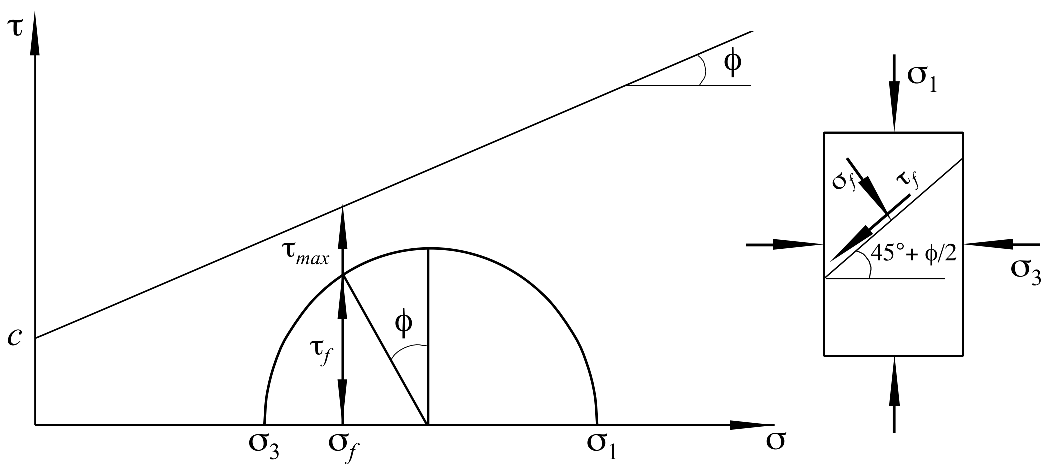

Figure 3.5 Mohr-Coulomb Representation of Shear Strength and Applied Stresses

The applied stress states on the failure plane to compute shear stress ratios in Figure 3.5 can be derived from the following equations:

$$\text{Shear Stress Ratio (SSR)} = \frac{\text{Mobilized Shearing Resistance}}{\text{Shear Strength}} = \frac{\tau_f}{\tau_{\max}} \tag{3.1}$$

$$\sigma_f = \frac{2\sigma_3\,(1 + tan^2\,\phi)\ + \sigma_\mathrm{d}\,(1 + tan^2\,\phi) - \sqrt{\sigma_\mathrm{d}^2\ tan^2\,\phi\,(\,1 +\ tan^2\,\phi)}}{2\,(\,1 +\ tan^2\,\phi)} \tag{3.2}$$

$$\tau_f = \sqrt{(\sigma_\mathrm{d}/2)^2 - [\sigma_f - (\sigma_3 + \sigma_\mathrm{d}/2)]^2} \tag{3.3}$$

where τ_f is the mobilized shearing resistance acting on failure plane; τ_{max} is shear strength obtained through Mohr-Coulomb failure criteria, $\tau_{max} = c + \sigma_f \tan \phi$; σ_f is normal stress acting on failure plane; σ_3 is minor principal stress or confining pressure in this case; σ_d is deviator stress, or $(\sigma_1 - \sigma_3)$; and ϕ is internal friction angle determined from shear strength tests.

The ratio between τ_f and shear strength of the material corresponding to that particular normal stress ($\tau_{max} = c + \sigma_f \tan \phi$) is defined as the Shear Stress Ratio (SSR). Lower SSR values essentially mean that the material is less likely to undergo bearing capacity type shear failure, whereas a unity value of SSR (SSR = 1.0) represents shear failure of the material. Unbound granular materials subjected to SSR values higher than 0.7 have been found to accumulate high permanent strains, ultimately leading to shear failure (Tutumluer et al. 2004; Kim and Tutumluer 2006). This phenomenon can be clearly seen in Appendix E. Noticeably, majority of the granular materials tested at SSR levels of 0.75 exhibits a greater slope at accumulating permanent deformations. Subsequently, it was decided to select SSR values of 0.25, 0.50 and 0.75 to cover the range from low to high states of stress without jeopardizing aggregate specimen failure and equipment damage. Table 3.5 lists the stress states applied to each granular material to achieve SSR values of 0.25, 0.50 and 0.75, representing low, intermediate and high stress states, respectively. Permanent deformation behavior of the granular materials was characterized by conducting repeated load triaxial tests under these three SSR conditions listed in the table.

Table 3.5 Computed Shear Stress Ratio (SSR) Values

	Confining Pressure, σ_3		τ_f / τ_{max} = 0.25				τ_f / τ_{max} = 0.50				τ_f / τ_{max} = 0.75				τ_f / τ_{max} = 1.0			
			σ_f		σ_d		σ_f		σ_d		σ_f		σ_d		$\sigma_{f,\, failure}$		$\sigma_{d,\, failure}$	
	psi	kPa	psi	kPa	psi	kPa	psi	kPa	psi	kPa	psi	kPa	psi	kPa	psi	kPa	psi	kPa
Arrowood	3.0	20.7	4.6	31.7	13.9	95.8	6.7	46.2	31.6	217.7	9.4	64.8	55.1	379.6	13.2	91.2	87.5	603.0
	5.0	**34.5**	**6.9**	**47.5**	**16.0**	**110.2**	**9.3**	**64.1**	**36.4**	**250.8**	**12.4**	**85.4**	**63.3**	**436.1**	**16.8**	**115.5**	**100.6**	**693.2**
	7.0	48.2	9.1	62.7	18.1	124.7	11.8	81.3	41.1	283.2	15.4	106.1	71.6	493.3	20.3	139.9	113.7	783.5
	10.0	68.9	12.5	86.1	21.2	146.1	15.6	107.5	48.2	332.1	19.8	136.4	83.9	578.1	25.6	176.4	133.4	918.8
	15.0	103.4	18.1	124.7	26.4	181.9	22.0	151.6	60.0	413.4	27.2	187.4	104.6	720.7	34.4	237.2	166.1	1144.4
Belgrade	3.0	20.7	3.5	23.8	2.7	18.8	4.0	27.7	6.1	42.3	4.7	32.7	10.5	72.5	5.7	39.3	16.4	112.8
	5.0	**34.5**	**5.7**	**39.1**	**4.1**	**28.1**	**6.5**	**44.9**	**9.2**	**63.1**	**7.6**	**52.4**	**15.7**	**108.3**	**9.0**	**62.3**	**24.5**	**168.5**
	7.0	48.2	7.9	54.4	5.4	37.3	9.0	62.1	12.2	84.0	10.5	72.1	20.9	144.1	12.4	85.3	32.6	224.3
	10.0	68.9	11.2	77.4	7.4	51.2	12.8	88.0	16.7	115.3	14.7	101.6	28.7	197.8	17.4	119.8	44.7	307.9
	15.0	103.4	16.8	115.7	10.8	74.4	19.0	131.1	24.3	167.6	21.9	150.9	41.7	287.3	25.7	177.3	64.9	447.2
Fountain	3.0	20.7	6.0	41.2	16.2	111.8	9.7	66.6	36.4	250.6	14.4	99.0	62.0	427.3	20.6	141.6	95.8	659.9
	5.0	**34.5**	**8.2**	**56.4**	**17.4**	**119.9**	**12.1**	**83.7**	**39.0**	**268.7**	**17.2**	**118.4**	**66.5**	**458.1**	**23.8**	**164.1**	**102.7**	**707.5**
	7.0	48.2	10.4	71.7	18.6	128.0	14.6	100.8	41.6	286.8	20.0	137.9	71.0	488.9	27.1	186.7	109.6	755.1
	10.0	68.9	13.7	94.6	20.3	140.1	18.4	126.4	45.6	313.9	24.2	167.0	77.7	535.2	32.0	220.4	120.0	826.5
	15.0	103.4	19.3	132.7	23.3	160.3	24.6	169.2	52.1	359.1	31.3	215.6	88.9	612.2	40.2	276.7	137.2	945.6
Franklin	3.0	20.7	4.1	28.5	5.2	35.7	5.5	38.1	11.5	79.1	7.3	50.0	19.3	133.3	9.5	65.3	29.4	202.5
	5.0	**34.5**	**6.3**	**43.7**	**6.1**	**41.8**	**8.0**	**54.9**	**13.5**	**92.8**	**10.0**	**68.9**	**22.7**	**156.3**	**12.6**	**86.8**	**34.5**	**237.5**
	7.0	48.2	8.5	58.8	7.0	48.0	10.4	71.7	15.5	106.5	12.7	87.7	26.0	179.3	15.7	108.3	39.5	272.4
	10.0	68.9	11.8	81.5	8.3	57.2	14.1	96.9	18.4	127.0	16.8	116.0	31.0	213.8	20.4	140.5	47.2	324.9
	15.0	103.4	17.3	119.4	10.5	72.6	20.2	138.9	23.4	161.1	23.7	163.1	39.4	271.3	28.2	194.2	59.8	412.3

Table 3.5 Computed Shear Stress Ratio Values (Cont'd)

	Confining Pressure, σ_3		τ_f / τ_{max} = 0.25				τ_f / τ_{max} = 0.50				τ_f / τ_{max} = 0.75				τ_f / τ_{max} = 1.0			
			σ_f		σ_d		σ_f		σ_d		σ_f		σ_d		$\sigma_{f,\ failure}$		$\sigma_{d,\ failure}$	
	psi	kPa	psi	kPa	psi	kPa	psi	kPa	psi	kPa	psi	kPa	psi	kPa	psi	kPa	psi	kPa
Goldhill	3.0	20.7	4.2	28.7	6.1	41.9	5.6	38.7	13.6	93.7	7.4	51.3	23.1	159.2	9.8	67.8	35.6	245.0
	5.0	**34.5**	**6.4**	**44.0**	**7.2**	**49.5**	**8.1**	**55.7**	**16.0**	**110.5**	**10.2**	**70.6**	**27.3**	**187.9**	**13.1**	**90.0**	**42.0**	**289.2**
	7.0	48.2	8.6	59.2	8.3	57.0	10.6	72.7	18.5	127.4	13.0	89.9	31.4	216.6	16.3	112.3	48.4	333.3
	10.0	68.9	11.9	82.0	9.9	68.3	14.3	98.3	22.2	152.7	17.2	118.8	37.7	259.7	21.1	145.7	58.0	399.5
	15.0	103.4	17.4	120.1	12.7	87.2	20.4	140.8	28.3	194.9	24.2	167.0	48.1	331.4	29.2	201.3	74.0	509.9
Hendersonville	3.0	20.7	4.3	29.9	9.2	63.2	6.0	41.6	20.7	142.8	8.2	56.8	35.8	246.4	11.2	77.3	56.1	386.6
	5.0	**34.5**	**6.6**	**45.3**	**10.7**	**74.0**	**8.6**	**59.0**	**24.3**	**167.4**	**11.1**	**76.7**	**41.9**	**288.8**	**14.6**	**100.8**	**65.8**	**453.1**
	7.0	48.2	8.8	60.7	12.3	84.9	11.1	76.3	27.9	192.0	14.0	96.7	48.1	331.2	18.0	124.3	75.4	519.7
	10.0	68.9	12.2	83.7	14.7	101.2	14.9	102.4	33.2	228.8	18.4	126.7	57.3	394.8	23.2	159.6	89.9	619.5
	15.0	103.4	17.7	122.2	18.6	128.4	21.2	145.9	42.1	290.3	25.6	176.7	72.7	500.8	31.7	218.4	114.1	785.8
Jamestown	3.0	20.7	3.8	25.9	4.4	30.3	4.7	32.4	9.9	68.0	5.9	40.7	16.9	116.4	7.5	51.7	26.2	180.7
	5.0	**34.5**	**6.0**	**41.2**	**5.7**	**39.1**	**7.2**	**49.6**	**12.7**	**87.8**	**8.8**	**60.3**	**21.8**	**150.3**	**10.8**	**74.6**	**33.9**	**233.2**
	7.0	48.2	8.2	56.5	7.0	47.9	9.7	66.7	15.6	107.6	11.6	79.9	26.7	184.2	14.1	97.4	41.5	285.8
	10.0	68.9	11.5	79.4	8.9	61.1	13.4	92.5	19.9	137.3	15.9	109.3	34.1	235.0	19.1	131.6	52.9	364.7
	15.0	103.4	17.1	117.6	12.1	83.1	19.7	135.5	27.1	186.8	23.0	158.3	46.4	319.6	27.4	188.7	72.0	496.1
Lemon Spring	3.0	20.7	3.5	24.4	3.1	21.5	4.2	29.0	7.0	48.4	5.1	34.9	12.0	82.8	6.2	42.8	18.6	128.4
	5.0	**34.5**	**5.8**	**39.7**	**4.4**	**30.3**	**6.7**	**46.2**	**9.9**	**68.2**	**7.9**	**54.5**	**16.9**	**116.6**	**9.5**	**65.6**	**26.3**	**181.0**
	7.0	48.2	8.0	55.0	5.7	39.1	9.2	63.4	12.8	87.9	10.8	74.1	21.8	150.5	12.8	88.4	33.9	233.6
	10.0	68.9	11.3	77.9	7.6	52.4	12.9	89.1	17.1	117.6	15.0	103.5	29.2	201.3	17.8	122.6	45.3	312.4
	15.0	103.4	16.9	116.1	10.8	74.4	19.2	132.1	24.3	167.1	22.1	152.5	41.5	286.0	26.1	179.7	64.4	443.9

Table 3.5 Computed Shear Stress Ratio Values (Cont'd)

	Confining Pressure, σ_3		τ_f / τ_{max} = 0.25				τ_f / τ_{max} = 0.50				τ_f / τ_{max} = 0.75				τ_f / τ_{max} = 1.0			
			σ_f		σ_d		σ_f		σ_d		σ_f		σ_d		$\sigma_{f,\,failure}$		$\sigma_{d,\,failure}$	
	psi	kPa	psi	kPa	psi	kPa	psi	kPa	psi	kPa	psi	kPa	psi	kPa	psi	kPa	psi	kPa
Moncure	3.0	20.7	3.4	23.3	3.4	23.8	3.9	26.7	7.9	54.1	4.5	31.2	13.7	94.4	5.4	37.4	21.8	150.4
	5.0	**34.5**	**5.6**	**38.8**	**5.7**	**38.9**	**6.4**	**44.3**	**12.9**	**88.8**	**7.5**	**51.7**	**22.5**	**154.8**	**9.0**	**61.9**	**35.8**	**246.5**
	7.0	48.2	7.9	54.3	7.9	54.1	9.0	62.0	17.9	123.4	10.5	72.2	31.2	215.1	12.5	86.4	49.7	342.6
	10.0	68.9	11.2	77.5	11.2	76.9	12.8	88.4	25.4	175.3	14.9	103.0	44.4	305.7	17.9	123.1	70.6	486.8
	15.0	103.4	16.9	116.1	16.7	114.8	19.2	132.5	38.0	261.8	22.4	154.2	66.3	456.6	26.8	184.4	105.5	727.0
Nash	3.0	20.7	3.7	25.4	4.0	27.3	4.5	31.2	8.9	61.2	5.6	38.7	15.2	104.8	7.1	48.6	23.6	162.7
	5.0	**34.5**	**5.9**	**40.7**	**5.2**	**36.1**	**7.0**	**48.4**	**11.8**	**81.0**	**8.5**	**58.3**	**20.1**	**138.7**	**10.4**	**71.5**	**31.2**	**215.2**
	7.0	48.2	8.1	55.9	6.5	44.9	9.5	65.6	14.6	100.8	11.3	77.9	25.0	172.6	13.7	94.3	38.9	267.8
	10.0	68.9	11.4	78.9	8.4	58.1	13.3	91.3	18.9	130.5	15.6	107.3	32.4	223.4	18.7	128.5	50.3	346.7
	15.0	103.4	17.0	117.1	11.6	80.1	19.5	134.3	26.1	180.0	22.7	156.3	44.7	308.0	26.9	185.6	69.4	478.1
N. Wilkesboro	3.0	20.7	4.1	28.5	8.1	55.8	5.6	38.4	18.3	126.3	7.4	51.3	31.7	218.4	10.0	68.9	49.9	343.6
	5.0	**34.5**	**6.4**	**43.9**	**9.8**	**67.3**	**8.1**	**55.8**	**22.1**	**152.3**	**10.4**	**71.4**	**38.2**	**263.3**	**13.4**	**92.6**	**60.1**	**414.2**
	7.0	48.2	8.6	59.3	11.4	78.7	10.6	73.2	25.9	178.3	13.3	91.5	44.7	308.2	16.9	116.3	70.4	484.8
	10.0	68.9	12.0	82.4	13.9	95.9	14.4	99.4	31.5	217.3	17.6	121.6	54.5	375.6	22.0	151.8	85.7	590.8
	15.0	103.4	17.5	120.8	18.1	124.6	20.7	143.0	41.0	282.2	24.9	171.8	70.8	487.8	30.6	211.0	111.4	767.4
Princeton	3.0	20.7	3.5	23.9	3.8	26.4	4.1	28.0	8.7	60.0	4.9	33.5	15.1	104.2	5.9	40.9	24.0	165.2
	5.0	**34.5**	**5.7**	**39.3**	**5.8**	**39.9**	**6.6**	**45.6**	**13.2**	**90.7**	**7.8**	**53.8**	**22.9**	**157.7**	**9.4**	**65.1**	**36.3**	**250.0**
	7.0	48.2	8.0	54.8	7.8	53.4	9.2	63.1	17.6	121.5	10.8	74.1	30.7	211.2	13.0	89.3	48.6	334.8
	10.0	68.9	11.3	77.9	10.7	73.7	13.0	89.5	24.3	167.7	15.2	104.6	42.3	291.5	18.2	125.6	67.0	462.0
	15.0	103.4	16.9	116.5	15.6	107.6	19.4	133.4	35.5	244.7	22.6	155.5	61.7	425.2	27.0	186.0	97.8	674.0

Table 3.5 Computed Shear Stress Ratio Values (Cont'd)

	Confining Pressure, σ_3		τ_f / τ_{max} = 0.25				τ_f / τ_{max} = 0.50				τ_f / τ_{max} = 0.75				τ_f / τ_{max} = 1.0			
			σ_f		σ_d		σ_f		σ_d		σ_f		σ_d		$\sigma_{f, failure}$		$\sigma_{d, failure}$	
	psi	kPa	psi	kPa	psi	kPa	psi	kPa	psi	kPa	psi	kPa	psi	kPa	psi	kPa	psi	kPa
Raleigh	3.0	20.7	3.7	25.2	4.0	27.3	4.5	30.8	8.9	61.4	5.5	38.1	15.3	105.4	6.9	47.8	23.8	164.0
	5.0	**34.5**	**5.9**	**40.5**	**5.3**	**36.6**	**7.0**	**48.1**	**11.9**	**82.3**	**8.4**	**57.8**	**20.5**	**141.2**	**10.3**	**70.8**	**31.9**	**219.7**
	7.0	48.2	8.1	55.8	6.7	45.9	9.5	65.3	15.0	103.2	11.2	77.5	25.7	177.0	13.6	93.8	40.0	275.5
	10.0	68.9	11.4	78.8	8.7	59.8	13.2	91.2	19.5	134.5	15.5	107.1	33.5	230.7	18.6	128.3	52.1	359.1
	15.0	103.4	17.0	117.1	12.0	83.0	19.5	134.2	27.1	186.7	22.7	156.3	46.5	320.2	27.0	185.8	72.3	498.4
Rockingham	3.0	20.7	4.0	27.4	5.9	40.6	5.2	35.8	13.3	91.4	6.8	46.6	22.8	156.8	8.9	61.0	35.4	244.0
	5.0	**34.5**	**6.2**	**42.7**	**7.2**	**49.9**	**7.7**	**53.0**	**16.3**	**112.3**	**9.6**	**66.3**	**27.9**	**192.6**	**12.2**	**84.0**	**43.5**	**299.7**
	7.0	48.2	8.4	58.0	8.6	59.2	10.2	70.3	19.3	133.2	12.5	86.0	33.1	228.4	15.5	107.0	51.6	355.4
	10.0	68.9	11.8	81.0	10.6	73.1	13.9	96.1	23.9	164.5	16.8	115.6	40.9	282.1	20.5	141.5	63.7	439.0
	15.0	103.4	17.3	119.3	14.0	96.3	20.2	139.2	31.5	216.7	23.9	164.8	53.9	371.6	28.9	199.0	83.9	578.4
Rocky Point	3.0	20.7	3.4	23.3	2.6	17.9	3.9	26.9	6.0	41.3	4.5	31.0	10.3	71.0	5.4	37.0	16.2	111.4
	5.0	**34.5**	**5.6**	**38.7**	**4.2**	**28.9**	**6.4**	**44.1**	**9.5**	**65.5**	**7.4**	**51.0**	**16.5**	**113.7**	**8.8**	**60.5**	**25.8**	**177.9**
	7.0	48.2	7.8	54.1	5.8	40.0	8.9	61.3	13.1	90.3	10.3	71.0	22.6	155.7	12.2	84.0	35.5	244.5
	10.0	68.9	11.2	77.1	8.2	56.5	12.7	87.5	18.5	127.5	14.7	101.3	31.8	219.1	17.3	119.3	50.0	344.3
	15.0	103.4	16.8	115.6	12.1	83.4	19.0	130.9	27.4	188.8	21.9	150.9	47.2	325.2	25.9	178.1	74.1	510.6
Rougemont	3.0	20.7	3.4	23.5	3.4	23.5	3.9	27.2	7.7	53.4	4.7	32.0	13.5	92.7	5.6	38.7	21.3	147.0
	5.0	**34.5**	**5.7**	**39.0**	**5.4**	**37.0**	**6.5**	**44.8**	**12.2**	**84.1**	**7.6**	**52.4**	**21.2**	**146.2**	**9.1**	**62.9**	**33.6**	**231.8**
	7.0	48.2	7.9	54.4	7.3	50.5	9.0	62.3	16.7	114.9	10.6	72.7	29.0	199.7	12.6	87.1	45.9	316.6
	10.0	68.9	11.3	77.6	10.3	70.8	12.9	88.7	23.4	161.1	15.0	103.2	40.6	280.0	17.9	123.3	64.4	443.8
	15.0	103.4	16.9	116.2	15.2	104.7	19.2	132.5	34.6	238.1	22.4	154.1	60.1	413.8	26.7	183.8	95.2	655.8

3.8 REPEATED LOAD TRIAXIAL TESTING FOR PERMANENT DEFORMATION CHARACTERIZATION

After establishing the stress states required to achieve the target SSR values for each aggregate type, repeated load triaxial tests were conducted to characterize the permanent deformation behavior of each aggregate materials. A confining pressure level of 5 psi (34.5 kPa) was selected for the repeated load permanent deformation tests to ensure that deviator stress values required for achieving the target SSR values remained within the equipment limits. All the repeated load permanent deformation tests in this study were conducted using an advanced triaxial testing device, referred to as the University of Illinois FastCell (UI-FastCell), presenting unique capabilities for independent pulsing in the vertical and horizontal directions (Tutumluer and Seyhan 1999). Figure 3.6 shows the setup of repeated load test specimen to the UI-FastCell loading frame for permanent deformation testing.

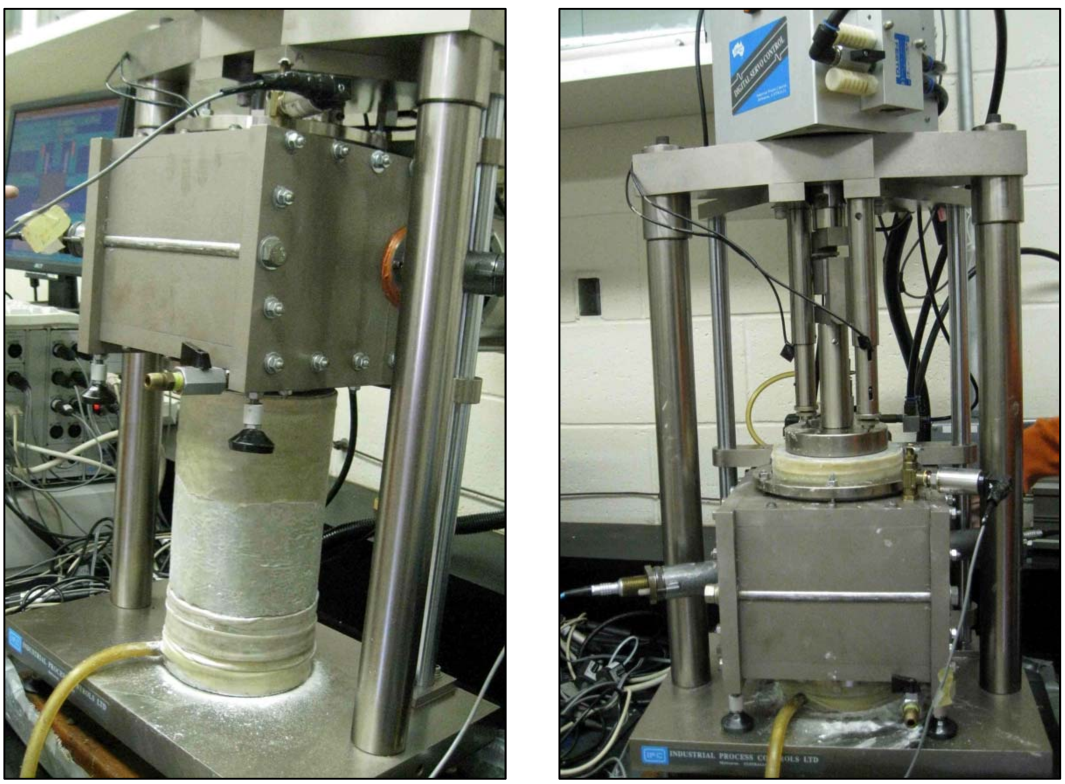

(a) (b)

Figure 3.6 University of Illinois FastCell: (a) Setting up specimen to FastCell loading frame. Internal vacuum is used to help holding the specimen; and (b) Confining cell is lowered to testing position before vacuum line is removed. Note that both axial and lateral LVDTs are used to measure axial and lateral deformations, respectively.

In the UI-FastCell, a pneumatic actuator applies the axial pressure, whereas the confining pressures are cycled through a hydraulic fluid within a rubber membrane. The driving cylinders on the back of the confining cell include an air-fluid interface, which provides “fast” application and switching of the dynamic loading in the confinement “cell.” Some of the unique capabilities are listed as follow:

- Measurement of specimen vertical and radial displacement, and axial force;
- Measurement of pore water pressure in undrained and/or cyclic loading by the use of a pressure transducer, which can be installed in the bottom platen;
- A bladder type horizontal confinement chamber with a built-in membrane, which is inflated to apply variable confining pressure during vertical cyclic loading;
- Ability to independently apply both static and dynamic vertical and radial stresses in phase or out of phase under compression or extension type loadings; and,
- Ability to reverse principal loading direction on the same specimen with applied radial pulse stresses exceeding the vertical ones.

The UI-FastCell cyclic loading system is a customary product of IPC Universal Testing Machine (UTM), a closed-loop servo control material testing machine. The main part of the system consists of loading frame, triaxial cell, air power supply, Control and Data Acquisition System (CDAS), and personal computer with an integrated software package. Within the servo hydraulic and servo pneumatic testing systems used together for horizontal confinement and axial loading, energy is transmitted to the specimen using high-pressure hydraulic fluid through a membrane and high-pressure air acting on a piston, respectively. The CDAS directly controls the servo valves to apply the predefined loading rate or waveform. The associated system transducers, a load cell and LVDTs, measure force and displacement, respectively. While the specimen is being subjected to load, the CDAS captures data from the transducers and transfers the data via a standard serial communication link to a personal computer for processing, display and storage. More details about capabilities of the UI-FastCell can be found elsewhere (Tutumluer and Seyhan, 1999).

3.8.1 Permanent Deformation Test Specimen Preparation

The specimen preparation for permanent deformation tests is similar to the triaxial shear strength test specimen preparation procedure described in the previous section. However, instead of 6-in. (152-mm) in diameter by 12-in. (305-mm) height, the cylindrical permanent deformation test specimens have the dimensions of 150-mm height and 150-mm diameter (approximately 6-in. in diameter by 6-in. high).

Aggregate specimens were prepared using a customized split-mold manufactured with the UI-FastCell. After the assembly of split-mold, a 25-mil (0.64-mm) thick membrane was lined to the bottom platen with an O-ring and the platen was placed in the split-mold. A vacuum line was attached to the mold to hold the membrane tight against the mold. A nonwoven geotextile was placed on top of the bottom platen to prevent the drainage port from being clogged. Aggregate mixture with target moisture content was compacted following the exact specimen preparation procedure as triaxial shear strength test, in three equal lifts. Essentially, with known volume and amount of aggregate material placed in the mold, the target density and moisture content were the MDD and OMC, respectively.

After compaction, the specimen was carefully moved to UI-FastCell loading frame for testing. Internal vacuum was switched from mold to the bottom port to maintain specimen stability. The top platen was then placed on top of the specimen before split-mold was taken apart. A second 25-mil (0.64-mm) thick membrane was placed on the specimen because of punctures during compaction procedure. Seyhan (2002) has reported that using two membranes on the specimen would not produce a significant discrepancy on radial strain measurement even at low stress states. Next, the specimen and the top and bottom platens were placed in the UI-FastCell loading frame, and the loading plate was lowered to make contact with top platen. Seating pressure of 0.3 psi (2.1 kPa) was applied axially. Finally, the UI-FastCell confining cell was lowered down, and confining pressure was applied before internal vacuum was removed.

3.8.2 Permanent Deformation Test Sequence

All the permanent deformation tests were performed at a confining pressure level of 5 psi (34.5 kPa), selected based on the calculated Shear Stress Ratios (SSRs) and equipment capabilities, by applying 10,000 cycles at each stress level using a haversine-shaped load pulse. The haversine load waveform was applied with a load pulse duration of 0.1-sec and a rest period of 0.9-sec. Details on the selection of load cycle was discussed in Section 3.3. Tests at the three stress levels (low, medium and high), i.e. Shear Stress Ratios of 0.25, 0.50 and 0.75, were conducted on three different specimens in single-stage loading. The fourth specimen was tested under multi-stage loading conditions involving the application of a total of 30,000 cycles with consecutively increasing SSR or stress levels (0.25, 0.50, and 0.75, applied sequentially). After the completion of each test, the specimen was weighed and oven-dried for moisture content measurement.

3.9 SUMMARY

This chapter covered the laboratory test matrix that was completed in this research study to investigate the permanent deformation behavior of the 16 different aggregate materials. The following primary factors, established in the past to affect aggregate permanent deformation behavior, were considered in the test matrix:

- Particle shape, texture and angularity;
- Grading;
- Moisture-density relationship;

- Plasticity of fines;
- Shear strength properties; and
- State of stress and stress history.

The sieving, size separation, and material blending to achieve a target specimen gradation ensured that the effects of particle size distribution on aggregate behavior were eliminated from the test matrix. .

CHAPTER 4: TEST RESULTS AND ANALYSES

4.1 INTRODUCTION

The results from the moisture-density tests and the applied stress states on each aggregate material, and their interpretations were given in Chapter 3. This chapter presents results from the imaging-based particle shape characterization and the triaxial tests, which consist of (i) monotonic shear strength tests and (ii) repeated load permanent deformation tests along with the analyses of the test data. Test results are interpreted for significant trends identified in the strength and deformation response in accordance with the developed test matrix, and possible causes for any differences in the aggregate material behavior are discussed.

4.2 PARTICLE SHAPE, TEXTURE AND ANGULARITY TEST RESULTS

The use of a validated image analysis system, the Enhanced-University of Illinois Aggregate Image Analyzer (E-UIAIA), was pursued during the course of this project to give timely consideration to imaging based shape (flatness and elongation), angularity and surface texture property determinations of the selected coarse aggregates (Moaveni et al. 2013). Basic components of the imaging equipment and its principle of operation have already been introduced in Chapter 3. The E-UIAIA based imaging indices for the 16 coarse aggregate materials studied fall into the following two categories: (1) particle sizes, which include maximum, intermediate and minimum dimensions, and volume of the aggregate particle (Tutumluer et al. 2000; Rao 2001); (2) particle morphological or shape indices, which include the Flat and Elongated Ratio (FER) (Rao et al. 2001), Angularity Index (AI) (Rao et al. 2002), and Surface Texture Index (STI) (Rao et al. 2003; Pan et al. 2004). Both categories of these imaging based coarse aggregate shape indices have been validated in the past by measuring aggregate properties using the UIAIA and successfully linking results to corresponding laboratory strength data and field rutting performances (Rao et al. 2002; Pan et al. 2004).

For quantifying the shape and angularity aspects of the 16 aggregate materials studied in this project, 50 particles of each material were analyzed using the E-UIAIA. The Surface Texture Index (STI) and the Angularity Index (AI) were computed using the automated algorithms by Rao et al. (2002 and 2003). The STI and AI can be directly linked to shear strength and permanent deformation properties of the studied aggregates to realistically account for the contributions of crushed and uncrushed particles in the development of aggregate thickness correction factors.

Tables 4.1, 4.2 and 4.3 are average values of AI, STI and FER, respectively, based on selected 50 particles having average sizes of 1.0-in. (25.4-mm) and 0.5-in. (12.5-mm). The shape properties to some level reflect the mineralogical properties of the aggregate particles eventually influenced by the type of crushers used in the quarry production. For both the Belgrade and Rocky Point limestone materials, the AI is high and STI and FER appear to be low. On the other hand, when compared to shear strength properties, stronger materials such as Arrowood, Hendersonville and North Wilkesboro are consistently found to have relatively lower AI, higher STI and higher FER values. The higher STI results are reasonable because rougher surface texture provides higher shearing resistance, and higher FER values may suggest particles are susceptible to crushing or breakage, resulting in denser packing during compaction. However, a correct interpretation of highly angular limestone particles should be associated with the hardness of the particles. Because limestone is often formed from skeletal fragments of marine organisms (i.e. shells), newly crushed stones may produce higher AI values but limestone materials do not generally exhibit higher strength and they are prone to abrasion (rounding) and polishing (smoother texture) under repeated traffic loading

.

Table 4.1 Imaging based Angularity Index (AI) Properties

Quarry	Average AI in Degrees (Particle Size)				
	AI (0.5-in.)	*Std. Dev.*	*AI (1.0-in.)*	*Std. Dev.*	*AI for All Sizes*
Arrowood	384	70	431	96	408
Belgrade	557	113	560	90	558
Fountain	457	91	430	69	444
Franklin	360	78	428	109	394
Goldhill	464	89	463	88	464
Hendersonville	484	91	496	100	490
Jameston	456	80	412	66	434
Lemon Spring	430	73	418	66	424
Moncure	444	88	432	74	438
N. Wilkesboro	439	95	394	73	416
Nash	421	72	389	90	405
Princeton	467	83	458	72	462
Raleigh	426	75	401	81	414
Rockingham	451	77	524	71	488
Rocky Point	497	89	526	114	511
Rougemont	552	85	481	78	516

Table 4.2 Imaging based Surface Texture Index (STI) for Roughness

Quarry	Average STI (Particle Size)				
	STI (0.5-in.)	*Std. Dev.*	*STI (1.0-in.)*	*Std. Dev.*	*STI for All Sizes*
Arrowood	1.710	0.520	2.722	0.969	2.216
Belgrade	1.966	0.572	1.799	0.487	1.883
Fountain	2.794	1.291	1.992	0.857	2.393
Franklin	1.560	0.743	1.946	1.240	1.753
Goldhill	2.381	0.914	2.072	0.775	2.226
Hendersonville	2.588	0.866	2.769	0.871	2.678
Jameston	2.306	0.751	1.597	0.535	1.951
Lemon Spring	1.698	0.501	1.847	0.955	1.773
Moncure	1.899	0.721	1.471	0.408	1.685
N. Wilkesboro	2.382	1.032	1.611	0.546	1.997
Nash	2.179	0.644	1.636	0.808	1.908
Princeton	2.468	0.883	2.229	0.789	2.348
Raleigh	2.684	1.022	2.035	0.710	2.360
Rockingham	1.877	0.498	2.401	0.724	2.139
Rocky Point	1.960	0.575	1.906	0.686	1.933
Rougemont	2.805	1.297	2.686	1.113	2.746

4.3 RESILIENT MODULUS TEST RESULTS

As described in Chapter 3, resilient modulus (M_R) tests were performed in accordance with AASHTO T307-99 procedure at the NCDOT Material and Tests Unit. Unlike permanent deformation behavior, resilient response of granular materials is quite well studied and directly related to a given state of stress applied on the specimen. Resilient modulus test results, as provided in Appendix C, were fitted with two commonly used resilient modulus models: (1) K-θ Model (Hicks and Monismith 1971) and (2) MEPDG Model (Ayres 2002; NCHRP 1-37A study), to compare the differences in model performances:

K-θ Model: $$M_R = K\,\theta^n \qquad (4.1)$$

MEPDG Model: $$M_R = K_1\, p_a \left(\frac{\theta}{p_a}\right)^{K_2} \left(\frac{\tau_{oct}}{p_a} + 1\right)^{K_3} \qquad (4.2)$$

where bulk stress $\theta = \sigma_1 + \sigma_2 + \sigma_3$; σ_d is deviator stress; σ_3 is confining pressure; p_a is atmospheric pressure (14.7 psi or 101.3 kPa); octahedral stress, $\tau_{oct} = \sqrt{2}/3 * \sigma_d$; n, K, K_1, K_2 and K_3 are model parameters. The resulting model parameters for both resilient modulus models are listed in Table 4.4. Both models fit very well to the resilient modulus data, with coefficient of determination (R^2) values often exceeding 0.990.

Table 4.3 Imaging based Flatness and Elongation Ratio (FER)

Quarry	Average FER (Particle Size)				
	FER (0.5-in.)	*Std. Dev.*	*FER (1.0-in.)*	*Std. Dev.*	*FER for All Sizes*
Arrowood	2.470	0.730	2.628	0.731	2.549
Belgrade	1.884	0.399	1.834	0.392	1.859
Fountain	3.001	0.975	2.667	0.956	2.834
Franklin	2.373	0.773	2.257	0.722	2.315
Goldhill	2.442	0.867	2.307	0.581	2.375
Hendersonville	2.528	0.702	2.479	0.807	2.504
Jameston	2.336	0.626	2.239	0.471	2.287
Lemon Spring	2.557	0.896	2.355	0.631	2.456
Moncure	2.340	0.608	2.049	0.581	2.194
N. Wilkesboro	2.767	0.900	2.519	0.786	2.643
Nash	2.792	0.825	2.343	0.668	2.567
Princeton	2.484	0.901	2.299	0.789	2.392
Raleigh	2.897	0.862	2.580	0.784	2.739
Rockingham	2.103	0.527	1.876	0.471	1.990
Rocky Point	2.119	0.564	1.829	0.386	1.974
Rougemont	2.478	0.848	2.667	0.855	2.573

Figures 4.1(a)-(d) represent resilient modulus trends of each material subjected to a confining pressure level of 5 psi (34.5 kPa) at SSR values of 0.25, 0.50, and 0.75. The 5-psi confining pressure was selected to compare the results from various models mainly because 5-psi was the only confining pressure used while conducting the permanent deformation tests. It is apparent, overall, that the differences between the predicted resilient modulus values are insignificant for both models. As clearly shown in the figures, Arrowood material has the highest resilient modulus values. On the contrary, resilient modulus values were the lowest for Fountain and Rougemont materials at the same stress state. This is true for all deviator stresses, and becomes much more noticeable for the high Shear Stress Ratio (SSR = 0.75), or deviator stress. This is believed to be an indication of material quality. Later on, the analysis of permanent deformation response (see Figure 4.5) indicated that higher resilient moduli tended to produce lower permanent deformation at a given stress state. However, the difference in permanent deformation is not sensitive to the magnitude of resilient modulus. Take 15 psi (103.4 kPa) deviator stress as an example, approximated permanent strains of Arrowood (0.3%), Belgrade (0.6%), Hendersonville (0.6%), and Fountain (0.7%) materials can be traced back to the decreasing resilient modulus trends [i.e. Arrowood (26 ksi), Hendersonville (22 ksi), Belgrade (17 ksi), Fountain (14 ksi)] from Figure 4.1. Permanent strains of Hendersonville and Belgrade were minuscule, but the resilient modulus of both

materials varied by 5 ksi, suggesting that the resilient modulus property is not affecting significantly the permanent deformation predictions.

Table 4.4 Resilient Modulus Model Parameters obtained from Regression Analyses

Quarry	K-θ Model			MEPDG 1-37A Model			
	K	n	R^2	K_1	K_2	K_3	R^2
Arrowood	3.50E+03	0.586	0.998	1.16E+03	0.611	-0.027	0.999
Belgrade	1.95E+03	0.707	0.992	8.57E+02	0.611	0.105	0.997
Fountain	9.90E+02	0.756	0.999	5.11E+02	0.740	0.018	0.999
Franklin	1.50E+03	0.734	0.995	7.23E+02	0.672	0.068	0.996
Goldhill	2.08E+03	0.648	0.997	8.14E+02	0.652	-0.004	0.998
Hendersonville	1.59E+03	0.701	0.999	7.16E+02	0.711	-0.011	1.000
Jamestown	2.41E+03	0.625	0.997	8.75E+02	0.597	0.031	0.997
Lemon Spring	2.23E+03	0.637	0.996	8.29E+02	0.589	0.053	0.997
Moncure	2.47E+03	0.632	0.992	8.86E+02	0.542	0.091	0.997
Nash County	6.04E+02	0.994	0.989	6.10E+02	1.018	-0.027	0.990
N. Wilkesboro	2.90E+03	0.587	0.998	9.68E+02	0.609	-0.024	0.999
Princeton	1.48E+03	0.737	0.992	7.25E+02	0.681	0.062	0.993
Raleigh	2.50E+03	0.628	0.993	9.52E+02	0.713	-0.093	0.997
Rockingham	2.00E+03	0.659	0.996	8.20E+02	0.721	-0.067	0.998
Rocky Point	1.94E+03	0.730	0.994	9.41E+02	0.703	0.029	0.994
Rougemont	1.18E+03	0.725	0.994	5.71E+02	0.730	-0.006	0.994

For a given granular material, an average resilient modulus is computed from the two M_R models for a specified stress state. The M_R values of the granular materials are exclusively used in the analysis by the Pavement ME Design program directly influencing the rutting damage model predictions as outlined in Chapter 2. Whereas, a newly proposed permanent deformation model in this study will incorporate both shear strength properties and applied stress states for predicting rutting in an unbound aggregate base course (Chapter 5).

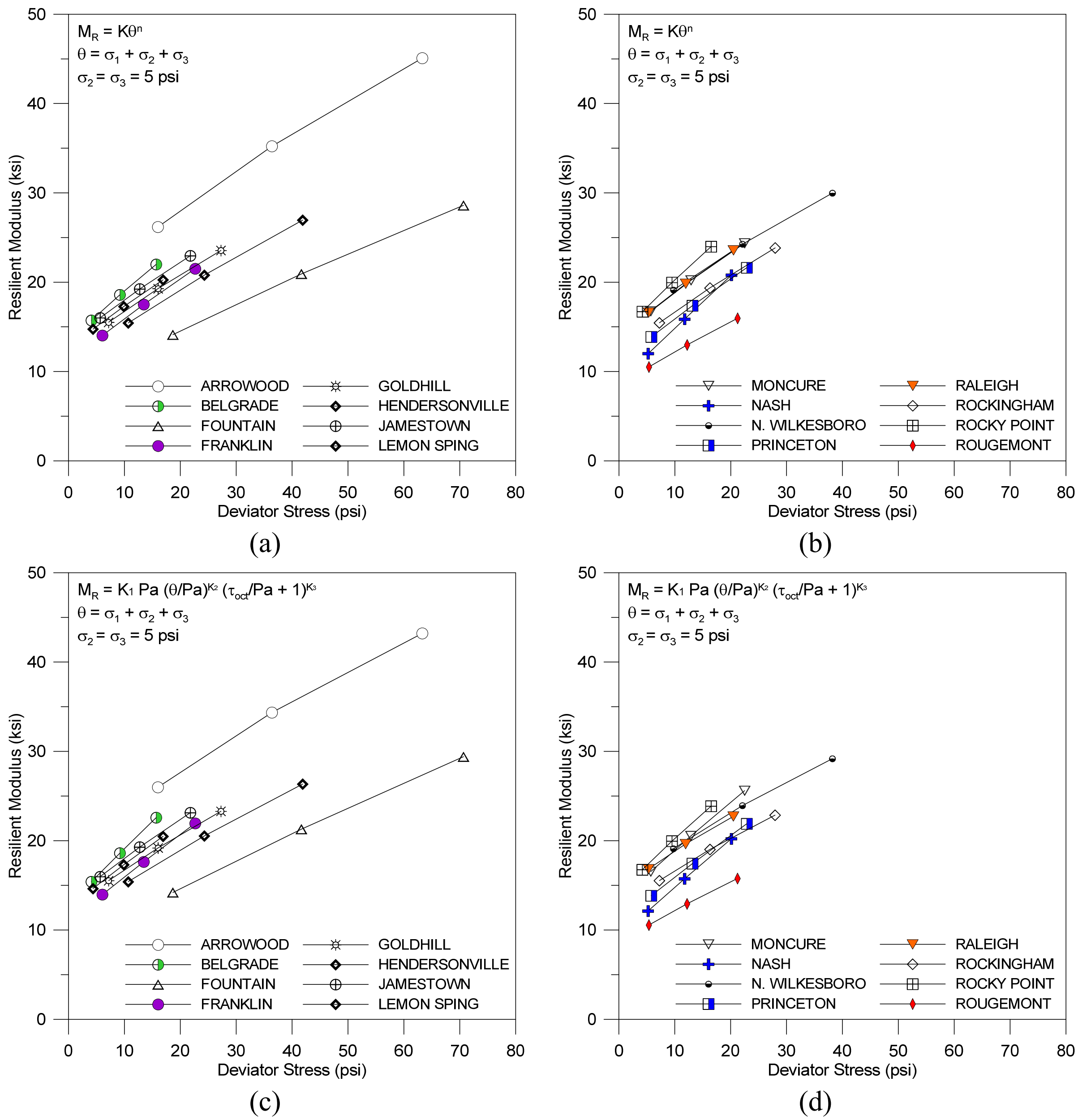

Figure 4.1 Resilient Modulus Plotted at Three States of Stress of Permanent Deformation Testing for Each Granular Material: (a)-(b) K-θ Model and (c)-(d) MEPDG NCHRP 1-37A Model. Each of the Three Data Points Represents Stress States at SSR of 0.25, 0.50 and 0.75 at 5 psi Confining Pressure

4.4 SHEAR STRENGTH TEST RESULTS

Monotonic shear strength tests were conducted for the 16 aggregate materials by compacting specimens under OMC-MDD conditions to establish the shear strength properties. All triaxial compression tests were performed in accordance with the procedure described in Chapter 3, at the Illinois Center for Transportation. The peak deviator stress values recorded at specimen failure can be used as an indicator to evaluate the shear strength behavior of an aggregate sample for comparison purposes. The significant trends observed in the strength behavior of all studied granular materials are reported in this section.

Stress-strain plots established from shear strength testing of all 16 aggregate materials are presented in Appendix B. The majority of the stress-strain curves are qualitatively similar to that of dense sand, which exhibits a well-defined peak value then a decrease after the peak, post-peak softening. The peak stress value or the deviator stress at failure for a given confining pressure was used to interpret friction angle (ϕ) and cohesion intercept (c) values of the tested granular materials. The shear strength properties are summarized in Table 4.5.

Almost all the aggregate materials tested in this study had friction angles ranging from 40-50 degrees. Notably, Arrowood and Moncure materials exhibited the two highest friction angles of 50 degrees. In contrast, the lower end friction angle values from mid to high 30 degrees correspond to Fountain, Franklin, and Goldhill materials. In spite of having the second highest dry density (151.5 pcf), Franklin material exhibited the lowest friction angle. Additional tests were repeated at the same confining pressure to confirm the results. Note that although the Fountain material has a lower friction angle, the high cohesion intercept value as obtained from the linear interpretation suggests the material exhibits high shear strength in accordance with Equation (4.1). The friction angle values ranging from 40 to 50 degrees are reasonable for base course granular materials when compared to drained friction angles of around 45 degrees for dense, well-graded, and angular granular soils (Terzaghi et al. 1996).

Figures 4.2 and 4.3 present for all the tested materials the linear Mohr-Coulomb failure envelopes computed from Equation (4.3) using the strength properties listed in Table 4.5. It becomes distinguishable that Arrowood, Fountain, Hendersonville and North Wilkesboro materials exhibit the highest shear strength at any given normal stress at failure. On the other hand, Belgrade, Franklin, Goldhill and Rocky Point materials are much weaker. Note that the linearly interpolated c and ϕ may not be definite in representing the strength properties of the test aggregate materials. Alternatively, ϕ_{sec} values are also provided to better differentiate the strength trends. For the purpose of this study, Arrowood and Belgrade materials are selected for comparison and subsequent analyses in this report.

Table 4.5 Shear Strength Properties of the Aggregate Materials

Quarry	Friction Angle, ϕ	ϕ_{sec}[a]	Cohesion, c	
	(degree)	(degree)	(psi)	(kPa)
Arrowood	50.2	65.2	12.4	85.1
Belgrade	41.8	42.5	0.9	6.5
Fountain	39.3	66.9	23.3	139.4
Franklin	34.1	51.1	5.8	39.9
Goldhill	37.7	50.5	6.3	43.6
Hendersonville	45.3	59.4	8.6	59.4
Jamestown	41.2	49.4	3.4	23.3
Lemon Spring	41.4	46.6	1.6	11.3
Moncure	50.6	47.1	0.2	1.1
Nash County	41.4	51.2	2.8	19.1
N. Wilkesboro	46.0	58.0	7.0	48.0
Princeton	49.1	45.3	1.0	7.1
Raleigh	42.3	51.1	2.6	17.9
Rockingham	41.7	54.3	5.2	35.7
Rocky Point	44.9	42.4	0.3	2.4
Rougemont	48.8	51.3	0.5	3.7

[a] ϕ_{sec} values reported here were interpreted from shear strength tests at 5-6 psi confining pressure by drawing the secant Mohr-Coulomb envelope from the origin.

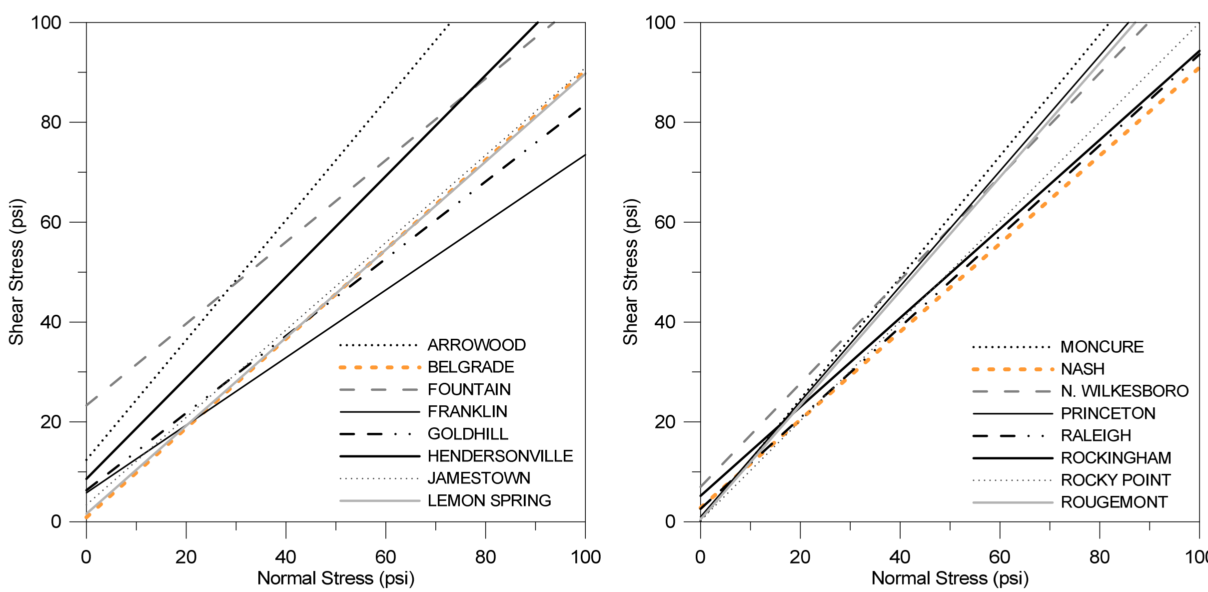

Figure 4.2 Interpretation of Linear Mohr-Coulomb Failure Envelope

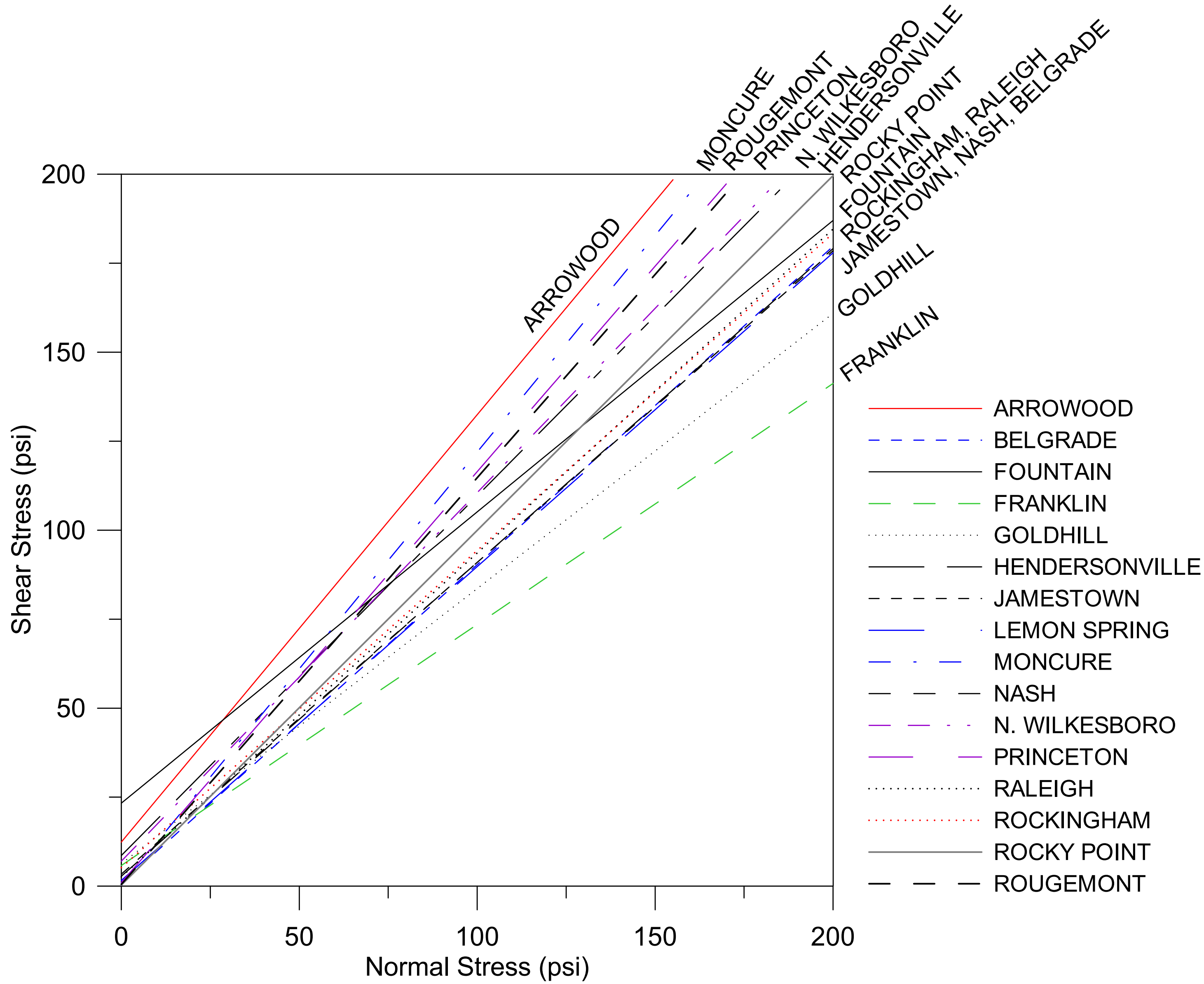

Figure 4.3 Mohr-Coulomb Failure Envelopes of all the Tested Aggregate Materials

4.4.1 Determination of Shear Strength Properties: *c* and ϕ

There are many methods to interpret strength properties (i.e. *c* and ϕ) of granular materials from triaxial test data. In this study, the Mohr-Coulomb yield criteria were based on the overall development of the plastic deformation model. The Mohr-Coulomb failure criteria assume a simplified linear relationship between shear and normal stresses:

$$\tau_{max} = c + \sigma_f \tan \phi \tag{4.3}$$

where τ_{max} is shear strength of material; σ_f is normal stress at failure; *c* is cohesion intercept; and ϕ is internal friction angle. The tensile strength of a material is usually controlled by cohesion intercept (*c*), which is a constant and often varies with the size of particles (i.e. fine-grained soils) and suction (as a function of moisture content) in unsaturated soils. Note that the dilatational behavior of granular soils under triaxial states of stress results in a nonlinear Mohr-Coulomb failure envelope. However, for simplifications, this study assumes the validity of a linear Mohr-Coulomb failure envelope, and hence, the friction angle (ϕ) and cohesion intercept (*c*) values presented in Table 4.5 were computed by establishing a linear regression relation following Equation (4.4).

$$\sigma_{1,f} = a + b\,\sigma_3 \tag{4.4}$$

where $\sigma_{1,f}$ is major principal stress at failure; σ_3 is confining pressure, or minor principal stress; and, *a* and *b*, which are the constant and slope from the regression line, were used to determine ϕ and *c* of granular material from the two following equation:

$$c = \frac{a}{2\sqrt{b}} \tag{4.5}$$

$$\phi = \sin^{-1}\left(\frac{b-1}{b+1}\right) \tag{4.6}$$

For simplicity, cohesion intercept and friction angle values as determined from Equations (4.5) and (4.6) were used to compute Shear Stress Ratio components such as τ_{max}, τ_f, and σ_f in Section 3.7.2.

Essentially, a minimum of three test results at different confining pressures (i.e. 5 psi, 10 psi and 15 psi) needs to be plotted to give the linear equation between minor and major principal stresses at failure. In order to obtain a more representative ϕ and *c* values, additional shear strength tests, e.g. for Franklin material, were repeated to produce a minimum coefficient of determination (R^2) value of 0.90. Accordingly, the R^2 values were found to fall within the range of 0.89 to 0.99 for 15 granular materials, except that Fountain material has the lowest R^2 value of 0.81 after conducting seven shear strength tests at various confining pressures.

Secant friction angle, or symbolically termed as, ϕ_{sec} has been alternatively used in this research study to establish the relationship of shear strength in granular soils. The primary advantage of using ϕ_{sec} is to better evaluate friction angles of different granular materials without the influence of linearly interpolated cohesion intercept. All ϕ_{sec} values reported in this report were based on triaxial shear strength test results at 5-6 psi (34.5-41.3 kPa) confining pressure, and helped to compare permanent deformation trends for the tests conducted at the same confining pressure. Fundamentally, Equation (4.7) to compute ϕ_{sec} comes from Rankine states of plastic equilibrium. According to this equation, the ratio between major and minor principal stresses in a cohesionless material cannot exceed the value:

$$\tan^2\left(45+\frac{\phi_{sec}}{2}\right)=\frac{\sigma_{1,f}}{\sigma_3} \tag{4.7}$$

where $\sigma_{1,f}$ is peak normal stress at major principal direction and σ_3 is minor principal stress or confining pressure of 5-6 psi (34.5-41.3 kPa) from laboratory shear strength tests. Secant friction angles values are reported in Table 4.5.

4.4.2 Correlations between Dry Density and Friction Angle

A vast amount of studies have concluded that soil-aggregate strength properties are directly related to void ratio, particle shape and surface roughness, grading, moisture content, particle size and stress history. Void ratio, related to density of granular materials, is the single most important parameter that affects aggregate material strength. Generally, increasing void ratio (or density), particle angularity and surface roughness, and coefficient of uniformity (C_u) resulted in an increase in the friction angle ϕ while higher moisture content tends to reduce ϕ (Terzaghi et al. 1996).

In this study, gradation was engineered to follow a mid-spec gradation curve. Subsequently, Figure 4.4 highlights a low correlation coefficient between the maximum dry densities and the secant friction angles of the tested aggregate materials. Secant friction angle (ϕ_{sec}) was used in the comparison to better understand the dense-graded granular material behavior when subjected to shear. Each hollow circle in Figure 4.4 represents secant friction angle and the corresponding maximum dry density for one aggregate material as interpreted from the shear strength tests at 5-6 psi (34.5-41.3 kPa) confining pressure. In conclusion, the shear strength test results are in strong agreement with the density results; higher dry density exhibits higher friction angle.

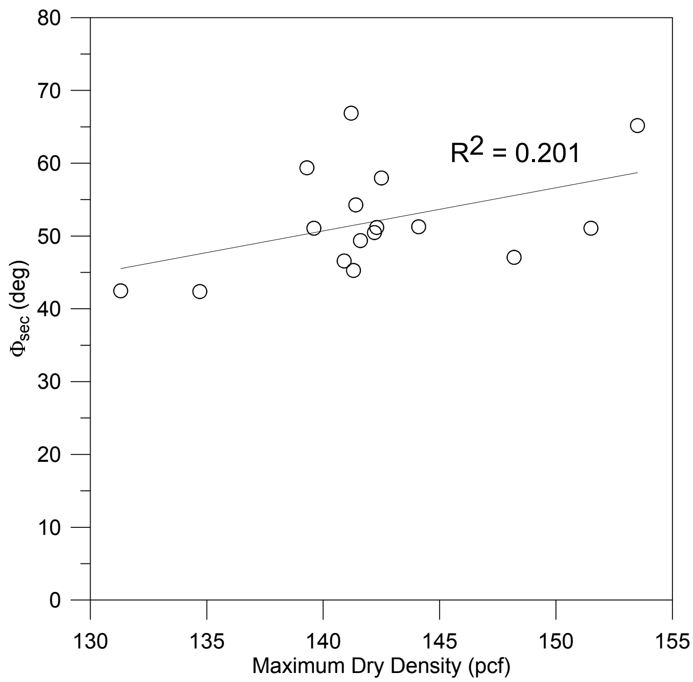

Figure 4.4 Maximum Dry Densities Graphed with Secant Friction Angles (ϕ_{sec}) of the Tested Aggregate Materials

4.5 PERMANENT DEFORMATION TEST RESULTS

As already discussed in Chapter 3, permanent deformation tests were conducted by subjecting the triaxial cylindrical samples to 10,000 cycles of haversine type dynamic pulse loading applied at 0.1-sec with a 0.9-sec rest period at confining pressure of 5 psi (34.5 kPa) at three Shear Stress Ratios (SSRs), as shown in Table 3.5 for each material. In addition, a multi-stage permanent deformation testing was also performed at each of the Shear Stress Ratios up to a total of 30,000 cycles.

4.5.1 Multi-Stage Permanent Deformation Test Results

All multi-stage permanent deformation test results are included in Appendix D. As depicted in the figures, the stress history effect is significant when evaluating the permanent deformation response of unbound materials under increasing applied stresses. From Table 4.6, it appears that the rapid increase in deformation occurs at the first hundreds of load cycles during the first stage of loading. Subsequently, the second and third stages of loading accumulated much less deformation in each of the 10,000 cycles. This behavior seems to be influenced primarily by the applied stress states, SSR levels and accordingly, the stress history. Note that Arrowood, as an example for strong material, accumulated 0.62% strain after second-stage loading, followed by 0.30% after the third stage loading. Whereas, weaker Rocky Point exhibited differences of 0.31% and 0.11% during second and third stages of loading, respectively. More interestingly, Goldhill material with plastic fines initially accumulated very large deformation followed by relatively mild accumulation at consecutive stress levels. This was believed to be the cause of densification and particle rearrangement during the early stage loading. In addition to stress history effects, the differences between the two stages are about 2-3 times (i.e. 0.31% ÷ 0.11% = 2.82) less than the preceding stages at 25% increment in the stress/strength level. Even Goldhill material with plastic fines showed identical response of about 3 times less deformation than the previous loading, in spite of being arguably the weakest material amongst all tested materials. This observation may suggest the densification from the preceding loading is crucial in predicting permanent deformation, or it is evident that permanent deformation accumulation is "restarted" whenever higher load is applied. Accordingly, in order to obtain comparable data to eliminate the effect of stress history, permanent strains from the first 10,000 cycles were only included in the later analyses.

Table 4.6 Permanent Strain Accumulated at Individual Stage of Multi-Stage Loading

Quarry	Permanent Strain per 10,000 Cycle (%)				
	Stage - Shear Stress Ratio (SSR)				
	I - 0.25	*Difference (II-I)*	*II - 0.50*	*Difference (III-II)*	*III - 0.75*
Arrowood	0.50	0.62	1.11	0.29	1.41[a]
Belgrade	0.18	0.44	0.62	0.20	0.82
Fountain	0.86	0.97	1.84	0.41	2.24[b]
Franklin	0.24	0.27	0.52	0.06	0.58
Goldhill	1.37	0.50	1.87	0.15	2.02
Hendersonville	0.54	0.75	1.29	0.33	1.62
Jamestown	0.32	0.51	0.83	0.14	0.97
Lemon Spring	0.15	0.28	0.43	0.08	0.51
Moncure	0.24	0.50	0.74	0.18	0.91
Nash County	0.24	0.47	0.71	0.17	0.88
N. Wilkesboro	0.40	0.28	0.68	0.05	0.72
Princeton	0.18	0.31	0.50	0.11	0.61
Raleigh	0.20	0.35	0.55	0.09	0.64
Rockingham	0.26	0.68	0.94	0.24	1.19
Rocky Point	0.17	0.31	0.48	0.11	0.59
Rougemont	0.25	0.58	0.83	0.22	1.04

[a] Achieved SSR level of 0.68
[b] Achieved SSR level of 0.67

4.5.2 Single-Stage Permanent Deformation Test Results

Detailed permanent deformation responses from the single-stage tests are presented in Appendix E to clearly indicate that the accumulation of permanent deformation is proportional to increasing stress/strength levels. Notably, Arrowood and Fountain materials could not be tested at a SSR level at 0.75, as deviator stresses required to achieve an SSR value of 0.75 exceeded the equipment capabilities. Therefore, the test results for Arrowood and Fountain materials correspond to SSR values of 0.68 and 0.67, respectively. Figure 4.5 combines the single-stage and the first 10,000 cycles of multi-stage permanent deformation test results. Each data point represents low, intermediate and high SSR levels; in addition, multistage-stage low SSR level results are also given. Note that permanent strains recorded for Goldhill material (top right figure) as 3.25% and 5.14% at SSR levels of 0.50 and 0.75, respectively, are out of the 2.5% range as plotted. In general, it can be observed from Figure 4.5 that higher applied deviator stress or stress/strength level produces higher permanent deformations. This relationship appears to be fitted well with linear approximation.

From Figure 4.5, it also appears that weaker materials such as Belgrade and Rocky Point materials accumulated low levels of permanent strain, 0.6% and 0.5%, respectively, even at an SSR level of 0.75. However, this is in contradiction with the results from the shear strength tests, which consistently indicated lower peak deviator stress values at failure for both materials (see Table 3.5 and Figure 4.2). Note that SSR values are calculated using material shear strength properties, and therefore, for a material with lower shear strength, a reasonable low deviator stress value may correspond to a significantly high SSR value. Accordingly, even a high SSR value of 0.75 corresponds to quite low peak deviator stresses at failure for Belgrade and Rocky Point materials. In conclusion, SSR alone may not be used as the sole variable but instead the magnitude of applied deviator stress also needs to be taken into account when comparing the permanent deformation accumulation in unbound materials.

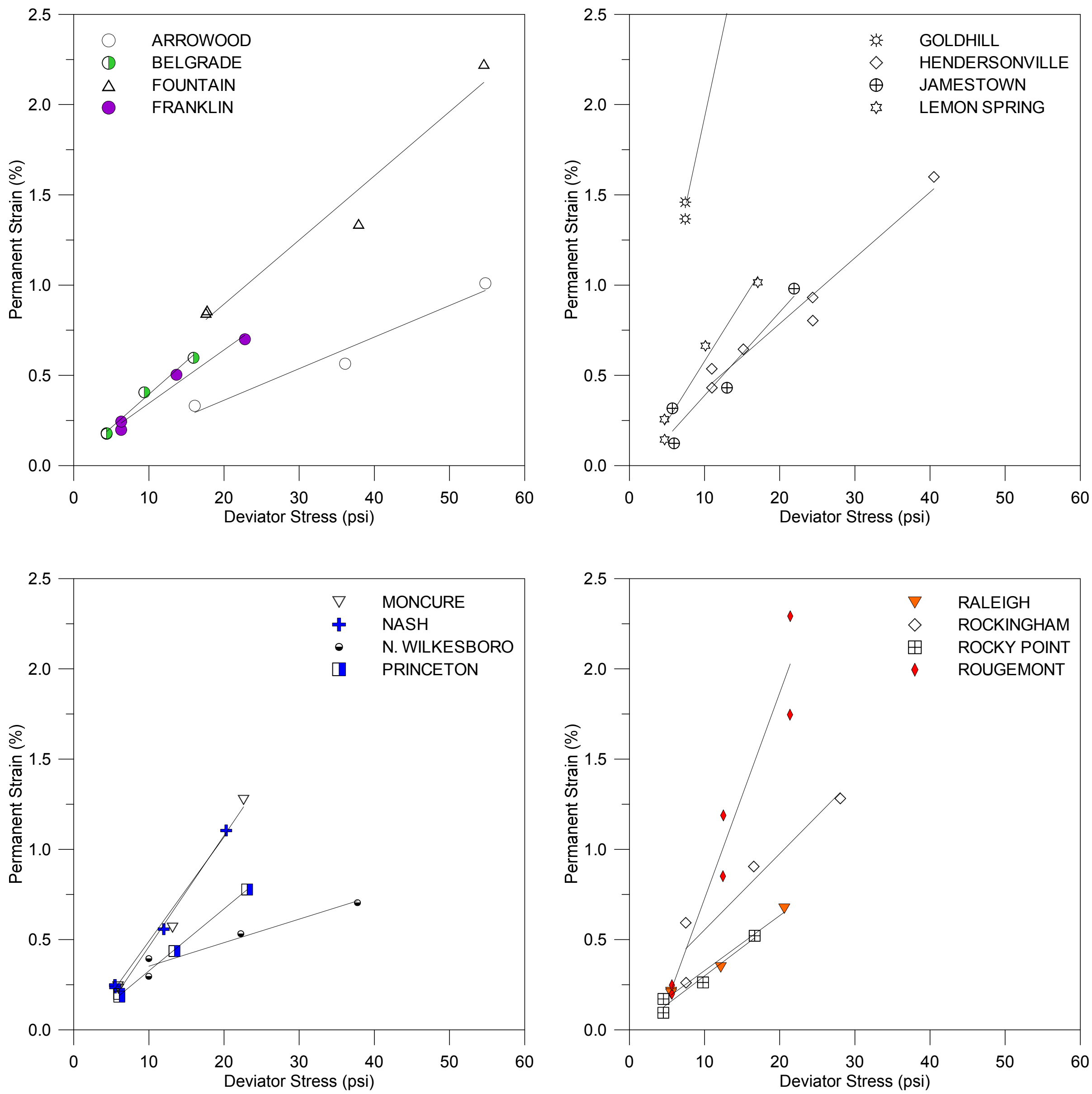

Figure 4.5 Relationships between Permanent Strain and Applied Deviator Stress

Goldhill material has plastic fines reported earlier with a Plasticity Index of 6%. Although the as-received Goldhill material had only 2.5% passing No. 200 sieve (75-μm) fines, the tested specimens were engineered to contain 8% fines. Accordingly, as clearly shown in Figures 4.5 and 4.6, exceptionally high permanent strains were recorded for Goldhill material, greater than 3% and 5% after 10,000 loading cycle at the intermediate and high stress/strength levels, respectively. When these results are compared to the stress-strain relationships at 5 psi (34.5 kPa) confinement, the tested specimen was likely to have undergone shear failure under such heavy loading, resulting in very high plastic deformation.

To conclude, granular materials with plastic fines perform quite poorly in rutting resistance, which is in good agreement with the recent findings by Mishra and Tutumluer (2012).

Figure 4.6 presents permanent strain data for all the materials plotted with applied deviator stress representing low, intermediate and high stress/strength (SSR) levels. This figure can be used to determine for any material the approximate value of permanent deformation recorded at a known stress state. For instance, at 5 psi confining pressure and 15 psi deviator stress, Arrowood, North Wilkesboro and Rocky Point materials accumulated the lowest permanent strains. In contrast, Goldhill, Rougemont and Rockingham materials accumulated the highest permanent strains. Note that although Rocky Point seems to perform better than other stronger materials, its corresponding stress state yields a high stress/strength or SSR level. Further increase in applied stress is expected to produce larger permanent strains and accordingly, the Rocky Point would approach failure condition. In other words, if used in a granular base layer, Rocky Point material would not survive under, e.g., 30 psi applied wheel load deviator stress values (greater than SSR=100%), whereas, for Arrowood material, this load level would only generate quite low and stable permanent strains due to a lower than SSR=50% applied stress to strength ratio.

Figure 4.7(a)-(c) present the imaging based aggregate shape indices in comparison to the 10,000th cycle permanent deformations from repeated load triaxial tests. Figure 4.7(a) suggests that granular materials with higher strength (i.e. Arrowood and North Wilkesboro) do not necessarily possess higher AI, but they consistently exhibit higher STI or rougher surfaces. In spite of low AI, Arrowood and North Wilkesboro materials produced quite low permanent strains. It also becomes apparent that permanent strains of materials with STI of less than about 2.00 are relatively intermediate in performance. Note that these granular materials also have intermediate strength properties. Whereas much stronger materials, such as Hendersonville, Arrowood, North Wilkesboro and Fountain, were observed to have higher FER values; this may be as a result of the type of crushers used during quarry production and much less breakage experienced by the stronger rock mineralogy, such as granites and basalts. On the other hand, Figure 4.7(c) presents both Belgrade and Rocky Point materials to have lower FER values of 1.859 and 1.974, respectively. This could be due to the fact that weaker limestone particles tend to break more easily during transport even if they might be produced more flat and elongated during quarry production.

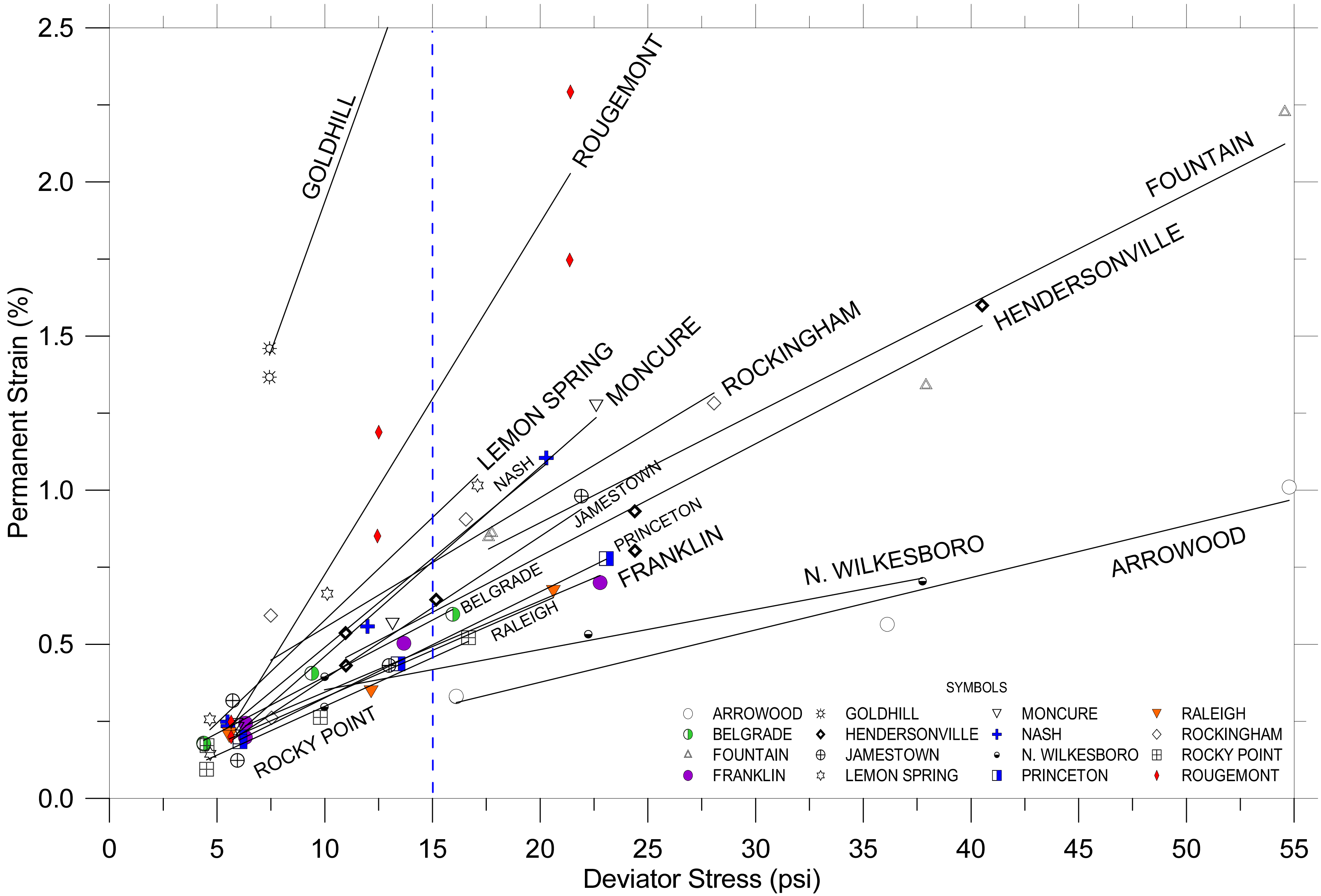

Figure 4.6 Permanent Strain Responses from Single-stage Tests after 10,000 Cycles (5 psi Confining Pressure)

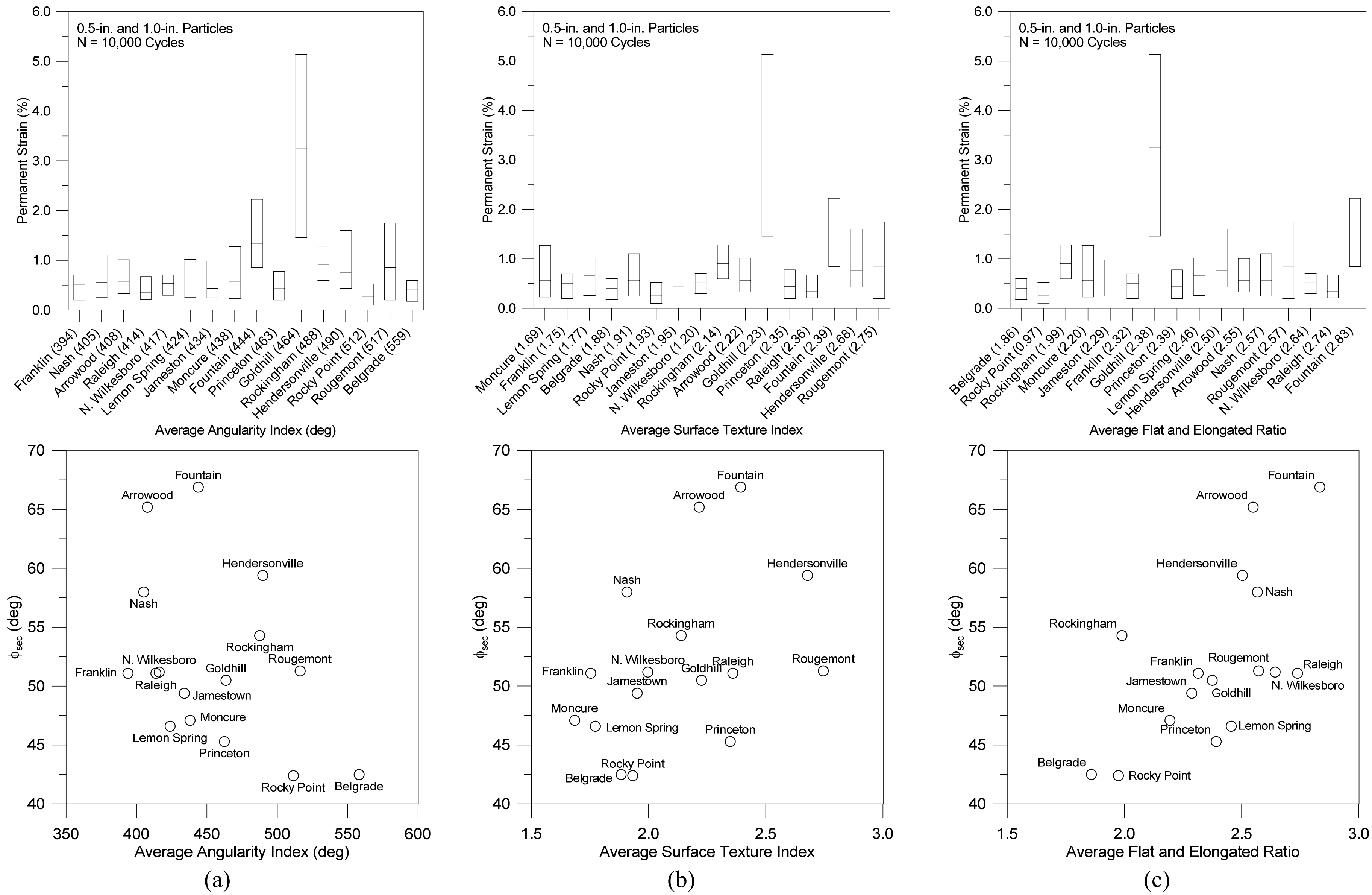

Figure 4.7 Comparisons between Imaging based Aggregate Shape Indices and Permanent Deformation: (a) AI; (b) STI; and (c) FER

4.6 SUMMARY

All resilient modulus, aggregate imaging, shear strength and permanent deformation test results were critically reviewed and discussed in this chapter. The findings of noteworthy trends in the generated test results are summarized as follows:

- Friction angle (ϕ) and cohesion intercept (c) were determined through a regression analysis type linear interpolation method based on peak stresses at different confining pressures. Secant friction angle (ϕ_{sec}), slope of the line extended from the origin to the tangent point of the Mohr circle for 5-psi confining pressure, has shown better correlations with density for the strength properties of granular materials.
- Both multi-stage and single-stage permanent deformation test results showed convincing arguments that permanent deformation response is stress dependent.
- In multi-stage tests, permanent strains accumulated in the second and third stages were observed to be 2-3 times less than the accumulated values in the preceding 10,000 cycle with only 25% increment in the stress/strength level between the different stages;
- In single-stage tests, the accumulated permanent strains after 10,000 cycles exhibited a linear relationship with applied deviator stress levels for all the sixteen granular materials tested.
- Goldhill material with plastic fines (i.e. PI = 6) produced undesirable high permanent deformation.
- Imaging based shape, texture and angularity analysis was performed on two particle sizes (1.0-in. and 0.5-in.) for all the sixteen aggregate materials. Aggregate particles from weaker granular materials (i.e. limestone) were observed to have high AI, low STI and low FER values. On the other hand, aggregate particles from stronger granular materials were found to have lower AI, but higher STI and FER values. The particle shape properties were likely to be influenced by the aggregate mineralogy and the type of crusher used during aggregate production.

CHAPTER 5: RECOMMENDED DESIGN APPROACH FOR PAVEMENT UNBOUND AGGREGATE BASE LAYER

5.1 INTRODUCTION

Several of the currently available permanent deformation predictive models and their dependencies on the applied stress states were clearly highlighted in Chapter 2. Similarly, the permanent deformation characteristics of the sixteen unbound aggregate materials tested in the current study were found to be highly dependent on the applied load levels (see Chapter 4). Any allowable deformation before reaching shear failure in the tested specimens was directly related to the shear strength of material, hence, the fundamental mechanical property of granular soils. On the contrary, the rutting damage model implemented in the MEPDG and the Pavement ME Design approach does not incorporate the effects of shear strength or applied stress states for predicting plastic deformations. In this chapter, a new model is proposed to incorporate stress/strength and applied stress states into the prediction of unbound aggregate permanent deformation behavior. The model is discussed in detail and compared with the simulation results obtained from the Pavement ME Design program. Finally, based on the experimental findings and utilizing the proposed model, a design approach is recommended for predicting flexible pavement aggregate base course rutting potentials.

5.2 PREDICTIVE METHOD FOR RUTTING ACCUMULATION

The following sections present both the application of the AN^b phenomenological model to the experimental data and the development of a newly proposed permanent deformation prediction model and its mathematical form. The laboratory test results in this research study were extensively used to justify the validity of the proposed model and its model parameters to be discussed in the next sections.

5.2.1 Discussion of AN^b Model with Experimental Data

The development of the new proposed model was based on the phenomenological model (Monismith et al. 1975) ($\epsilon_p = AN^b$) reviewed in Chapter 2. As a result, regression analyses were first performed to determine model parameters A and b for the phenomenological model. Table 5.1 lists the model parameters A and b for each individual permanent deformation test. Note that A-value represents initial compaction/deformation during the repeated loading and increases with the increase in the SSR shear stress ratios for all cases. In addition, the A-value is observed to be dependent on material types and properties. For example, Goldhill material with plastic fines is consistently assigned with the highest A-values amongst all the tested aggregate materials. Belgrade and Rocky Point materials, which are weaker materials, have the lowest *A*-values because lower stresses were commonly applied to these materials. These observations are in strong agreement with Khedr (1985) and Garg (1997) that parameter *A* varies with and is strongly dependent on the repeated load stress state and material strength.

Table 5.1 Parameters of the AN^b Phenomenological Model for the Three SSR Levels

Quarry	SSR = 0.25			SSR = 0.50			SSR = 0.75		
	A	***b***	**R^2**	***A***	***b***	**R^2**	***A***	***b***	**R^2**
Arrowood	0.2350	0.0889	0.936	0.2817	0.0776	0.917	0.3427	0.1163	0.993
Belgrade	0.0569	0.1262	0.926	0.1446	0.1156	0.927	0.1939	0.1251	0.947
Fountain	0.1001	0.2334	0.999	0.3185	0.1597	0.976	0.3629	0.1995	0.988
Franklin	0.0728	0.1132	0.905	0.2043	0.1018	0.867	0.2922	0.0977	0.907
Goldhill	0.2302	0.2062	0.846	0.9930	0.1341	0.886	1.4780	0.1386	0.839
Hendersonville	0.1623	0.1086	0.964	0.2619	0.1316	0.977	0.3290	0.1706	0.997
Jamestown	0.0460	0.1109	0.881	0.1702	0.1050	0.859	0.4765	0.0815	0.803
Lemon Spring	0.0877	0.1242	0.763	0.2589	0.1090	0.718	0.4268	0.1006	0.762
Moncure	0.0799	0.1181	0.886	0.2276	0.1025	0.845	0.5171	0.1031	0.741
Nash County	0.0915	0.1128	0.884	0.2151	0.1084	0.812	0.4403	0.1066	0.663
N. Wilkesboro	0.1629	0.0669	0.852	0.3154	0.0583	0.862	0.4061	0.0607	0.938
Princeton	0.0645	0.1269	0.871	0.1597	0.1118	0.950	0.2669	0.1180	0.980
Raleigh	0.0729	0.1194	0.918	0.1235	0.1141	0.948	0.2355	0.1164	0.938
Rockingham	0.2910	0.0826	0.641	0.4673	0.0764	0.668	0.4309	0.1187	0.967
Rocky Point	0.0307	0.1275	0.901	0.0899	0.1208	0.902	0.1652	0.1279	0.943
Rougemont	0.0663	0.1242	0.880	0.3091	0.1152	0.820	0.7095	0.1037	0.690

Garg (1997) evaluated aggregate materials used in the Mn/ROAD low volume road field study by means of mechanistic-based laboratory strength, modulus and deformation testing. It was observed that aggregate materials used in base/subbase applications exhibited a strong correlation between the rutting parameter *A* and the deviator stress at 1% axial strain obtained from the shear strength tests. However, it was reported that no significant relationship was found for estimating the *b* term (Garg 1997).

Figure 5.1 shows for the currently studied aggregate materials the relationships obtained between the rutting parameter *A* and the deviator stress at 1% axial strain for each of the SSR levels. It becomes obvious that higher stress/strength levels correspond to higher *A*-values in a predictive form, with the most reliable predictive *A*-value obtained at lower stress/strength levels. Note that an SSR level of 0.25 also includes data points from the first stage of the multi-stage test results, whereas 0.50 and 0.75 SSR levels only contain data points from the single-stage tests. In addition, Goldhill material data points are eliminated from this plot for the purpose of comparing only granular materials with nonplastic fines. As observed in the stress-strain relationships given in Appendix B, majority of the granular materials, except

Rocky Point, already failed at axial strain magnitudes greater than 1% at the applied 5 psi confining pressure. As a result, deviator stress at 1% axial strain was selected to represent the mobilized shearing resistance of the corresponding granular material at 5-psi confinement.

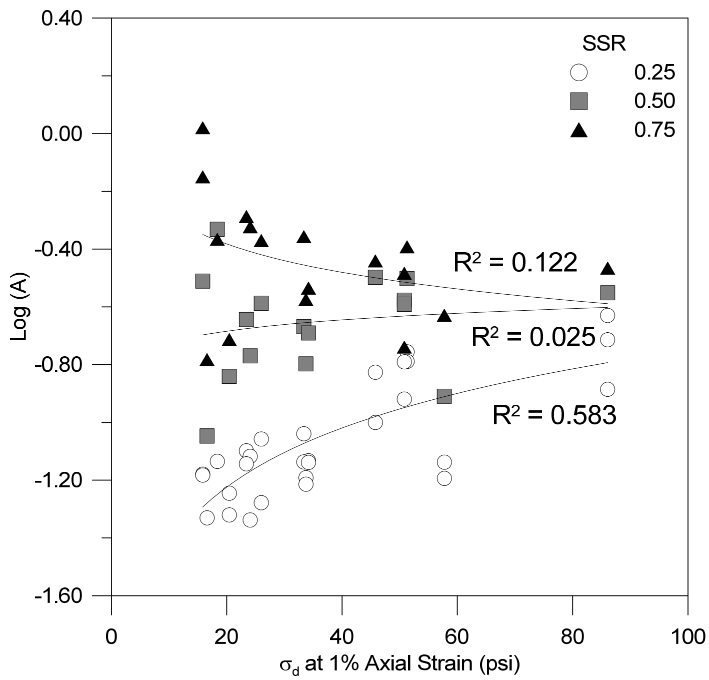

Figure 5.1 Relationships between *A*-value and Material Strength (σ_d at 1% axial strain)

The following interpretation can be offered in the light of the trends observed in Figures 5.1 and 5.2. The applied deviator stress at a high SSR level nearly mobilizes shear strength of granular materials, and hence, *A*-values at this SSR level are consistently higher compared to the intermediate and low SSR levels. For weaker materials (i.e. Rocky Point), the deviator stresses at 1% axial strain tend to be small and the difference between the *A*-values at different stress/strength levels are high. Whereas for stronger materials (i.e. Arrowood), a change in *A*-value is smaller. The funnel-shape trend is the product of this relationship.

Another attempt was made to correlate *A*-value to secant friction angles (see Figure 5.2): *A*-value is linearly related with ϕ_{sec} values at low SSR level. However, the relationship is not consistent across higher SSR levels. From both Figures 5.1 and 5.2, *A*-value is highly dependent on applied stress, hence, shear strength of materials based on the SSR concept. High stress levels produce greater *A*-value. However, the *A*-value alone cannot quantitatively differentiate the effects of applied stress states and material quality (expressed in terms of shear strength) on the aggregate permanent deformation behavior. Accordingly, an improved permanent deformation prediction approach is needed for better prediction of unbound aggregate rutting behavior.

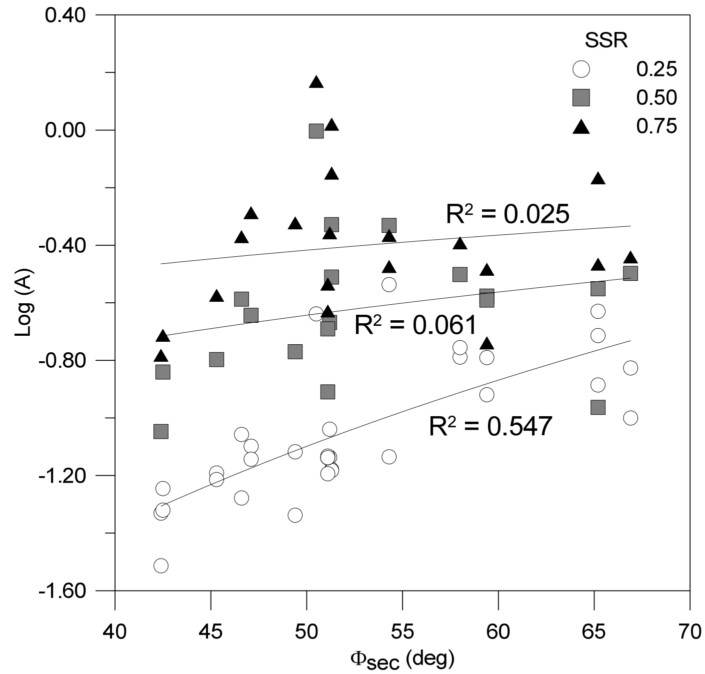

Figure 5.2 *A*-value (*AN^b*) Correlated with Secant Friction Angle (ϕ_{sec})

5.2.2 Development of a Newly Proposed Permanent Deformation Model

Laboratory results obtained from single-stage repeated load triaxial testing reported herein were used to propose a new permanent deformation model, referred to hereafter as the Chow-Mishra-Tutumluer (CMT) Rutting Model, to predict the permanent deformation accumulation trends of the unbound aggregate materials. Adequately considering the effects of applied stress levels as well as shear strength properties during the prediction of permanent deformation accumulation, this proposed model incorporates three primary components, namely number of load cycles, applied deviator stress, and shear stress ratio. Equations (5.1) and (5.2) are the basic and expanded formulations, respectively, for the CMT Rutting Model:

Chow-Mishra-Tutumluer (CMT) Rutting Model:

$$\epsilon_p(N) = AN^B \sigma_d{}^C \left(\frac{\tau_f}{\tau_{max}}\right)^D \tag{5.1}$$

$$\epsilon_p(N) = AN^B \sigma_d{}^C \left(\frac{\tau_f}{c+\sigma_f \tan\phi}\right)^D \tag{5.2}$$

where ϵ_p (N) is the permanent strain (%) corresponding to N-load applications; A, B, C and D are regression parameters; σ_d is applied deviator stress; τ_f is mobilized shearing resistance acting on failure plane; τ_{max} is available shear strength obtained through Mohr-Coulomb failure criteria, ($\tau_{max} = c + \sigma_f \tan \phi$); and, σ_f is normal stress acting on failure plane.

The primary advantage of the CMT Rutting Model is that the effects of stress levels applied on the specimens are adequately captured when predicting the permanent strain accumulation. Moreover, proper consideration is given to the shear strength properties of the materials by incorporating the SSR (τ_f / τ_{max}) term. Note that the proposed model does not consider at this time the effects of moisture content on permanent deformation accumulation. This is primarily because all shear strength and permanent deformation tests under the scope of this study were conducted at OMC-MDD conditions. Accordingly, moisture content was not used as a variable in this model. Furthermore, accuracy of the model has been verified at one confining pressure only, 5 psi (34.5 kPa). Therefore, the effect of confining pressure is indirectly reflected in the calculation for both σ_f and τ_f [see Equations (3.2) and (3.3)]. Note that the effects of material moisture content, particle shape, surface texture as well as stress history on permanent deformation accumulation can further be incorporated into the developed rutting model framework in the future. Table 5.2 lists the model parameters A, B, C and D for the combined sets of the three stress/strength levels conducted in this study.

Note that the model parameters for the Hendersonville material were calculated based on the test results at SSR levels of 0.25, 0.50 and 0.75, only. However, an additional test was also completed for this material at an SSR level of 0.34 (see Appendix E). Accordingly, Figure 5.3(a) compares the measured experimental data and the permanent deformation model predictions for this particular material. The model predicts permanent strain levels of 0.618% corresponding to an SSR level of 0.34, falling within the range between 0.406% (SSR = 0.25) and 0.958% (SSR = 0.50). This validates the prediction ability of the model at a confining pressure level of 5 psi. Figure 5.3(b) presents the laboratory-measured, and CMT model-predicted permanent strain values for the Arrowood material at different SSR levels. Laboratory measured permanent strain values are reported at three different SSR levels (SSR = 0.25, 0.50, and 0.68), whereas the CMT model-predicted permanent strain values at two other SSR levels (SSR = 0.40 and 0.85) are also plotted on the same graph. Note that permanent strain values of 0.495% and 1.981% were predicted at SSR levels of 0.40 and 0.85, respectively using the CMT model. The predicted high permanent deformations expectedly demonstrate the effects of high applied stresses that approach failure. Overall, the CMT model predicts permanent strains within a reasonable range of the assumed model input variables, i.e., the applied deviator stress and computed stress/strength level. Figure 5.4 is the compilation of the CMT model-predicted permanent strains from Table 5.2 fitted with the experimental data for all the sixteen aggregate materials.

Table 5.2 Model Parameters of the Proposed CMT Rutting Model

Material Number	Quarry	*A*	*B*	*C*	*D*	R^2
1	Arrowood	1.652E-12	0.0988	5.9649	-6.2489	0.996
2	Belgrade	6.460E+02	0.1227	-2.5291	4.2775	0.993
3	Fountain	3.778E-14	0.1959	6.7787	-6.9203	0.991
4	Franklin	8.430E+05	0.1046	-4.2325	6.2581	0.994
5	Goldhill	5.551E+00	0.1659	-0.3291	1.6501	0.982
6	Hendersonville	1.392E-02	0.1392	0.9248	0.0085	0.995
7	Jamestown	3.422E-03	0.0994	1.5569	0.0611	0.997
8	Lemon Spring	6.050E+02	0.1220	-2.2506	4.0630	0.986
9	Moncure	1.925E-06	0.1017	3.7611	-3.0862	0.994
10	Nash County	2.838E-06	0.1045	3.7036	-3.1253	0.990
11	N. Wilkesboro	2.985E+01	0.0632	-1.0292	2.0756	0.995
12	Princeton	3.015E-03	0.1180	1.3897	-0.4778	0.996
13	Raleigh	5.639E-10	0.1169	6.0100	-6.3182	0.994
14	Rockingham	1.814E-01	0.0925	0.3418	0.2204	0.965
15	Rocky Point	1.352E-02	0.1266	0.9338	0.4428	0.996
16	Rougemont	2.771E+02	0.1250	-1.6669	4.1391	0.994

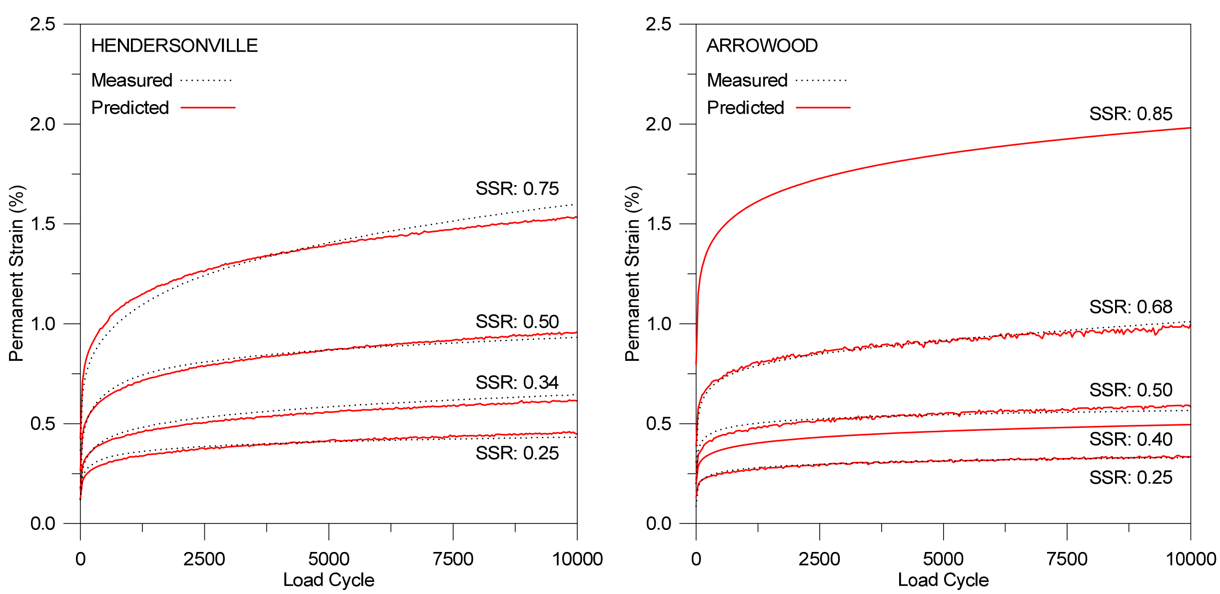

(a) (b)

Figure 5.3 Measured and Predicted Permanent Strains by CMT Rutting Model: (a) Hendersonville and (b) Arrowood Materials

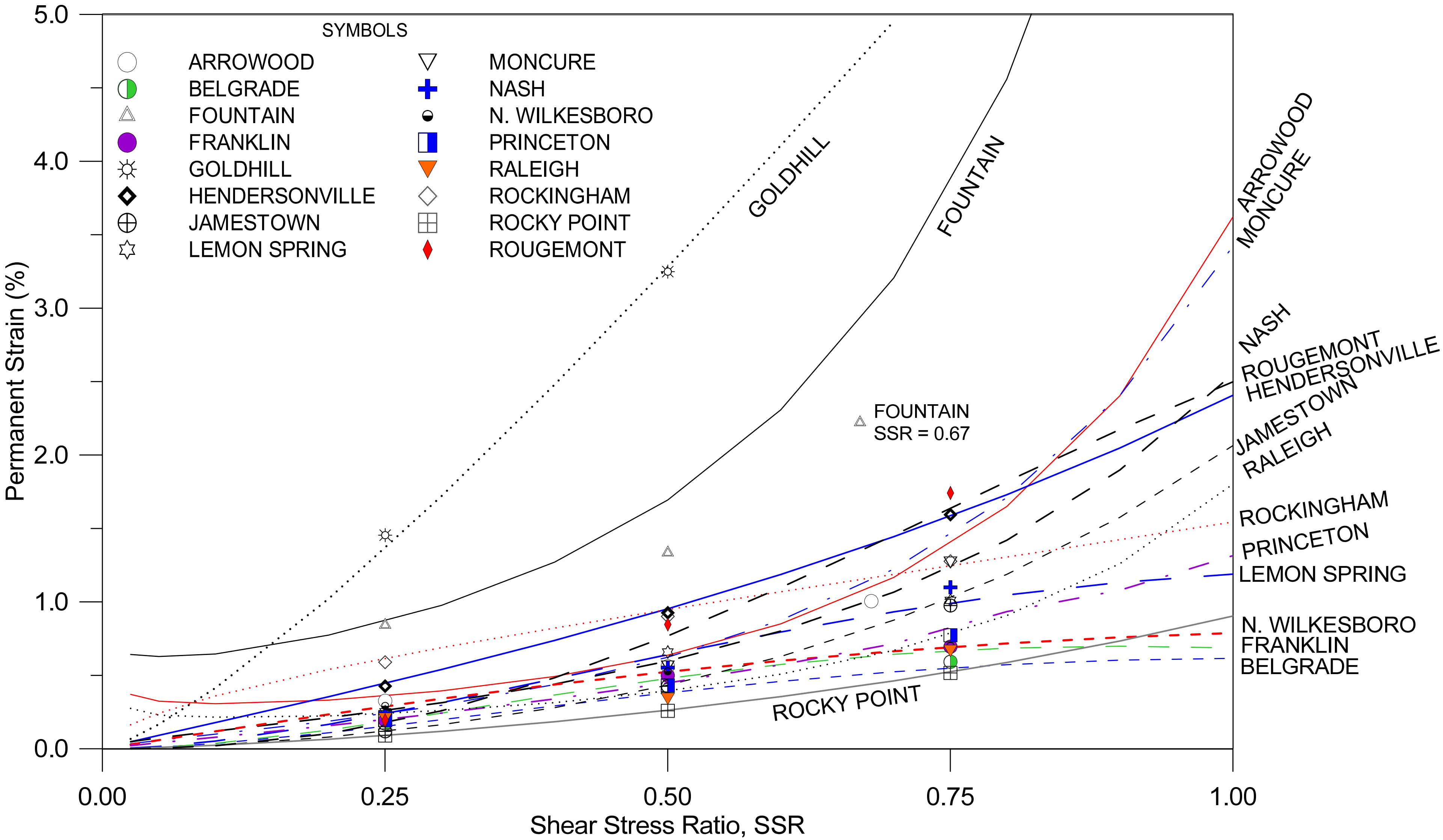

Figure 5.4 New CMT Rutting Model Predicted Permanent Strains Graphed with SSR Levels

5.2.3 CMT Rutting Model Parameters

The CMT rutting model parameters *C* and *D*, as listed in Table 5.2, may be questionable because both the applied deviator stress and the SSR terms should have positive powers to conform with the common observation that higher deviator stress as well as higher SSR levels usually lead to higher permanent deformation accumulations. An attempt was made to calibrate the model parameters *A*, *B*, *C* and *D* as part of this study. Shown in Figures 5.5 and 5.6 are the sensitivity analysis results of the different model parameters to material types and shear strength properties, respectively. Material types in Figure 5.5 are sorted in alphabetical order of quarry names. Large scatter and variation was observed in the ranges and values of all the four model parameters with no physical significance found for any single model parameter. The quite high variations in model parameter *A* and the positive and negative trends observed in model parameters *C* and *D* are merely the results of the numerical schemes in multiple regression analyses for obtaining the best fit resulting in the least sum of squared errors (SSE). For example, Figure 5.6 attempts to show any correlations between the shear strength property ϕ_{sec} and the model parameters. Again, no significant trends with strong correlations were found, suggesting the four model parameters from the CMT model are purely the outcome from regression analyses and do not carry any physical significance. However, the negative inclined trend of *A*-value with respect to ϕ_{sec} values implies stronger materials have the tendency to produce lower *A*-value from the CMT model, which is in agreement with common wisdom and engineering judgment.

5.2.4 Effects of Confining Pressure

As previously discussed in Chapter 2, confining stress level is one of the most important factors that influence the behavior of soils. Particularly for permanent deformation behavior, many researchers have concluded that accumulated permanent deformation is highly dependent on the magnitude of confining pressure. Barksdale (1972) observed that decreasing confining pressure resulted in higher accumulated permanent strains after a certain number of load cycles were applied on laboratory specimens of granular materials. In a more recent FAA study, Tutumluer et al. (2004) found that permanent strains of an airport pavement aggregate base material, when compared at the same applied deviator stress, were 0.60% at 5 psi (34.5 kPa) and 0.35% at 8 psi (55.1 kPa) confining pressures, respectively.

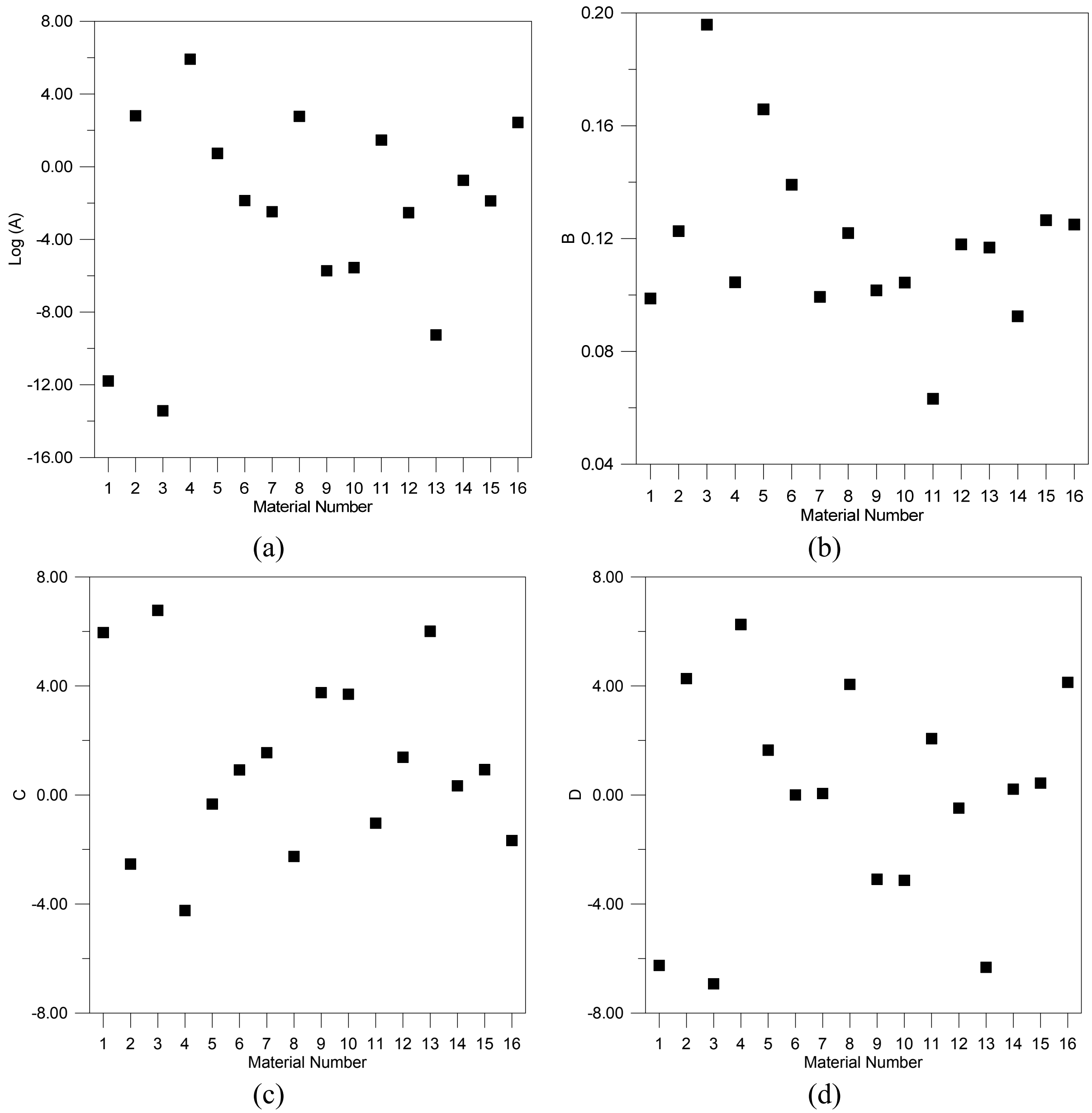

Figure 5.5 CMT Rutting Model Parameters Correlated with Material Types (Numbers indicate alphabetical order of quarry names)

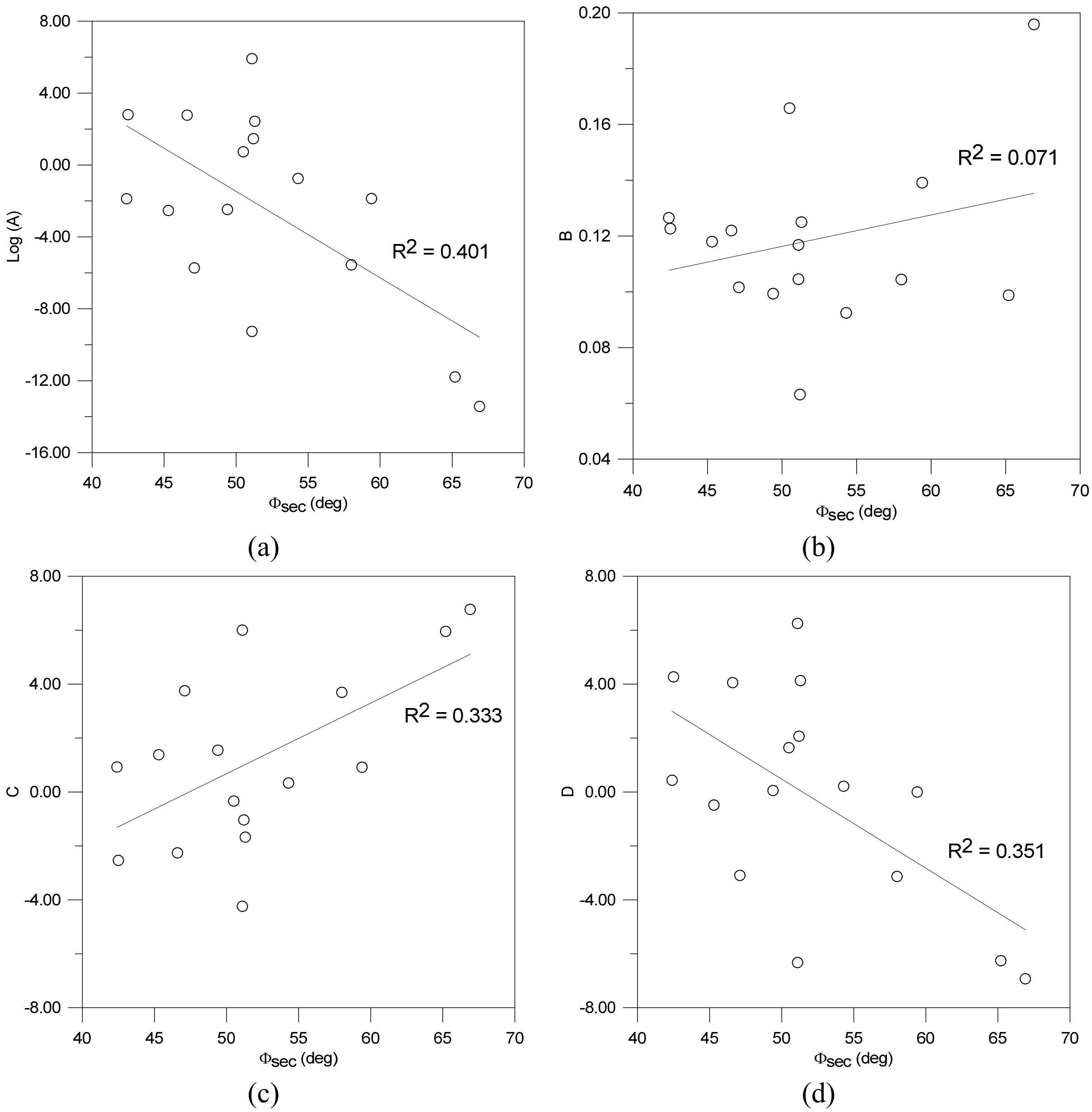

Figure 5.6 CMT Rutting Model Parameters Correlated with Secant Friction Angle (ϕ_{sec})

To check the "robustness" of the CMT model at different confining pressure levels, two additional repeated load triaxial tests were performed on strong and weak materials, Arrowood and Belgrade, respectively. Due to testing equipment limitations and the practical seating load requirements, the additional tests were performed at a confining pressure as low as 3 psi (20.7 kPa) to study the effects of lower confining pressure on permanent deformation behavior at SSR level of 0.75. The applied deviator stress values for Arrowood and Belgrade materials were 55.1 psi (379.6 kPa) and 10.5 psi (72.5 kPa), respectively (see Table 3.5). Tests results for the two materials at two different confining pressures are presented in Figure 5.7. It is clearly seen that with the 2 psi (13.8 kPa) decrease in confining pressure, the accumulated permanent strains were greater for both materials at an SSR level of 0.75. Note that the effect of confining pressure on permanent strain accumulation was much more significant on the Arrowood material [Figure 5.7(a)] compared to the Belgrade material [Figure 5.7(b)]. This can be directly linked to the magnitude of deviator stress (σ_d) applied during testing. Note that to achieve an SSR value of 0.75, deviator stress values of 63.1 psi and 55.1 psi had to be applied to the Arrowood material, whereas the corresponding σ_d values for the Belgrade material were 15.7 and 10.5 psi, respectively. Furthermore, changing the confining pressure level from 5 psi to 3 psi led to a change in principal stress ratio (σ_1/σ_3) of 12.66 to 18.36 for Arrowood, whereas the corresponding change for Belgrade was only 3.14 to 3.5. This indicates that the effect of change in confining pressure on permanent deformation can be linked to the corresponding change in principal stress ratios. Accordingly, it was clear from the comparisons that the CMT model permanent deformation predictions and the model parameters used for all the sixteen granular materials were only valid at a confining pressure of 5 psi.

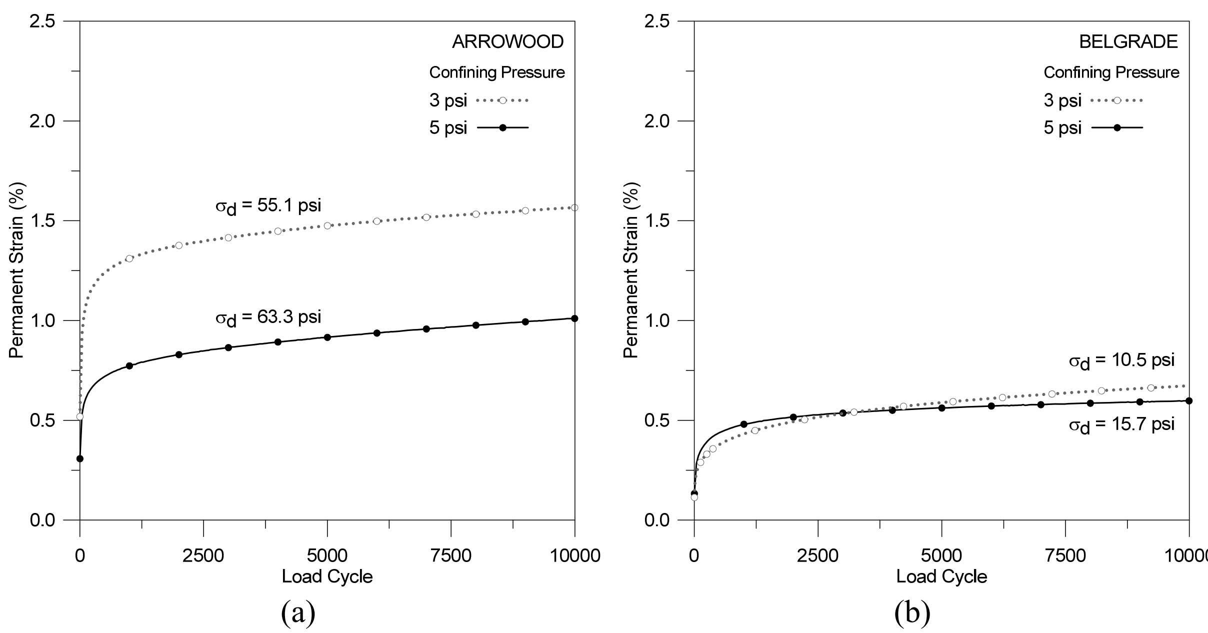

Figure 5.7 Effects of Confining Pressure on Permanent Deformation Behavior

Note that in many cases, horizontal stresses, very low in compression or even in tension, can be computed in the granular base from layered elastic analyses of conventional flexible pavements. These analyses usually do not take into account initial (existing field) conditions after pavement construction. Compaction induced lateral stresses in granular materials have been studied by many researchers (Duncan et al. 1991, Terzaghi 1996). Lateral pressure in compacted dense sand was measured to approach passive earth pressure at rest, K_p condition, with the assumption of rigid wall (Cheng and Fang 2008; Massarsch and Fellenius 2005). In pavements, they are often called residual stresses and exist in the granular layers as locked-in compressive stresses due to pavement construction or compaction and subsequent repeated traffic loading. Uzan (1985) reported measured horizontal residual stress to be as high as 2-5 psi (13.8-34.5 kPa) in pavement granular base materials. Barksdale and Alba (1993) also reported the measurement of horizontal residual stress of around 3 psi (20.7 kPa) in a 12-in. (305-mm) thick aggregate base due to the application of a 10-ton (8.9-MN) vibratory compactor. Based on the above findings, 5 psi (34.5 kPa) confining pressure selected for all permanent deformation testing in this study has been satisfactory and adequately considers the effects of compaction induced residual stresses.

5.2.5 Comparison: Permanent Deformation Predictions from CMT Rutting Model and Pavement ME Design

To demonstrate the need to modify the existing approach used in AASHTO Pavement ME Design procedure for predicting unbound aggregate layer rutting, an example pavement layered analysis was performed using the Pavement ME Design program. The analyzed pavement section comprised a 4-in. (100-mm) thick hot mix asphalt (HMA) layer over a 12-in. (305-mm) thick unbound aggregate base constructed over a prepared subgrade with CBR = 10%. Champaign, Illinois was selected as the pavement location, and the corresponding climatic data file was used in the Enhanced Integrated Climatic Model (EICM). The ground water table depth was set to 5 ft. (1.5 m) below the pavement surface. In addition, grain size distribution inputs for the aggregate base followed the engineered target gradation (Table 3.3 and Figure 3.1) and the material index properties including density, gravimetric water content, liquid limit and plasticity index were input accordingly for each granular material (see Table 3.4). All other factors were set equal to the default values used in the Pavement ME Design program and the analysis was performed for a new flexible pavement with a design life of 20 years.

Figure 5.8 presents the comparison charts for the permanent deformations predicted by the Pavement ME Design and the CMT rutting model. Resilient modulus (M_R) values for each aggregate material was obtained at an approximate stress state computed using layered elastic analysis in the middle of the granular base (σ_3 = 1.1 psi and σ_d = 13.4 psi), and were sorted in the order of magnitude for the purpose of graphical representation. As clearly seen in Figures 5.8(a)-(b), permanent strains predicted using Pavement ME Design are primarily linked to the unbound aggregate resilient modulus values, i.e., higher resilient modulus resulted in lower permanent strain. This is the outcome of an oversimplification of the original equations proposed by Tseng and Lytton (1989). Whereas, in Figures 5.8(c)-(d), the CMT rutting model predicts permanent strains with magnitudes varying quite differently than the M_R trends observed. In Figures 5.8(c)-(d), the example case is illustrated with the assumed 5 psi confinement and 15 psi deviator stress. The M_R values were recalculated accordingly, and the predicted results from CMT rutting model are more reasonable. Clearly, it is not the M_R but the level of stress in relation to the strength of the material that dictates the permanent strain accumulation. Strong materials such as Arrowood, Hendersonville and North Wilkesboro, consistently show lower deformations. Also noticeably, the estimated accumulated permanent strain of Goldhill material (PI = 6) was 2.33%, which indicated that this granular material with plastic fines produced significantly large permanent deformation.

Figures 5.8(e) and (f) compare predictions for the case of this 4-in. HMA and 12-in. aggregate base conventional pavement section. At 10,000 cycles, most predictions from the CMT rutting model are considerably lower those predicted by Pavement ME Design approach. At 1 million cycles (expected to simulate the life span of a low volume road), the predicted strains from the CMT rutting model are still lower except that Goldhill indicates very large deformations due to plastic fines, which is completely ignored by the Pavement ME Design software. Finally, except for Goldhill material, all permanent strains predicted by the CMT rutting model are much less than those predicted by the Pavement ME Design approach.

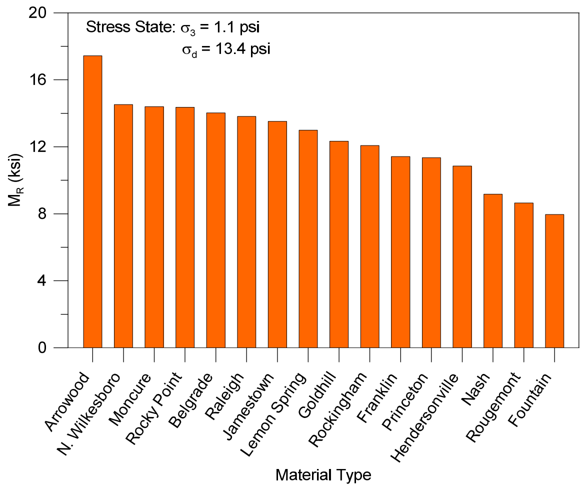

Stress State: σ_3 = 1.1 psi
σ_d = 13.4 psi
M_R (ksi)
0
4
8
12
16
20
Arrowood
N. Wilkesboro
Moncure
Rocky Point
Belgrade
Raleigh
Jamestown
Lemon Spring
Goldhill
Rockingham
Franklin
Princeton
Hendersonville
Nash
Rougemont
Fountain
Material Type

(a)

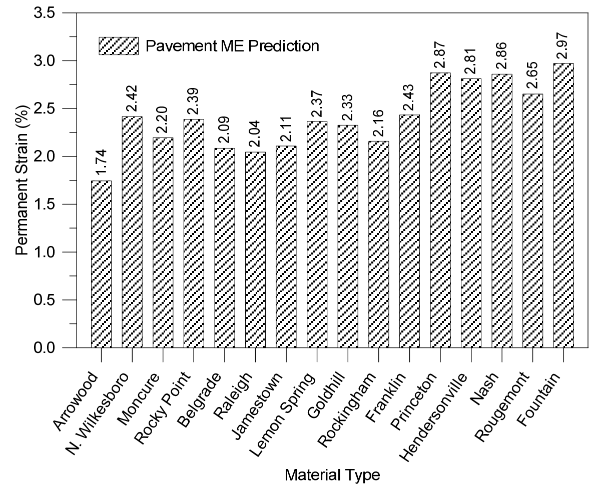

Pavement ME Prediction
Permanent Strain (%)
0.0
0.5
1.0
1.5
2.0
2.5
3.0
3.5
1.74
2.42
2.20
2.39
2.09
2.04
2.11
2.37
2.33
2.16
2.43
2.87
2.81
2.86
2.65
2.97
Arrowood
N. Wilkesboro
Moncure
Rocky Point
Belgrade
Raleigh
Jamestown
Lemon Spring
Goldhill
Rockingham
Franklin
Princeton
Hendersonville
Nash
Rougemont
Fountain
Material Type

(b)

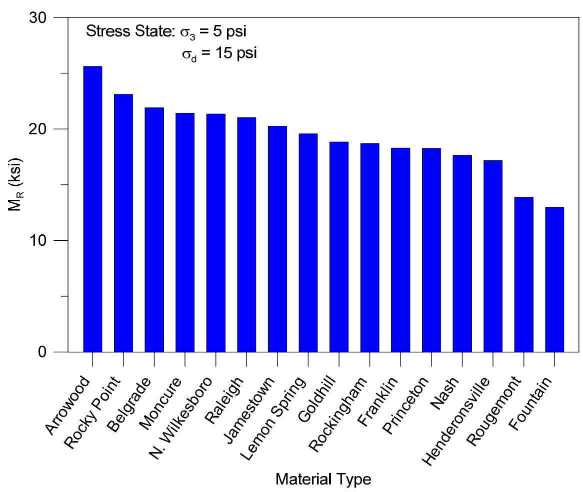

Stress State: σ_3 = 5 psi
σ_d = 15 psi
M_R (ksi)
0
10
20
30
Arrowood
Rocky Point
Belgrade
Moncure
N. Wilkesboro
Raleigh
Jamestown
Lemon Spring
Goldhill
Rockingham
Franklin
Princeton
Nash
Hendersonville
Rougemont
Fountain
Material Type

(c)

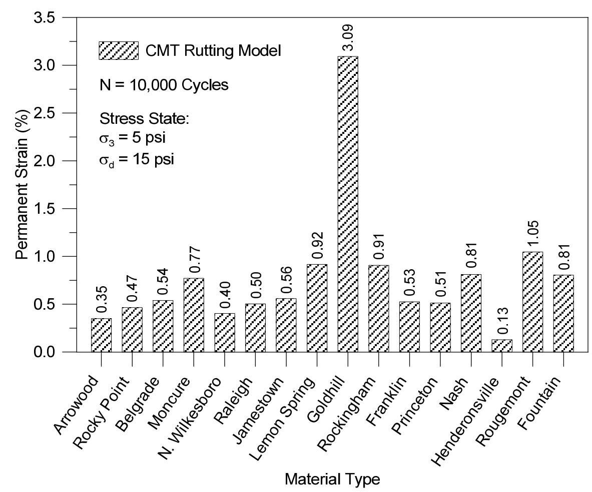

CMT Rutting Model
N = 10,000 Cycles
Stress State:
σ_3 = 5 psi
σ_d = 15 psi
Permanent Strain (%)
0.0
0.5
1.0
1.5
2.0
2.5
3.0
3.5
0.35
0.47
0.54
0.77
0.40
0.50
0.56
0.92
3.09
0.91
0.53
0.51
0.81
0.13
1.05
0.81
Arrowood
Rocky Point
Belgrade
Moncure
N. Wilkesboro
Raleigh
Jamestown
Lemon Spring
Goldhill
Rockingham
Franklin
Princeton
Nash
Hendersonville
Rougemont
Fountain
Material Type

(d)

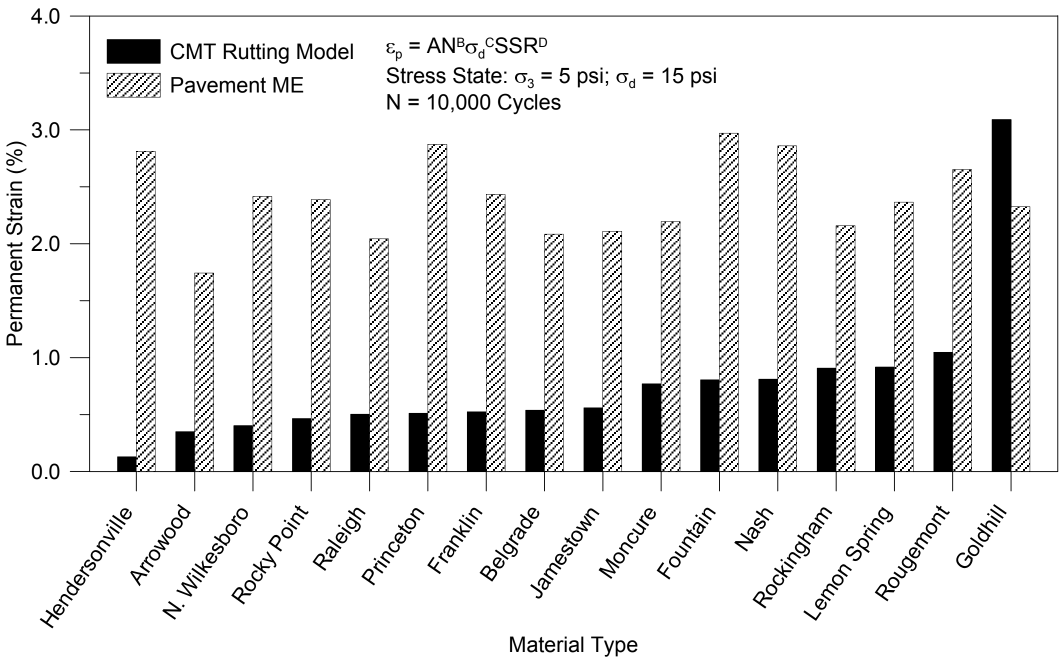

(e)

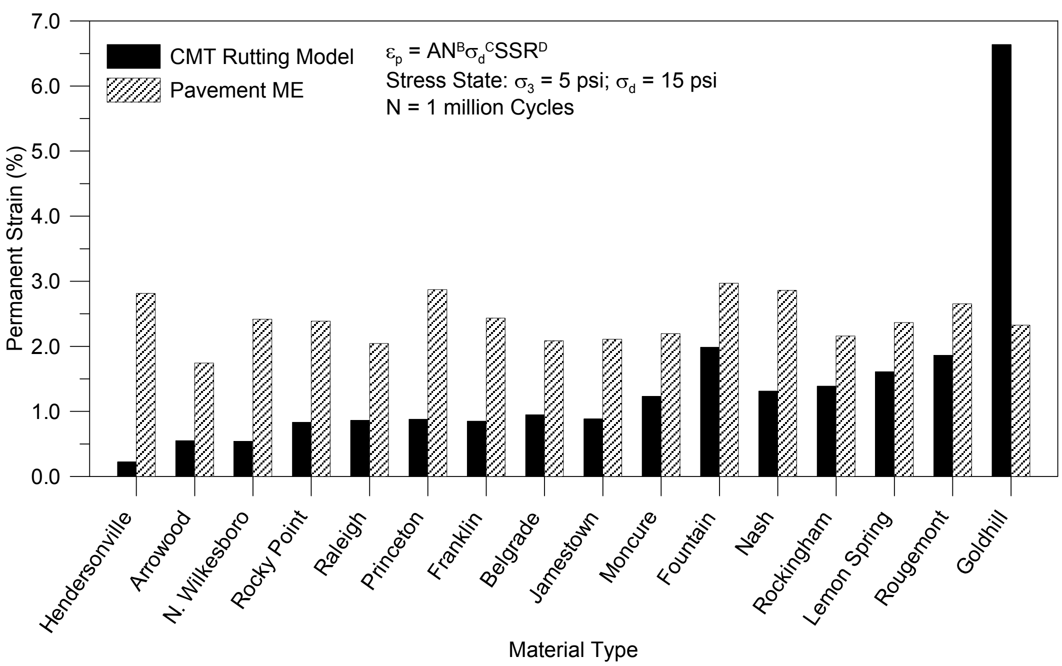

(f)

Figure 5.8 Comparison: Predicted Permanent Strains from Pavement ME Design and CMT Rutting Model: (a) Inputted Resilient Modulus (4" HMA + 12" ABC); (b) Results from Pavement ME Design; (c) Resilient Modulus based on 5 psi σ_3 and 15 psi σ_d; (d) Results from CMT Rutting Model; (e) Permanent Strains at 10,000 Cycles; and (f) Permanent Strains at 1 million Cycles

5.3 RECOMMENDED DESIGN APPROACH FOR TYPICAL NORTH CAROLINA PAVEMENT SECTIONS

For the sixteen (16) granular materials tested in this study, the rut accumulations within the unbound aggregate base/subbase layers can be predicted using the CMT rutting model parameters provided in Table 5.2, which assumes the use of 5 psi (34.5 kPa) confining pressure. The CMT rutting model is applicable and can be used with any of the sixteen aggregate materials to predict permanent strains or deformations for the designs of low, moderate and high volume road pavement sections.

Unlike the empirical CBR and the 1986-1993 AASHTO design methods, the mechanistic-empirical (M-E) design methodology is principally based on the analysis of the layered pavement structure. Accordingly, mechanistic pavement analysis considers the stress-strain-deformation response caused by traffic loading. Subsequently, the M-E design methodology often relies on computer analyzed results associated with laboratory characterizations of the pavement layer material behavior. Due to its applicability to various layer designs and changing climatic, material and loading conditions, the M-E methodology is scientifically more accurate and reliable when compared to empirical approaches. However, the empirical of the M-E methodology still requires accurate rutting damage models, such as the proposed CMT rutting model [Equations (5.1) and (5.2)] developed in this study. The applied stress state and shear stress ratio (SSR) components as integrated in the model must be considered and estimated in order for the model to work properly.

The following road construction practices are routinely employed in the state of North Carolina for building conventional flexible pavement sections:

- **Low Volume Road**: 3.0-in. (76-mm) HMA and 8.0-in. (203-mm) aggregate base;
- **Moderate Volume Road**: 6.0-in. (152-mm) HMA and 8.0-in. (203-mm) aggregate base; and
- **High Volume Road**: 9.0-in. (229-mm) HMA and 10.0-in. (254-mm) aggregate base.

The typical stress states at mid-depths of the aggregate base layers were approximated by using a finite element analysis program, ILLI-PAVE. Developed at the University of Illinois (Raad and Figueroa, 1980), ILLI-PAVE is an axisymmetric finite element (FE) program commonly used in the structural analysis of flexible pavements. The nonlinear, stress dependent resilient modulus geomaterial models are already incorporated into ILLI-PAVE. Numerous research studies have validated that the ILLI-PAVE model provides a realistic pavement structural response prediction for highway and airfield pavements (Thompson and Elliot 1985; Thompson 1992; Garg et al. 1998). Recent research at the Federal Aviation Administration's Center of Excellence established at the University of Illinois also supported the development of a new, updated version of the program, now known as the ILLI-PAVE 2000 (Gomez-Ramirez et al. 2002).

The primary advantages of using ILLI-PAVE finite element program include the elimination of tension effects in the elastic layered analysis and producing more accurate stress state estimation. Iterative process is started with average resilient modulus values assigned in the base and subgrade layers and completed when convergence is reached. Similar to the pavement configuration setting in Section 5.2.3, 9-kip (40-kN) wheel load and 100-psi (689-kPa) tire pressure were used for loading the pavement surface. The HMA layer was assigned an elastic modulus (E_{HMA}) of 500 ksi (3445 MPa) and Poisson's ratio (μ_{HMA}) of 0.35; the aggregate base layer was assigned a Poisson's ratio (μ_{base}) of 0.40; and resilient modulus values for the base layers were calculated using the K-θ relationship ($M_R = K\theta^n$); resilient modulus for the subgrade was assigned using the established correlation with CBR of ($M_R = 2555 \times CBR^{0.64}$; M_R = 11.2 ksi or 77 MPa, for a subgrade with CBR = 10%); a Poisson's ratio (μ_{subg}) of 0.45 was used for the subgrade.

For the case of 4-in. (102-mm) thick HMA layer and 12-in. (305-mm) thick aggregate base layer, the computed mid-depth aggregate base layer average stress states were σ_3 = 1.1 psi (7.6 kPa) and σ_d = 13.4 psi (92.3 kPa). Table 5.3 summarizes the stress states computed at mid-depth aggregate base layers of the four pavement sections. The computed values were used in the rutting predictions for low, moderate and high volume road pavement sections.

Table 5.3 ILLI-PAVE Results: Stress States at Mid-Depth Aggregate Base Layer

Pavement Section	Depth		$\sigma_{xx} = \sigma_{yy} = \sigma_3$		$\sigma_{zz} = \sigma_1$		σ_d	
	in.	m	psi	kPa	psi	kPa	psi	kPa
4-in. HMA + 12-in. base	10.0	0.254	1.1[a]	7.6	14.5	99.9	13.4[b]	92.3
3-in. HMA + 8-in. base	7.0	0.178	1.4[a]	9.6	26.0	179.1	24.6	169.5
6-in. HMA + 8-in. base	10.0	0.254	1.9[a]	13.1	9.1	62.7	7.2	49.6
9-in. HMA + 10-in. base	14.0	0.356	1.6[a]	11.0	5.0	34.5	3.4	23.4

[a] σ_3 values were adjusted to 5 psi (34.5 kPa) to account for residual stresses
[b] 15.0 psi σ_d for 4-in. HMA + 12-in. aggregate base layer was used in example

Earlier discussion on the undeniable existence of horizontal compressive residual stresses due to pavement construction/compaction activity and subsequent trafficking justified the use of 5 psi (34.5 kPa) confining pressure in the CMT rutting model permanent deformation predictions. Note that the lateral stress or confining pressure values in Table 5.3 computed from ILLI-PAVE are exclusive from such residual stress effects. Hence, in order to account for the effects of residual stresses, all confining pressures used in predicting permanent deformation were predominantly set equal to 5 psi (34.5 kPa), whereas deviator stresses computed from ILLI-PAVE and listed in Table 5.3 were used in permanent strain predictions. As a result, Table 5.4 lists the calculated SSR levels and the predicted permanent strains of each aggregate base material for up to 10,000 load cycles. Note that for low volume roads, the estimated deviator stress values at mid-depth aggregate base layer were found to approach failure conditions of the weaker materials, such as Belgrade, Rocky Point and Lemon Spring, indicated by the SSR levels close to 1.0 (see Table 5.4 in bold).

Table 5.4 Predicted Permanent Strains for Each Pavement Section

Quarry	ϕ	c	*Low Volume*		*Moderate Volume*		*High Volume*	
			SSR	ϵ_p	SSR	ϵ_p	SSR	ϵ_p
	(deg)	(psi)	(-)	(%)	(-)	(%)	(-)	(%)
Arrowood	50.2	12.4	0.36	0.45	0.12	0.31	0.06	0.32
Belgrade	41.8	0.9	**1.00**	**0.62**	0.41	0.30	0.21	0.12
Fountain	39.3	23.3	0.34	1.08	0.11	0.65	0.05	0.62
Franklin	34.1	5.8	0.80	0.68	0.29	0.23	0.15	0.07
Goldhill	37.7	6.3	0.70	4.96	0.25	1.38	0.13	0.56
Hendersonville	45.3	8.6	0.50	0.17	0.17	0.08	0.09	0.05
Jamestown	41.2	3.4	0.81	1.24	0.31	0.17	0.16	0.05
Lemon Spring	41.4	1.6	**0.96**	**1.17**	0.38	0.45	0.20	0.16
Moncure	50.6	0.2	0.80	1.69	0.31	0.31	0.16	0.15
Nash County	41.4	2.8	0.86	1.69	0.33	0.35	0.17	0.18
N. Wilkesboro	46.0	7.0	0.54	0.56	0.19	0.22	0.09	0.11
Princeton	49.1	1.0	0.79	0.86	0.30	0.25	0.15	0.12
Raleigh	42.3	2.6	0.85	1.06	0.33	0.27	0.17	0.22
Rockingham	41.7	5.2	0.68	1.17	0.25	0.61	0.12	0.41
Rocky Point	44.9	0.3	**0.97**	**0.85**	0.40	0.18	0.21	0.07
Rougemont	48.8	0.5	0.83	1.92	0.32	0.30	0.16	0.07

5.3.1 Low Volume Roads

Figure 5.9 presents the pavement geometry, layer material properties and the predicted permanent strains corresponding to the computed mid-depth aggregate base layer deviator stress in a typical low volume road pavement section. With a mid-layer deviator stress of 24.6 psi (169.5 kPa), the predicted permanent strains from the CMT rutting model for up to 10,000 load cycles are given in Table 5.4 and plotted in Figure 5.9(b). As expected from the laboratory test results, a pavement section comprising a base course layer constructed with the Goldhill material accumulated the highest rutting of 0.4-in. (10.2-mm) levels; this can be attributed to the existence of 8% plastic fines in this particular aggregate type. It can be seen that strong materials such as Hendersonville, Arrowood, and North Wilkesboro materials are expected to accumulate the lowest rutting amounts.

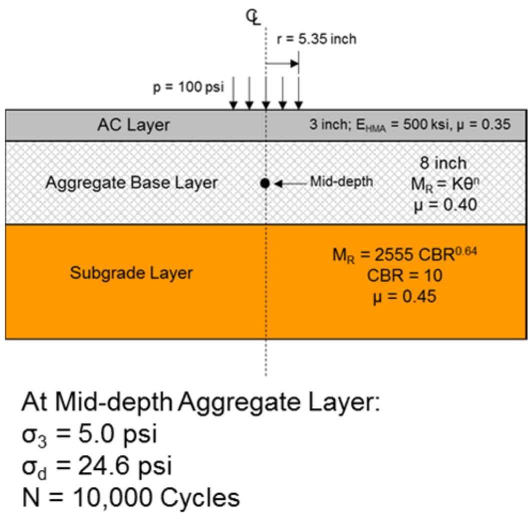

(a)

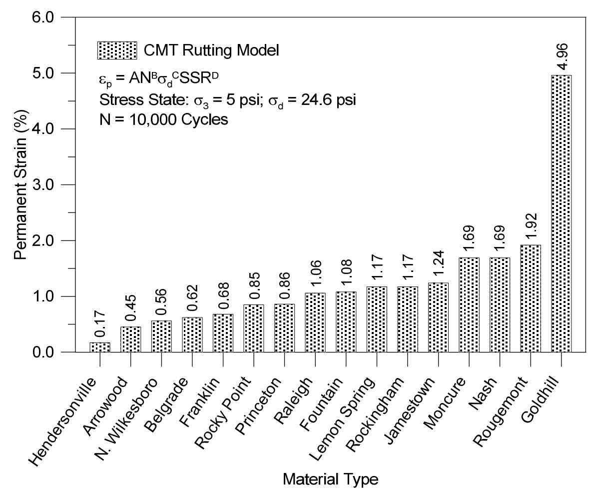

(b)

Figure 5.9 Low Volume Road Case Predicted Permanent Strains

Note that although Belgrade, Lemon Spring and Rocky Point materials had relatively low permanent strains predicted, the SSR = 1.0 level for each of the materials has been reached and through examining the stress-strain relationships of these materials (see Appendix B), they are expected to rapidly accumulate permanent deformations to fail the pavement. This observation may be used to highlight a limitation of the CMT rutting model in its current form. The CMT rutting model fails to capture the shear failure of an aggregate layer when the SSR value approaches unity. Accordingly, the rutting levels predicted using the CMT model are likely valid when SSR values fall in the range between 0.25 and 0.75. Extending the model predictions beyond this SSR range may be erroneous.

5.3.2 Moderate Volume Roads

Figure 5.10 presents the pavement geometry, layer material properties and the predicted permanent strains corresponding to the computed mid-depth aggregate base layer deviator stress in a typical moderate volume road pavement section. With almost 71% reduction in the mid-layer deviator stress, the predicted permanent strains for moderate volume road are substantially lower compared to the low-volume road configuration. The Goldhill material was expected to accumulate maximum rutting of 0.11-in. (2.79-mm) after 10,000 load applications. All other aggregate materials were predicted to accumulate less than 1% strain or 0.08-in. (2.0-mm) deformation due to the much lower base course wheel load deviator stress.

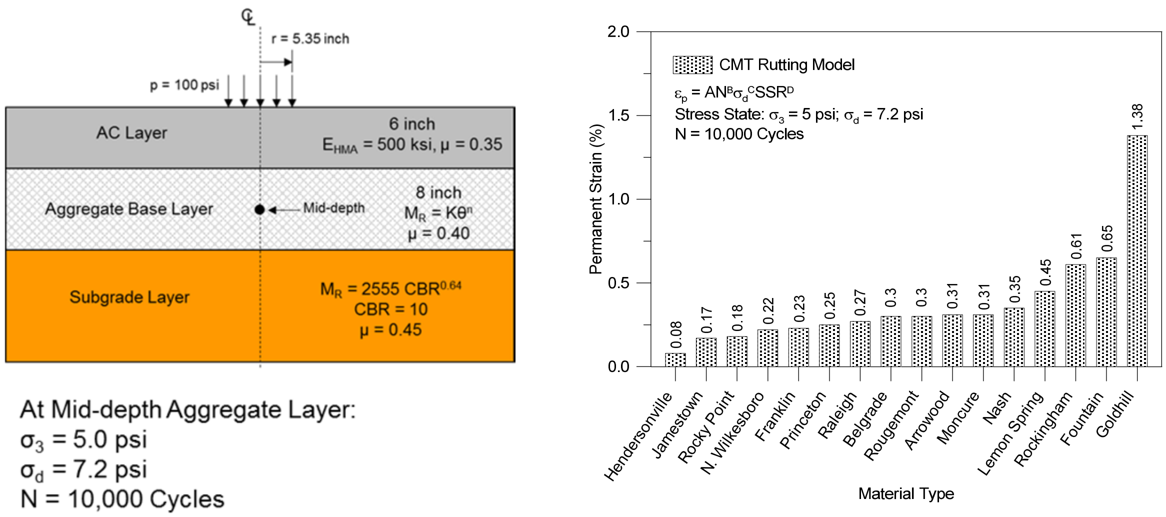

(a) (b)

Figure 5.10 Moderate Volume Road Case Predicted Permanent Strains

5.3.3 High Volume Roads

Figure 5.11 presents the pavement geometry, layer material properties and the predicted permanent strains corresponding to the computed mid-depth aggregate base layer deviator stress in a typical high volume road pavement section. The thick HMA layer greatly reduces the wheel load-induced deviator stress in the aggregate base layer. Accordingly, the confining pressure in the aggregate base should be expected to slightly increase with depth. However, for the purpose of comparison, similar confining pressure of 5 psi (34.5 kPa) was assumed to show the effects of stress state in predicting permanent strains of the aggregate materials. After 10,000 load applications, the Fountain material was found to produce the highest deformation. Second to Fountain material, Goldhill material accumulated permanent deformation of about 0.06-in (1.5-mm). In this case, the low stress states resulted in very low and negligible permanent deformations which are significantly smaller for all the tested granular materials when compared to the deformations predicted for the low and moderate volume road cases.

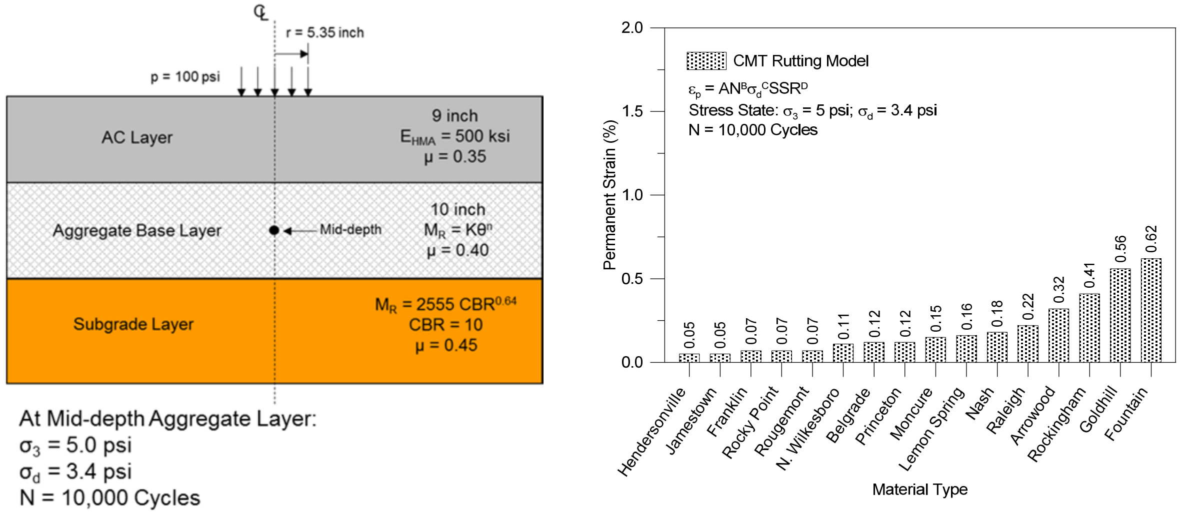

(a) (b)

Figure 5.11 High Volume Road Case Predicted Permanent Strains

5.3.4 Design Approach for Other Aggregate Base Materials

The predictive method introduced herein was developed for the sixteen aggregate materials studied in this research study. The proposed design approach uses the shear strength and applied stress states as two primary factors in predicting permanent deformations. Shear strength of the aggregate material, however, also varies with moisture content, compaction effort, changes in gradation or grain size distribution for different as-received material grading, mode of shear, rate of shear loading, etc. Therefore, careful quality control in laboratory testing and materials characterization to accurately capture the shear strength properties is the most important task prior to predicting permanent strains.

All repeated load triaxial tests in the current study were conducted at a confining pressure level of 5 psi (34.5 kPa) by subjecting the specimens to repeated loading for 10,000 load cycles. Accordingly, the proposed predictive model (CMT Rutting Model) is said to be valid only at a confining pressure level of 5 psi. However, Section 5.2.4 has shown that the varying confining pressures can have significant effects on unbound aggregate permanent deformation behavior. Note that appropriate selection of confining pressure levels during laboratory experimentation to ensure close simulation of field condition is difficult and challenging. Considering that most finite element or layered elastic programs estimate low horizontal stresses, often negative (tensile), in aggregate base layer, 5 psi (34.5 kPa) confining pressure selected for all permanent deformation testing in this study has been satisfactory and adequately considered the effects of compaction induced residual stresses.

Finally, with design criteria established for allowable rutting, predicted permanent deformation is obtained by multiplying strain with layer thickness. The design approach flowchart shown in Figure 5.12 is recommended for predicting permanent strain accumulation in aggregate base courses.

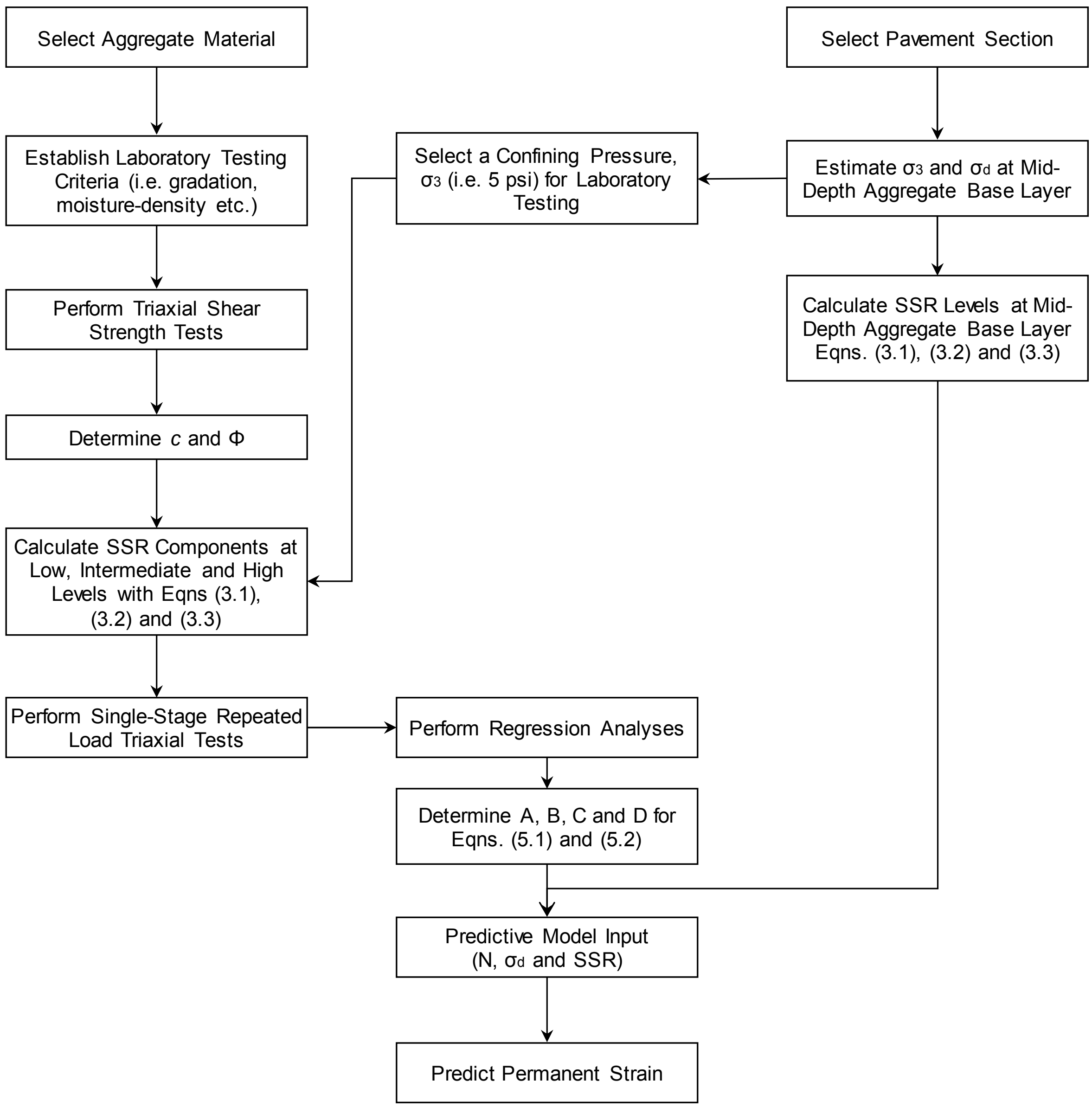

Figure 5.12 Recommended Design Approach for Predicting Aggregate Base Rutting

5.4 SUMMARY

Based on the current state-of-the-art knowledge and previous study findings on the behavior of aggregate base course materials, critical factors affecting permanent deformation accumulation were successfully reviewed and implemented in a newly proposed predictive model. This chapter discussed the development of the so called CMT Rutting Model based on the laboratory test results. The following are the summary findings and highlights.

- The phenomenological model ($\epsilon_p = AN^b$) does not incorporate shear strength and stress state components in permanent strain prediction. Therefore, improvement over this basic form of model was needed to adequately capture the effects of applied stress in relation to the strength of material in predicting permanent deformation accumulation in unbound granular materials.
- The newly proposed CMT rutting model was developed to incorporate into the predictive model shear stress to strength ratio (SSR) and applied deviator stress as input variables.
- When compared to the Pavement ME Design rutting predictions, the new model was able to predict much lower permanent strains, quite reasonably and adequately based on the number of load cycles, applied stress state and stress/strength (SSR) level.
- The model parameters assigned in the CMT rutting model appear to be only relevant for the best statistical fit and do not necessarily carry any physical relevance. However, one trend was observed was that higher secant friction angles (ϕ_{sec}) corresponded to lower model parameter *A*-values.
- It was observed that the CMT rutting model was only valid at confining pressure of 5 psi (34.5 kPa), which was found to adequately represent typical stress states of the mid-depth aggregate base layer considering compaction induced locked-in residual stresses.
- Estimations of wheel load deviator stresses from layered elastic solutions resulted in reasonable granular base rutting predictions using the CMT rutting model for the low, moderate and high volume road pavement sections.

CHAPTER 6: CONCLUSIONS AND RECOMMENDATIONS

The overall objective of this research study was to evaluate the rutting potentials of selected aggregate materials used in pavement base course applications in North Carolina and develop and calibrate rutting damage models based on primarily laboratory as well as field (if available) performance data. To accomplish the overall objective, the project specific goals linked to the proposed tasks were: (1) identify and select local base course aggregates from quarries in NC, (2) conduct a custom-designed suite of shear strength and permanent deformation tests, (3) investigate effects of applied stress states, shear strength properties, applied stress to strength ratios, and aggregate properties on the plastic shakedown and determine realistic rutting predictions of aggregate bases through permanent deformation testing, (4) based on this laboratory performance based evaluation, evaluate the adequacy of the rutting damage model in AASHTO's Pavement ME Design software and propose a new and improved rutting damage model based on the experimental data, and finally, (5) prepare a set of recommendations for developing new performance based specifications including strength criteria for these unbound aggregate layers.

Shear strength and permanent deformation tests were conducted at the Illinois Center for Transportation (ICT) at different applied stress/strength ratios. Accordingly, a framework was established to properly consider the strong correlation that commonly exists between permanent deformation and shear strength characteristics, as opposed to resilient modulus properties, in the laboratory characterization of aggregate materials for permanent deformation behavior.. The trends of permanent strain accumulations from repeated load triaxial tests were adequately captured in a new rutting model, referred to as the Chow-Mishra-Tutumluer or CMT rutting model, developed by taking into account the applied shear stresses levels as certain fractions of the material shear strength under similar confinement conditions. When compared to the results of the Pavement ME Design software, the CMT rutting model used for unbound aggregate base/subbase courses predicted much lower permanent strain values based on the number of load cycles, applied stress state and stress/strength (SSR) level and aggregate material properties.

6.1 SHEAR STRENGTH AND PERMANENT DEFORMATION BEHAVIOR

The complete database of shear strength and permanent deformation test results produced in this study is the product of more than 150 laboratory tests performed on sixteen different aggregate materials obtained from various quarries in the state of North Carolina. The laboratory test matrix was systematically and attentively organized to ensure all aggregate materials were tested under similar conditions. This included testing all specimens at one engineered target gradation and compacting all specimens by employing a method similar to that used by NCDOT to establish the maximum dry density and optimum moisture content values. Shear strength tests were first performed to establish the Mohr-Coulomb failure envelope for each aggregate material, and subsequently compute the target stress states to be used in repeated load permanent deformation testing. Through incorporation of stress/strength or Shear Stress Ratio (SSR) concept, this study has successfully accounted for the effects of material shear strength and applied stress levels on permanent deformation accumulation.

Important findings related to the laboratory testing and material characterization are outlined below:

- Resilient modulus (M_R) of unbound materials is used in the MEPDG and the Pavement ME Design approaches as a primary governing factor to predict the rut accumulation in pavement base/subbase layers. The laboratory characterization framework established in this study has adequately proven that a strong correlation exists between permanent deformation and shear strength characteristics, as opposed to resilient modulus properties. Furthermore, permanent deformation behavior is governed by the applied wheel load-induced stress states, shear strength of the material and the aggregate material properties.
- The concept of Shear Stress Ratio (SSR) is fundamentally a plastic equilibrium approach to normalize the stress states applied on a given material. The establishment of failure criteria based on this concept allowed this research study to successfully examine aggregate permanent deformation behavior at low, intermediate and high order of stress levels.
- Both multi-stage and single-stage permanent deformation test results showed convincing arguments that permanent deformation accumulation is stress dependent and the laboratory permanent deformations increased in direct proportion to applied stresses in a linear fashion.
- Plastic fines (i.e. PI = 6) produced undesirable high permanent deformation.
- Imaging-based shape, surface texture and angularity analyses performed on two particle sizes (1.0-in. and 0.5-in.) resulted in no clear trends with the permanent deformation behavior. Particle shape properties are likely to be influenced by the aggregate mineralogy and the type of crusher used during aggregate production.

6.2 RECOMMENDED DESIGN APPROACH

Since calibration of the rutting damage model used in the MEPDG and the Pavement ME Design approach was not feasible, the overall objective of this project was then to propose a new and improved rutting damage model based on the experimental data that would be readily implemented in the NCDOT pavement design practices. Based on the completeness of the experimental database consisting of the 16 aggregate base materials studied, a predictive CMT rutting model was proposed to capture the effects of stress state and incorporate the findings into a suggested performance-based design approach. Conventional flexible pavement case studies were analyzed to establish base course rutting performances for typical low, moderate and high volume NC pavement sections.

Important findings related to the CMT rutting model predictions and the key features of the recommended design approach are as follows:

- The newly proposed CMT rutting model was able to capture the effects of applied stress state, shear strength, and material properties, such as plastic fines, for predicting permanent deformation.
- When compared to the Pavement ME Design rutting predictions, the CMT rutting model was able to predict much lower permanent strains, based on the number of load cycles, applied stress state and stress/strength (SSR) level.
- A design flowchart has been established and recommended with the use of SSR concept and representative mid-depth base layer wheel load deviator stress (with a confining pressure of 5 psi assumed) to give reliable base course rutting predictions. This recommendation was included in Chapter 5, and is anticipated to be used by NCDOT for predicting the field permanent deformation potentials of the sixteen aggregate materials studied.

6.3 RECOMMENDATIONS FOR FUTURE RESEARCH

Some of the assumptions made and the limitations encountered in the course of this research study suggest potential improvements that can be made to the CMT rutting model to further develop the framework of the base course rutting prediction approach. Topics for future research may include the following:

- Additional aggregate material testing following the established laboratory characterization and testing framework will expand the current database and enhance reliability and accuracy of the permanent deformation model predictions.
- The model parameters assigned in the CMT rutting model can be correlated aggregate material properties when a satisfactory laboratory database is established.
- Aggregate properties, such as gradation, moisture content in relation to optimum moisture content, achieved dry density in relation to the maximum dry density, and amount and type (plastic or nonplastic) of fines, of a standard aggregate material can be studied individually to determine the sensitivities of the CMT rutting model predictions to material properties.

- In-situ testing and field measurement of lateral/vertical pressure in unbound aggregate base layer under real trafficking is required to establish representative stress states. Little attention has been given to residual stresses which exist in unbound aggregate base layer due to compaction and subsequent traffic loading. The effect of residual stress can be significant in permanent deformation accumulation (Chapter 5).

REFERENCES

Allen, J., "The Effect of Non-constant Lateral Pressures of the Resilient Response of Granular Materials," *Ph.D. Thesis*, University of Illinois at Urbana-Champaign, 1973.

Ayres, M.J., "Unbound Material Rut Model Modification," *Development of the 2002 Guide for the Design of New and Rehabilitated Pavement Structures, NCHRP 1-37A*, Inter Team Technical Report, 2002.

Barksdale, R.D., "Laboratory Evaluation of Rutting in Base Course Materials," *Proceedings of the 3rd International Conference on Asphalt Pavements*, University of Michigan, Ann Arbor, 1972, pp. 161-174.

Barksdale, R.D., and J.L. Alba, "Laboratory Determination of Resilient Modulus for Flexible Pavement Design," Interim Report No. 2, prepared for NCHRP, Transportation Research Board, National Research Council, Washington, D.C., 1993.

Barksdale, R.D. and S.Y. Itani, "Influence of Aggregate Shape on Base Behavior," *Transportation Research Record 1227*, Transportation Research Board, National Research Council, Washington, D.C., 1989, pp 173-182.

Brown, S.F. and F. Chan, "Reduced Rutting in Unbound Granular Pavement Layers through Improved Grading Design," *Proceedings of the Institution of Civil Engineers*, *Transport*, No. 117, 1996, pp. 40-49.

Brown, S.F. and A.F.L. Hyde, "Significance of Cyclic Confining Stress in Repeated-Load Triaxial Testing of Granular Material," *Transportation Research Record 537*, Transportation Research Board, National Research Council, Washington, D.C., 1975, pp 49-58.

Chen, T.J. and Y.S. Fang, "Earth Pressure due to Vibratory Compaction," *ASCE Journal of Geotechnical and Geoenvironmental Engineering*, Vol. 134, No. 4, 2008, pp. 437-444.

Chow, L.C. and J.F. Labuz, "Undrained Behavior of a Granular Base Material Subjected to Free-Thaw Conditions," *Unpublished technical report*, *University of Minnesota – Twin Cities, Minneapolis, MN,* 2010.

Dawson, A.R., N.H. Thom, and J.L. Paute, "Mechanical Characteristics of Unbound Granular Materials as a Function of Condition," *Flexible Pavements, Proceedings of European Symposium Euroflex 1993*, A.G. Correia, ed., Balkema, Rotterdam, the Netherlands, 1996, pp. 35-44.

Dempsey, B.J., “Laboratory and Field Studies of Channeling and Pumping,” *Transportation Research Record 849*, Transportation Research Board, National Research Council, Washington, D.C., 1982.

Duncan, J.M., G.W. Williams, A.L. Sehn, and R.B. Seed, “Estimation Earth Pressures due to Compaction,” *ASCE Journal of Geotechnical Engineering*, Vol. 117, No. 12, 1991, pp. 1833-1847.

El-Mitiny, M.R., “Material Characterization for Studying Flexible Pavement Behavior in Fatigue and Permanent Deformation,” *Ph.D. Thesis*, Ohio State University, Columbus, 1980.

Garg, N., “Mechanistic-Empirical Evaluation of the Mn/ROAD Low-Volume Road Test Sections,” *Ph.D. Thesis*, University of Illinois at Urbana-Champaign, 1997.

Garg, N., Tutumluer, E. and M.R. Thompson, “Structural Modeling Concepts for the Design of Airport Pavements for Heavy Aircraft,” In Proceedings, 5th International Conference on the Bearing Capacity of Roads and Airfields, Trondheim, Norway, 1998.

Gidel G., P. Hornych, J.J Chauvin, D. Breysse, and A. Denis, “Nouvelle approche pour l’étude des déformations permanentes des graves non traitées à l’appareil à chargement répétés,” *Bulletin des Laboratoire des Ponts et Chausées*, 2001, pp. 5-21.

Gomez-Ramirez, F., Thompson, M.R. and M. Bejarano, “ILLI-PAVE based Flexible Pavement Design Concepts for Multiple Wheel Heavy Gear Load Aircraft,” In Proceedings, 9th International Conference on Asphalt Pavements, Copenhagen, Denmark, 2002.

Hicks, R.G. and C.L. Monismith, “Factors Influencing the Resilient Response of Granular Materials,” *Transportation Research Record 345*, Transportation Research Board, National Research Council, Washington, D.C., 1971.

Huurman, M., “Permanent Deformation in Concrete Block Pavements,” *Ph.D. Thesis*, Delft University of Technology, Delft, the Netherlands, 1997.

Khedr, S., “Deformation Characteristics of Granular Base Course in Flexible Pavement,” *Transportation Research Record 1043*, Transportation Research Board, National Research Council, Washington, D.C., 1985, pp 131-138.

Kim, I.T., “Permanent Deformation Behavior of Airport Flexible Pavement Base and Subbase Courses,” *Ph.D. Thesis*, University of Illinois at Urbana-Champaign, 2005.

Lekarp, F. and A. Dawson, “Modeling Permanent Deformation Behavior of Unbound Granular Materials,” *Construction and Building Materials*, Vol. 12, No. 1, 1998, pp 9-18.

Lekarp, F., U. Isacsson, and A. Dawson, “State of the Art II: Permanent Strain Response of Unbound Aggregates,” *ASCE Journal of Transportation Engineering*, Vol. 126, No. 1, pp. 76-83, 2000.

Maree, J.H, “Design Parameters for Crushed Stone in Pavements,” *M.S. Thesis,* University of Pretoria, South Africa, 1978.

Massarsch, K.R. and B.H. Fellenius, “Deep Vibratory Compaction of Granular Soils,” *Chapter 19 in Ground Improvement-Case Histories, Elsevier*, 2005, pp. 633-658.

Mishra, D. and E. Tutumluer, “Aggregate Physical Properties Affecting Modulus and Deformation Characteristics of Unsurfaced Pavements,” *ASCE Journal of Materials in Civil Engineering*, Vol. 24, No. 9, 2012, pp. 1144-1152.

Moaveni, M., Wang, S., Hart, J.M., Tutumluer, E., and N. Ahuja. “Aggregate Size and Shape Evaluation Using Segmentation Techniques and Aggregate Image Processing Algorithms,” Transportation Research Record 2335, Journal of the Transportation Research Board, National Research Council, Washington, D.C., 2013, pp 50-59.

Monismith, C.L., N. Ogawa, and C.R. Freeme, “Permanent Deformation Characteristics of Subgrade Soils Due to Repeated Loading,” *Transportation Research Record 537*, Transportation Research Board, National Research Council, Washington, D.C., 1975, pp 1-17.

Pan, T., E. Tutumluer, and S.H. Carpenter, “Imaging Based Evaluation of Coarse Aggregate used in the NCAT Pavement Test Track Asphalt Mixes,” *In Proceedings of the 1st International Conference on Design and Construction of Long Lasting Asphalt Pavements*, Auburn, AL, 2004.

Pan, T., and E. Tutumluer, “Quantification of Coarse Aggregate Surface Texture Using Image Analysis,” *ASTM Journal of Testing and Evaluation*, Vol. 35, No. 2, 2007.

Pappin, J.W., “Characteristics of a Granular Material for Pavement Analysis,” University of Notthingham, Nottingham, England, 1979.

Paute, J.L., P. Hornych, and J.P. Benaben, “Repeated Load Triaxial Testing of Granular Materials in French Network of Laboratories des Ponts et Chaussées,” *Flexible Pavements, Proceedings of the European Symposium Euroflex 1993*, A.G. Correia, Ed., Balkema, Rotterdam, the Netherlands, 1996, pp. 53-64.

Raad, L. and J.L. Figueroa, “Load Response of Transportation Support Systems,” *ASCE Transportation Engineering Journal*, 106(TE1), 1990.

Rada, G. and M.W. Witczak, "Comprehensive Evaluation of Laboratory Resilient Moduli Results for Granular Material," *Transportation Research Record 810*, Transportation Research Board, National Research Council, Washington, D.C., 1981, pp 23-33.

Rao, C., E. Tutumluer, and I.T. Kim, "Quantification of Coarse Aggregate Angularity based on Image Analysis," *Transportation Research Record 1787*, Transportation Research Board, National Research Council, Washington, D.C., 2002, pp 117-124.

Rao, C., E. Tutumluer, and J.A. Stefanski, "Flat and Elongated Ratios and Gradation of Coarse Aggregates Using a New Image Analyzer," *ASTM Journal of Testing and Standard*, Vol. 29, No. 5, 2001, pp. 79-89.

Saeed, A., J. Hall, and W. Barker, "Performance-related Tests of Aggregates for Use in Unbound Pavement layers," *NCHRP Report No. 453*, National Academy Press, Washington, D.C., 2001.

Seyhan, U. and E. Tutumluer, "Anisotropic Modular Ratios as Unbound Aggregate Performance Indicators," *ASCE Journal of Materials in Civil Engineering*, Vol. 14, No. 5, 2002, pp. 409-416.

Tao, M., M.N. Louay, N.D. Munir, Z. Zhang, and Z. Wu, "Application of Shakedown Theory in Characterizing Traditional and Recycled Pavement Base Materials," *Journal of Transportation Engineering*, Vol. 136, No. 3, 2010, pp. 214-222.

Terzaghi, K., R.B. Peck, and G. Mesri, "Soil Mechanics in Engineering Practice," *John Wiley and Sons, Inc*., New York, NY, 1996.

Thom, N.H. and S.F. Brown, "The Effect of Grading and Density on the Mechanical Properties of a Crushed Dolomitic Limestone," *Proceedings of the 14th ARRB Conference*, Part 7. 1988, pp. 94-100.

Thompson, M.R. "ILLI-PAVE based Conventional Flexible Pavement Design Procedure," In Proceedings, 7th International Conference on Asphalt Pavements, Nottingham, U.K., 1992.

Thompson, M.R., "State-of-the-Art: Unbound Base Performance," *Proceedings of the 6th Annual Symposium of International Center for Aggregate Research (ICAR)*, Austin, TX, 1998.

Thompson, M.R. and R.P. Elliott, "ILLI PAVE based Response Algorithms for Design of Conventional Flexible Pavements," *Transportation Research Record 1043*, Transportation Research Board, National Research Council, Washington, D.C., 1985, pp. 50-57.

Thompson, M.R. and Q.L. Robnett, "Resilient Properties of Subgrade Soils," *ASCE Transportation Engineering Journal,* Vol. 105, No. TE1, 1979.

Thompson, M.R. and D. Nauman, "Rutting Rate Analyses of the AASHO Road Test Flexible Pavements," *Transportation Research Record 1384*, Transportation Research Board, National Research Council, Washington, D.C., 1993, pp 36-48.

Tseng, K.H. and R.L. Lytton, "Prediction of Permanent Deformation in Flexible Pavement Materials," *Implication of Aggregates in the Design, Construction, and Performance of Flexible Pavements*, ASTM STP 1016, ASTM, Philadelphia, PA, 1989, pp. 154-172.

Tutumluer, E., I.T. Kim, and R.L. Santoni, "Modulus Anisotropy and Shear Stability of Geofiber-Stabilized Sands," *Transportation Research Record 1874*, Transportation Research Board, National Research Council, Washington, D.C., 2004, pp 125-135.

Tutumluer, E., C. Rao, and J.A. Stefanski, "Video Image Analysis of Aggregates," *Final Project Report, FHWA-IL-UI-278, Civil Engineering Studies UILU-ENG-2000-2015*, University of Illinois at Urbana-Champaign, 2000.

Tutumluer, E. and U. Seyhan, "Laboratory Determination of Anisotropic Aggregate Resilient Moduli using an Innovative Test Device," *Transportation Research Record 1687*, Transportation Research Board, National Research Council, Washington, D.C., 1999, pp 13-21.

Ullidtz, P., "Modeling of Granular Materials Using the Discrete Element Method," *Proceedings of the 8th International Conference on Asphalt Pavements*, Seattle, WA, 1997, pp. 757-769.

Uzan, J. "Characterization of Granular Materials," *Transportation Research Record 1022*, Transportation Research Board, National Research Council, Washington, D.C., 1985, pp 52-59.

van Niekerk, A.A. and M. Huurman, "Establishing Complex Behavior of Unbound Road Building Materials from Simple Material Testing," *Technical Report No. 7-95-200-16*, Delft University of Technology, Delft, the Netherlands, 1995.

Werkmeister, S., "Permanent Deformation Behavior of Unbound Granular Materials in Pavement Constructions," *Ph.D. Thesis*, Dresden University of Technology, Dresden, Germany, 2003.

Witczak, M.W. and M.M. El-Basyouny, "Appendix GG-1: Calibration of Permanent Deformation Models for Flexible Pavements," *In Guide for Mechanistic-Empirical Design of New and Rehabilitated Pavement Structures, NCHRP*, 2004, pp. 1-556.

Wolff, H., "Elasto-Plastic behavior of Granular Pavement Layers in South Africa," *Ph.D. Thesis*, University of Pretoria, Pretoria, Republic of South Africa, 1992.

APPENDIX A GRAIN SIZE DISTRIBUTIONS OF VIRGIN AGGREGATES

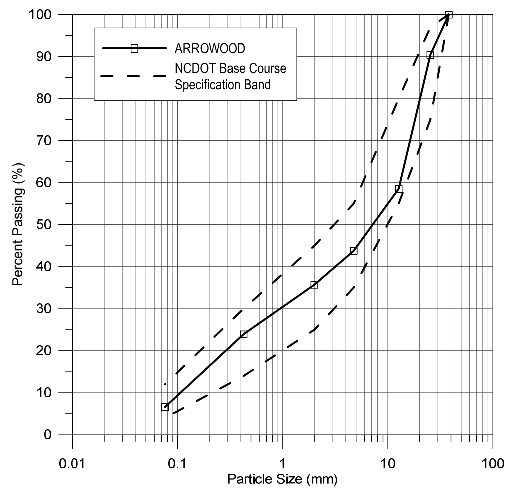

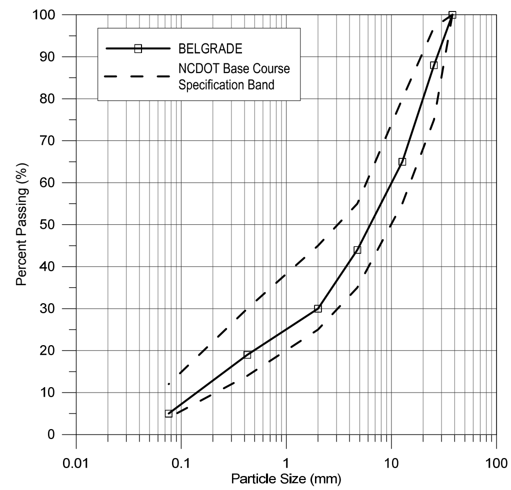

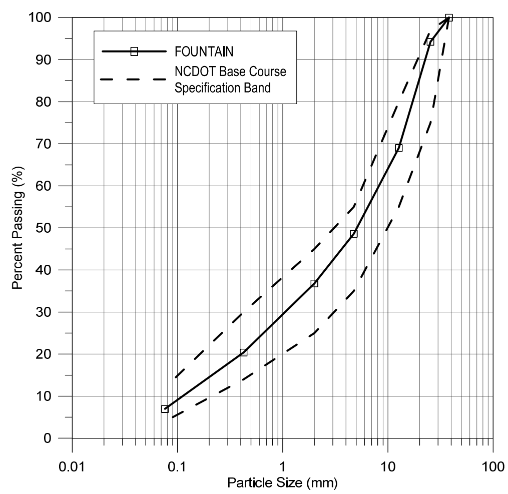

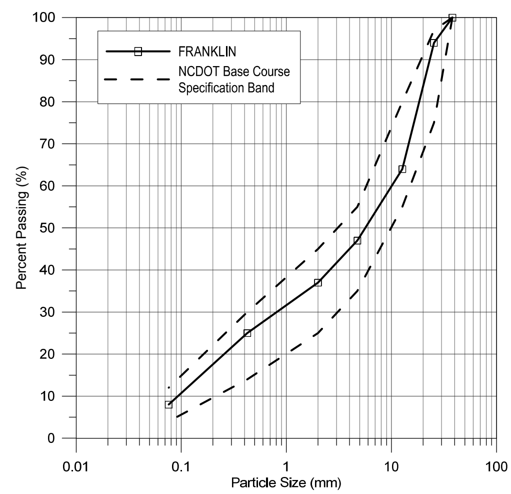

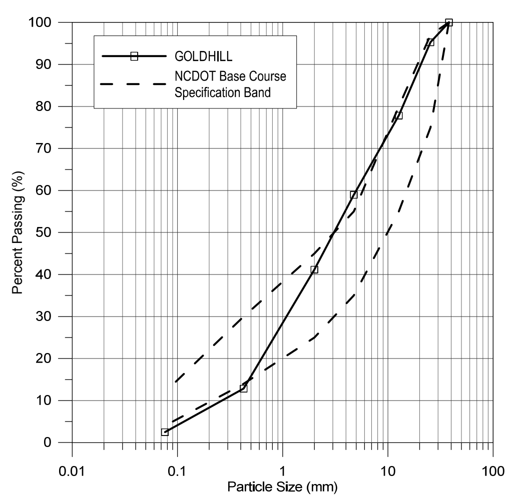

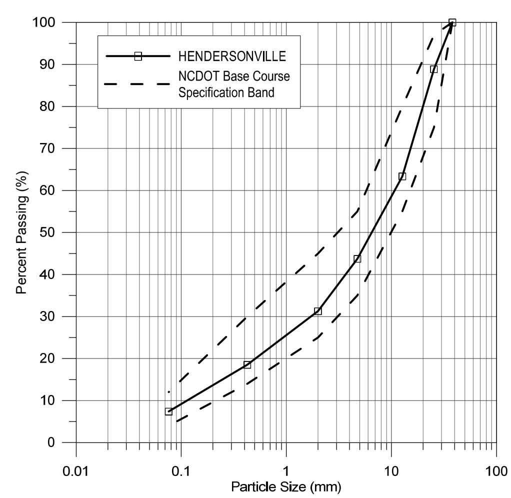

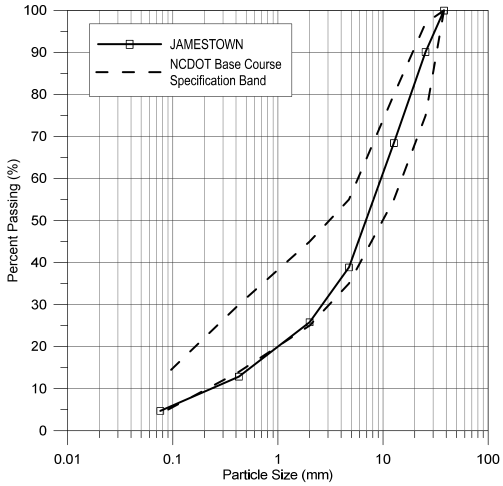
JAMESTOWN
NCDOT Base Course Specification Band
Percent Passing (%)
Particle Size (mm)

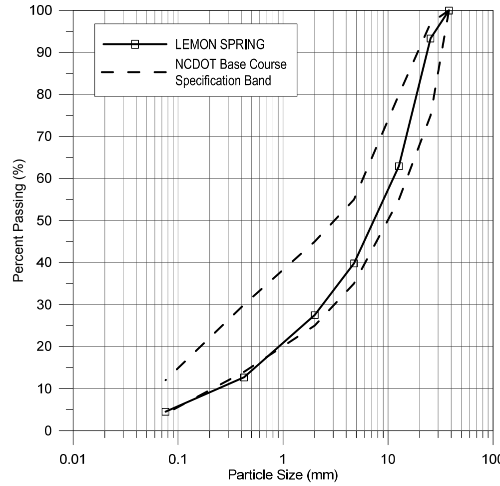
LEMON SPRING
NCDOT Base Course Specification Band
Percent Passing (%)
Particle Size (mm)

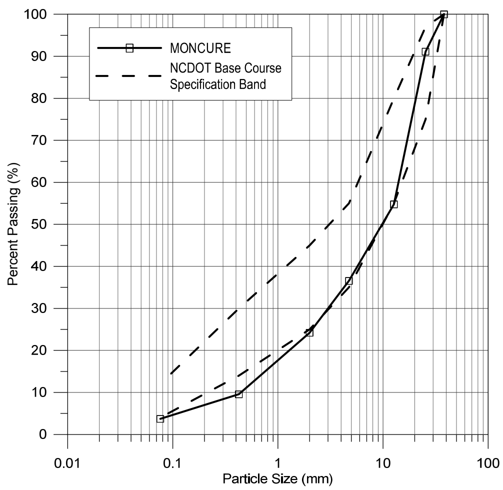
MONCURE
NCDOT Base Course Specification Band
Percent Passing (%)
Particle Size (mm)

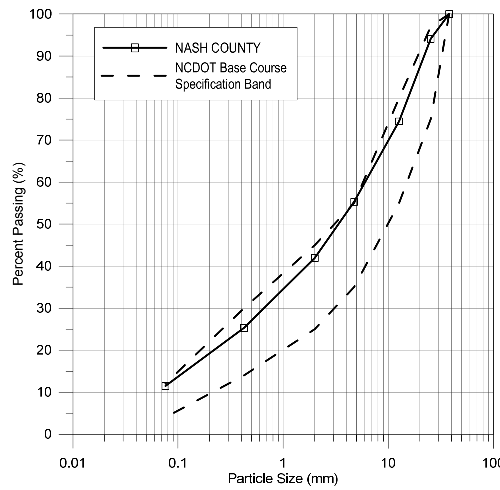
NASH COUNTY
NCDOT Base Course Specification Band
Percent Passing (%)
Particle Size (mm)

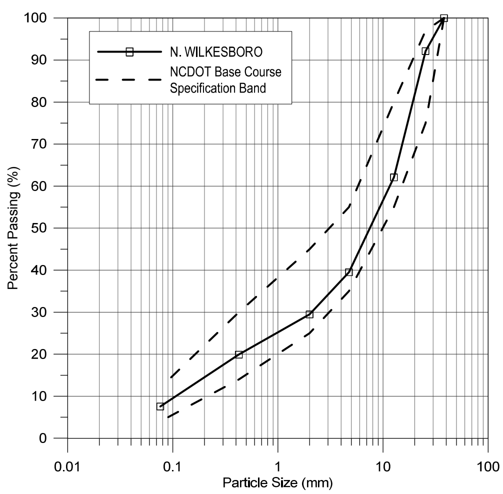
N. WILKESBORO
NCDOT Base Course Specification Band
Percent Passing (%)
Particle Size (mm)

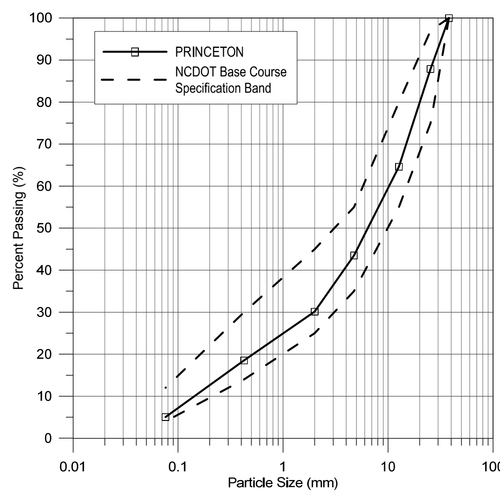
PRINCETON
NCDOT Base Course Specification Band
Percent Passing (%)
Particle Size (mm)

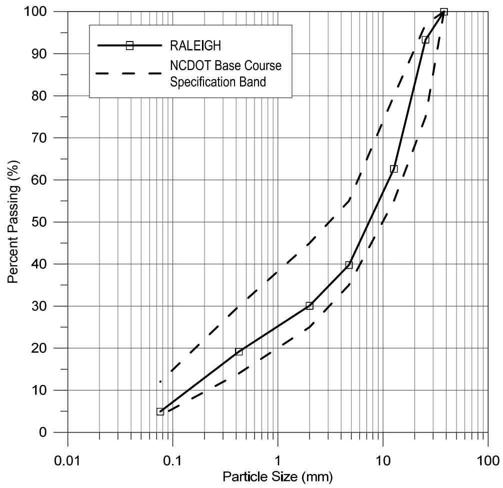
RALEIGH
NCDOT Base Course
Specification Band
Percent Passing (%)
Particle Size (mm)

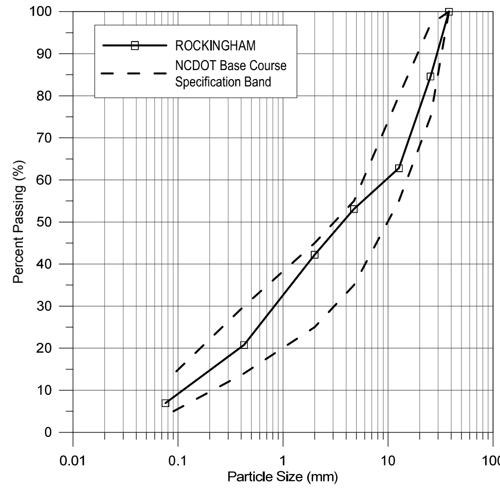
ROCKINGHAM
NCDOT Base Course
Specification Band
Percent Passing (%)
Particle Size (mm)

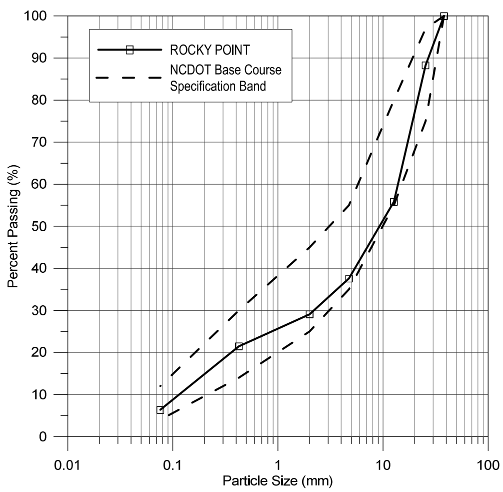
ROCKY POINT
NCDOT Base Course
Specification Band
Percent Passing (%)
Particle Size (mm)

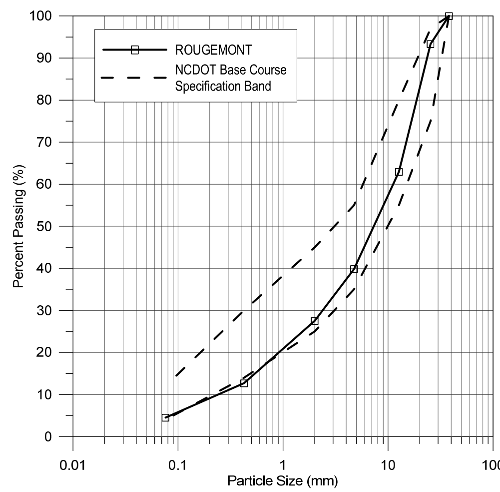
ROUGEMONT
NCDOT Base Course
Specification Band
Percent Passing (%)
Particle Size (mm)

APPENDIX B SHEAR STRENGTH TEST RESULTS

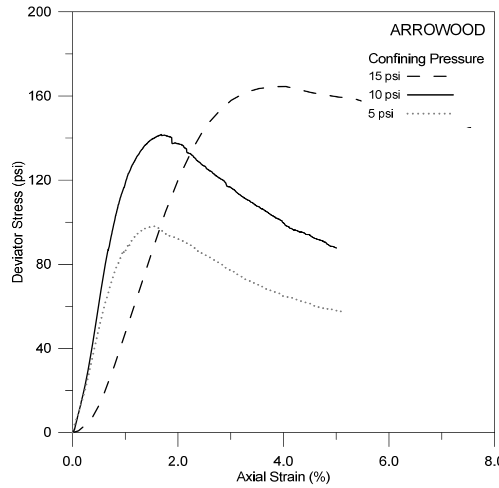

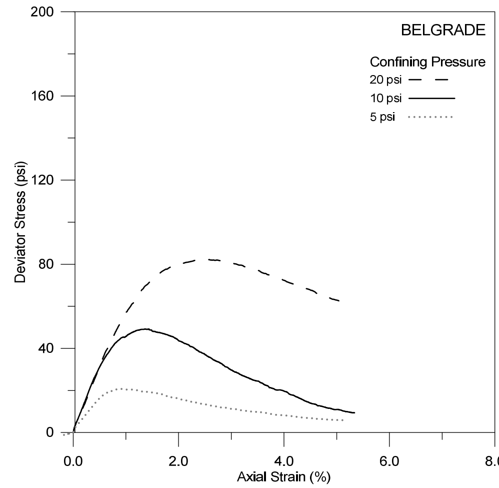

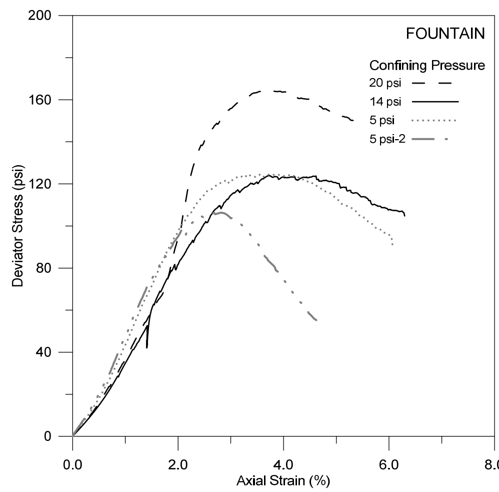

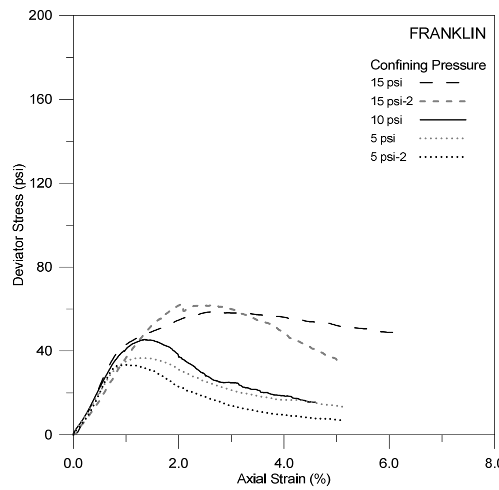

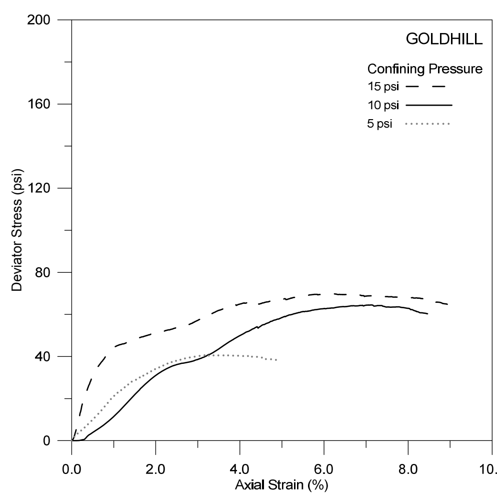

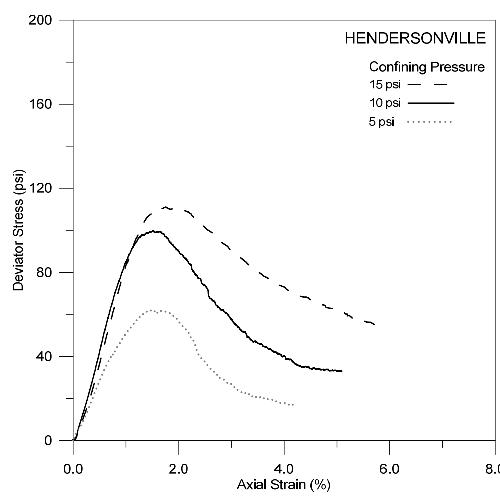

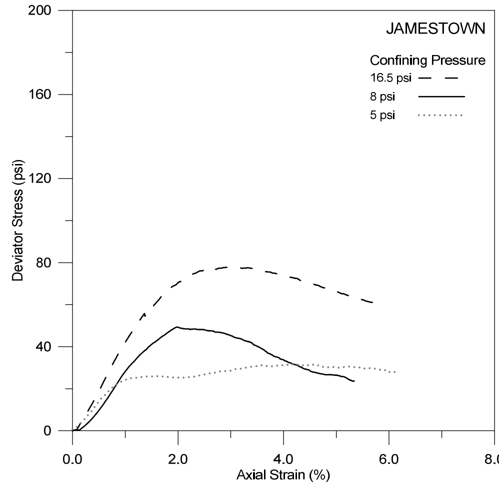
JAMESTOWN
Confining Pressure
16.5 psi
8 psi
5 psi
Deviator Stress (psi)
Axial Strain (%)
0
40
80
120
160
200
0.0
2.0
4.0
6.0
8.0

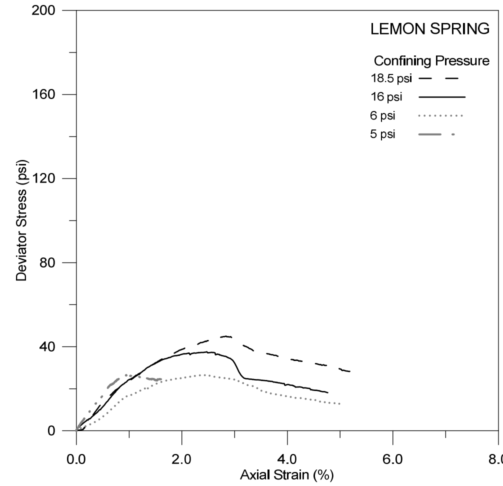
LEMON SPRING
Confining Pressure
18.5 psi
16 psi
6 psi
5 psi
Deviator Stress (psi)
Axial Strain (%)
0
40
80
120
160
200
0.0
2.0
4.0
6.0
8.0

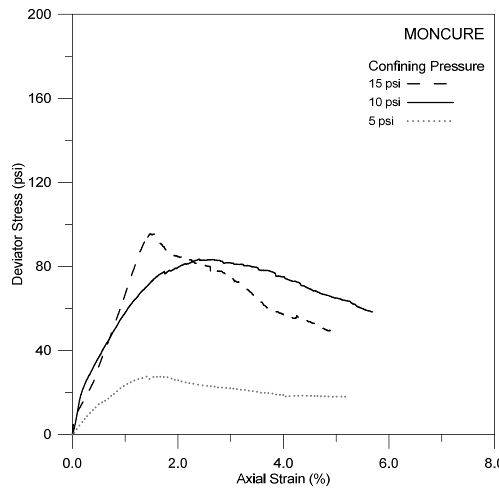
MONCURE
Confining Pressure
15 psi
10 psi
5 psi
Deviator Stress (psi)
Axial Strain (%)
0
40
80
120
160
200
0.0
2.0
4.0
6.0
8.0

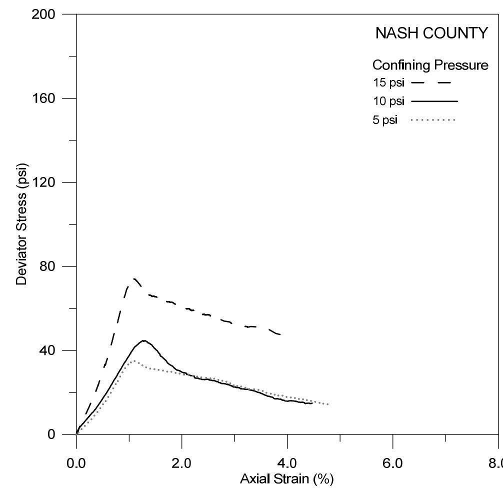
NASH COUNTY
Confining Pressure
15 psi
10 psi
5 psi
Deviator Stress (psi)
Axial Strain (%)
0
40
80
120
160
200
0.0
2.0
4.0
6.0
8.0

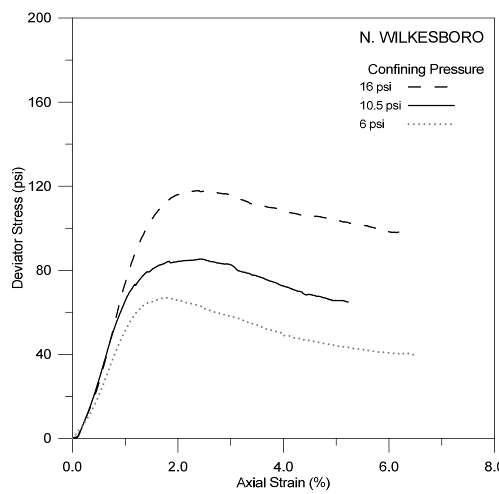
N. WILKESBORO
Confining Pressure
16 psi
10.5 psi
6 psi
Deviator Stress (psi)
Axial Strain (%)
0
40
80
120
160
200
0.0
2.0
4.0
6.0
8.0

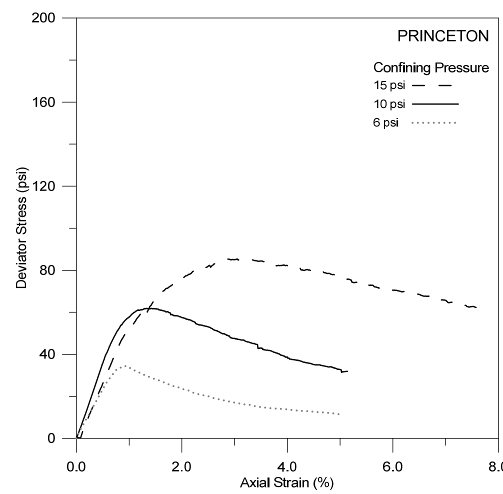
PRINCETON
Confining Pressure
15 psi
10 psi
6 psi
Deviator Stress (psi)
Axial Strain (%)
0
40
80
120
160
200
0.0
2.0
4.0
6.0
8.0

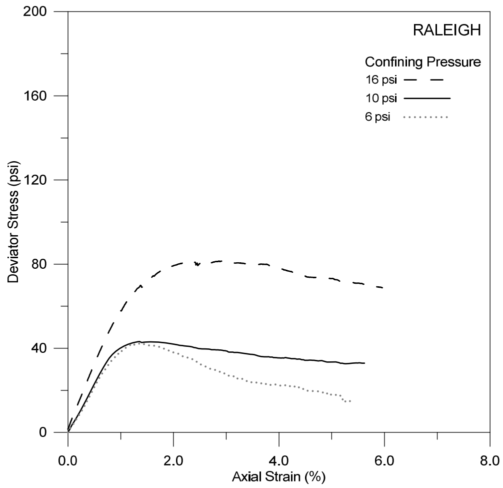
RALEIGH
Confining Pressure
16 psi
10 psi
6 psi
Deviator Stress (psi)
Axial Strain (%)
0
40
80
120
160
200
0.0
2.0
4.0
6.0
8.0

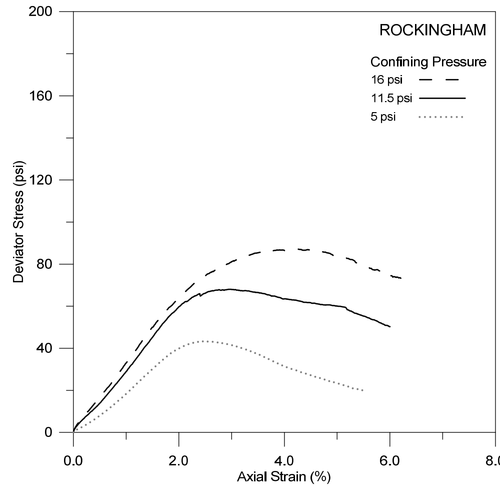
ROCKINGHAM
Confining Pressure
16 psi
11.5 psi
5 psi
Deviator Stress (psi)
Axial Strain (%)
0
40
80
120
160
200
0.0
2.0
4.0
6.0
8.0

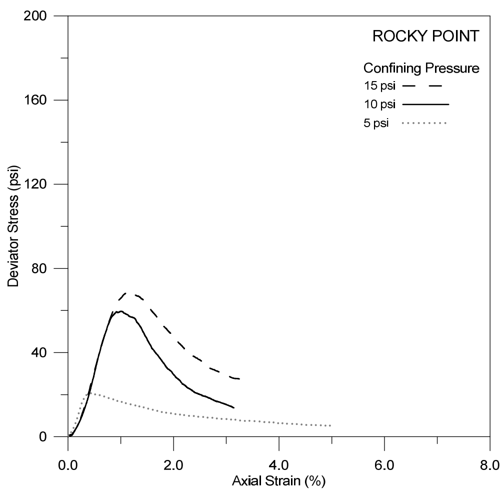
ROCKY POINT
Confining Pressure
15 psi
10 psi
5 psi
Deviator Stress (psi)
Axial Strain (%)
0
40
80
120
160
200
0.0
2.0
4.0
6.0
8.0

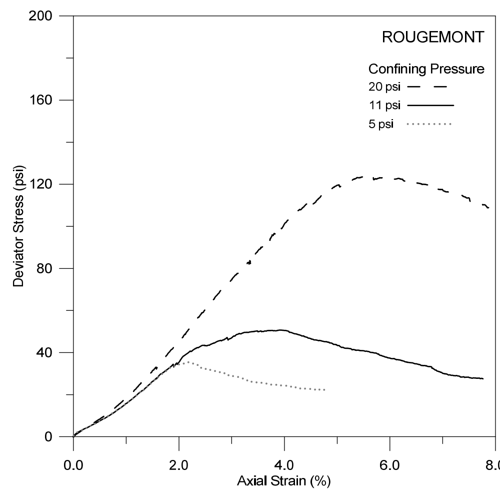
ROUGEMONT
Confining Pressure
20 psi
11 psi
5 psi
Deviator Stress (psi)
Axial Strain (%)
0
40
80
120
160
200
0.0
2.0
4.0
6.0
8.0

APPENDIX C RESILIENT MODULUS TEST RESULTS

Materials & Tests Unit

NCDOT

NORTH CAROLINA DEPARTMENT OF TRANSPORTATION
DIVISION OF HIGHWAY
MATERIALS & TESTS UNIT - SOILS LABORATORY
SUMMARY REPORT OF RESILIENT MODULUS TEST
Subgrade Soils and Untreated Base/Subgrade Materials

1. LAB NO.:	T-5692
2. PROJECT NO.:	5.672
3. SAMPLE NO.:	Q-#031
4. STATION NO.:	
5. SPECIMEN PROPERTIES:	103.9 % Maximum Dry Density at 3.9 % Moisture Content
6. SOURCE OF MATERIAL	Arrowood Quarry
7. TEST SPECIFICATION:	T-307
8. TEST DATE:	6-18-2013

PARAMETER	Chamber Confining Pressure	Nominal Maximum Axial Stress	Actual Applied Max. Axial Load	Actual Applied Cyclic Load	Actual Applied Contact Load	Actual Applied Max. Axial Stress	Actual Applied Cyclic Stress	Actual Applied Contact Stress	Average Recov Def. LVDT 1 and 2	Resilient Strain	Resilient Modulus
DESIGNATION	S_3	S_{cyclic}	P_{max}	P_{cyclic}	$P_{contact}$	S_{max}	S_{cyclic}	$S_{contact}$	H_{avg}	ε_r	M_r
UNIT	psi	psi	lbs	lbs	lbs	psi	psi	psi	in	in/in	psi
Sequence 1	3.0	3.0	87.1	78.1	9.0	3.1	2.8	0.3	0.00223	0.00019	15,131
Sequence 2	3.0	6.0	169.0	154.9	14.2	6.1	5.6	0.5	0.00409	0.00034	16,321
Sequence 3	3.0	9.0	253.5	231.8	21.7	9.1	8.3	0.8	0.00553	0.00046	18,102
Sequence 4	5.0	5.0	139.3	128.6	10.7	5.0	4.6	0.4	0.00272	0.00023	20,403
Sequence 5	5.0	10.0	283.3	259.4	24.0	10.2	9.3	0.9	0.00490	0.00041	22,830
Sequence 6	5.0	15.0	421.6	385.9	35.7	15.2	13.9	1.3	0.00668	0.00056	24,936
Sequence 7	10.0	10.0	281.9	258.7	23.3	10.1	9.3	0.8	0.00361	0.00030	30,946
Sequence 8	10.0	20.0	560.2	512.8	47.4	20.1	18.4	1.7	0.00640	0.00053	34,609
Sequence 9	10.0	30.0	843.5	770.7	72.8	30.3	27.7	2.6	0.00889	0.00074	37,415
Sequence 10	15.0	10.0	278.6	255.7	22.9	10.0	9.2	0.8	0.00301	0.00025	36,648
Sequence 11	15.0	15.0	421.9	385.9	36.0	15.2	13.9	1.3	0.00432	0.00036	38,519
Sequence 12	15.0	30.0	853.0	779.9	73.1	30.7	28.0	2.6	0.00783	0.00065	42,999
Sequence 13	20.0	15.0	421.4	386.7	34.7	15.2	13.9	1.2	0.00384	0.00032	43,418
Sequence 14	20.0	20.0	565.5	518.4	47.1	20.3	18.6	1.7	0.00498	0.00041	44,929
Sequence 15	20.0	40.0	1118.1	1022.1	96.0	40.2	36.8	3.5	0.00879	0.00073	50,197

TESTED BY Suriyati B S DATE 6-18-2013
REVIEWED BY DATE

Materials & Tests Unit

NCDOT

NORTH CAROLINA DEPARTMENT OF TRANSPORTATION
DIVISION OF HIGHWAY
MATERIALS & TESTS UNIT - SOILS LABORATORY

SUMMARY REPORT OF RESILIENT MODULUS TEST

Subgrade Soils and Untreated Base/Subgrade Materials

1. LAB NO.:	T-5707
2. PROJECT NO.:	5.262
3. SAMPLE NO.:	Q#038
4. STATION NO.:	
5. SPECIMEN PROPERTIES:	100.2 % Maximum Dry Density at 7.4 % Moisture Content
6. SOURCE OF MATERIAL	Belgrade Quarry
7. TEST SPECIFICATION:	T-307
8. TEST DATE:	7-3-2013

PARAMETER	*Chamber Confining Pressure*	*Nominal Maximum Axial Stress*	*Actual Applied Max. Axial Load*	*Actual Applied Cyclic Load*	*Actual Applied Contact Load*	*Actual Applied Max. Axial Stress*	*Actual Applied Cyclic Stress*	*Actual Applied Contact Stress*	*Average Recov Def. LVDT 1 and 2*	*Resilient Strain*	*Resilient Modulus*
DESIGNATION	S_3	S_{cyclic}	P_{max}	P_{cyclic}	$P_{contact}$	S_{max}	S_{cyclic}	$S_{contact}$	H_{avg}	ε_r	M_r
UNIT	psi	psi	lbs	lbs	lbs	psi	psi	psi	in	in/in	psi
Sequence 1	3.0	3.0	87.7	77.8	9.8	3.1	2.8	0.4	0.00308	0.00026	10,867
Sequence 2	3.0	6.0	173.7	158.7	14.9	6.2	5.7	0.5	0.00533	0.00044	12,827
Sequence 3	3.0	9.0	250.9	228.6	22.3	9.0	8.2	0.8	0.00657	0.00055	14,992
Sequence 4	5.0	5.0	138.7	126.9	11.7	5.0	4.6	0.4	0.00352	0.00029	15,516
Sequence 5	5.0	10.0	281.0	256.1	24.9	10.1	9.2	0.9	0.00571	0.00048	19,308
Sequence 6	5.0	15.0	419.2	382.0	37.2	15.0	13.7	1.3	0.00744	0.00062	22,122
Sequence 7	10.0	10.0	277.8	253.2	24.6	10.0	9.1	0.9	0.00414	0.00035	26,328
Sequence 8	10.0	20.0	565.7	515.8	49.9	20.3	18.5	1.8	0.00692	0.00058	32,082
Sequence 9	10.0	30.0	844.4	769.3	75.2	30.3	27.6	2.7	0.00928	0.00077	35,695
Sequence 10	15.0	10.0	280.9	256.7	24.2	10.1	9.2	0.9	0.00365	0.00030	30,284
Sequence 11	15.0	15.0	425.8	388.7	37.1	15.3	14.0	1.3	0.00500	0.00042	33,484
Sequence 12	15.0	30.0	854.4	779.7	74.6	30.7	28.0	2.7	0.00809	0.00067	41,493
Sequence 13	20.0	15.0	420.1	383.4	36.7	15.1	13.8	1.3	0.00430	0.00036	38,362
Sequence 14	20.0	20.0	566.0	516.8	49.2	20.3	18.5	1.8	0.00519	0.00043	42,855
Sequence 15	20.0	40.0	1146.0	1044.3	101.7	41.1	37.5	3.7	0.00881	0.00073	51,056

TESTED BY	Suriyati B S	DATE	7-3-2013
REVIEWED BY		DATE	

Materials & Tests Unit

NCDOT

NORTH CAROLINA DEPARTMENT OF TRANSPORTATION
DIVISION OF HIGHWAY
MATERIALS & TESTS UNIT - SOILS LABORATORY

SUMMARY REPORT OF RESILIENT MODULUS TEST

Subgrade Soils and Untreated Base/Subgrade Materials

1. LAB NO.: T-5722
2. PROJECT NO.:
3. SAMPLE NO.: Q#042
4. STATION NO.:
5. SPECIMEN PROPERTIES: 93.9 % Maximum Dry Density at 6.6 % Moisture Content
6. SOURCE OF MATERIAL MM Fountain Quarry
7. TEST SPECIFICATION: T-307
8. TEST DATE: 8-5-2013

PARAMETER	Chamber Confining Pressure	Nominal Maximum Axial Stress	Actual Applied Max. Axial Load	Actual Applied Cyclic Load	Actual Applied Contact Load	Actual Applied Max. Axial Stress	Actual Applied Cyclic Stress	Actual Applied Contact Stress	Average Recov Def. LVDT 1 and 2	Resilient Strain	Resilient Modulus
DESIGNATION	S_3	S_{cyclic}	P_{max}	P_{cyclic}	$P_{contact}$	S_{max}	S_{cyclic}	$S_{contact}$	H_{avg}	ε_r	M_r
UNIT	psi	psi	lbs	lbs	lbs	psi	psi	psi	in	in/in	psi
Sequence 1	3.0	3.0	87.8	77.5	10.3	3.2	2.8	0.4	0.00528	0.00044	6,321
Sequence 2	3.0	6.0	168.7	153.9	14.8	6.1	5.5	0.5	0.00885	0.00074	7,490
Sequence 3	3.0	9.0	258.1	235.3	22.9	9.3	8.4	0.8	0.01160	0.00097	8,737
Sequence 4	5.0	5.0	140.9	128.8	12.1	5.1	4.6	0.4	0.00594	0.00050	9,335
Sequence 5	5.0	10.0	285.2	259.5	25.7	10.2	9.3	0.9	0.01004	0.00084	11,139
Sequence 6	5.0	15.0	432.9	393.7	39.2	15.5	14.1	1.4	0.01344	0.00112	12,619
Sequence 7	10.0	10.0	286.7	261.3	25.4	10.3	9.4	0.9	0.00695	0.00058	16,192
Sequence 8	10.0	20.0	562.1	510.8	51.2	20.2	18.3	1.8	0.01183	0.00099	18,594
Sequence 9	10.0	30.0	855.4	777.1	78.4	30.7	27.9	2.8	0.01586	0.00132	21,098
Sequence 10	15.0	10.0	280.1	255.1	25.0	10.1	9.2	0.9	0.00562	0.00047	19,542
Sequence 11	15.0	15.0	425.6	387.3	38.4	15.3	13.9	1.4	0.00788	0.00066	21,176
Sequence 12	15.0	30.0	861.8	782.5	79.3	30.9	28.1	2.8	0.01332	0.00111	25,308
Sequence 13	20.0	15.0	428.2	389.6	38.7	15.4	14.0	1.4	0.00655	0.00055	25,609
Sequence 14	20.0	20.0	573.3	521.2	52.1	20.6	18.7	1.9	0.00823	0.00069	27,275
Sequence 15	20.0	40.0	1148.1	1040.9	107.2	41.2	37.4	3.8	0.01399	0.00117	32,036

TESTED BY Suriyati B S DATE 8-5-2013
REVIEWED BY DATE

Materials & Tests Unit

NCDOT

NORTH CAROLINA DEPARTMENT OF TRANSPORTATION
DIVISION OF HIGHWAY
MATERIALS & TESTS UNIT - SOILS LABORATORY
SUMMARY REPORT OF RESILIENT MODULUS TEST
Subgrade Soils and Untreated Base/Subgrade Materials

1. LAB NO.:	T-5720
2. PROJECT NO.:	
3. SAMPLE NO.:	Q#016
4. STATION NO.:	
5. SPECIMEN PROPERTIES:	99.4% Maximum Dry Density at 5.5 % Moisture Content
6. SOURCE OF MATERIAL	Harrison-Franklin Quarry
7. TEST SPECIFICATION:	T-307
8. TEST DATE:	7-30-2013

PARAMETER	*Chamber Confining Pressure*	*Nominal Maximum Axial Stress*	*Actual Applied Max. Axial Load*	*Actual Applied Cyclic Load*	*Actual Applied Contact Load*	*Actual Applied Max. Axial Stress*	*Actual Applied Cyclic Stress*	*Actual Applied Contact Stress*	*Average Recov Def. LVDT 1 and 2*	*Resilient Strain*	*Resilient Modulus*
DESIGNATION	S_3	S_{cyclic}	P_{max}	P_{cyclic}	$P_{contact}$	S_{max}	S_{cyclic}	$S_{contact}$	H_{avg}	ε_r	M_r
UNIT	psi	psi	lbs	lbs	lbs	psi	psi	psi	in	in/in	psi
Sequence 1	3.0	3.0	87.8	77.8	10.0	3.2	2.8	0.4	0.00395	0.00033	8,501
Sequence 2	3.0	6.0	171.4	157.0	14.3	6.2	5.6	0.5	0.00634	0.00053	10,667
Sequence 3	3.0	9.0	255.9	234.0	22.0	9.2	8.4	0.8	0.00801	0.00067	12,581
Sequence 4	5.0	5.0	140.8	128.9	11.8	5.1	4.6	0.4	0.00421	0.00035	13,199
Sequence 5	5.0	10.0	283.8	259.3	24.5	10.2	9.3	0.9	0.00684	0.00057	16,328
Sequence 6	5.0	15.0	428.5	391.7	36.8	15.4	14.1	1.3	0.00911	0.00076	18,524
Sequence 7	10.0	10.0	284.1	260.0	24.0	10.2	9.3	0.9	0.00494	0.00041	22,670
Sequence 8	10.0	20.0	567.6	518.8	48.8	20.4	18.6	1.8	0.00828	0.00069	26,979
Sequence 9	10.0	30.0	843.6	768.8	74.8	30.3	27.6	2.7	0.01108	0.00092	29,877
Sequence 10	15.0	10.0	283.3	258.9	24.5	10.2	9.3	0.9	0.00457	0.00038	27,274
Sequence 11	15.0	15.0	428.8	391.7	37.2	15.4	14.1	1.3	0.00569	0.00047	29,623
Sequence 12	15.0	30.0	845.4	771.1	74.3	30.3	27.7	2.7	0.00939	0.00078	35,365
Sequence 13	20.0	15.0	420.8	384.0	36.9	15.1	13.8	1.3	0.00483	0.00040	34,272
Sequence 14	20.0	20.0	561.9	513.1	48.8	20.2	18.4	1.8	0.00621	0.00052	35,573
Sequence 15	20.0	40.0	1140.3	1039.6	100.7	40.9	37.3	3.6	0.01052	0.00088	42,559

TESTED BY	Suriyati B S	DATE	7-30-2013
REVIEWED BY		DATE	

Materials & Tests Unit

NCDOT

NORTH CAROLINA DEPARTMENT OF TRANSPORTATION
DIVISION OF HIGHWAY
MATERIALS & TESTS UNIT - SOILS LABORATORY
SUMMARY REPORT OF RESILIENT MODULUS TEST
Subgrade Soils and Untreated Base/Subgrade Materials

1. LAB NO.:	T-5725
2. PROJECT NO.:	VM Gold Hill Q#085
3. SAMPLE NO.:	Q#085
4. STATION NO.:	
5. SPECIMEN PROPERTIES:	99.8 % Maximum Dry Density at 6.8 % Moisture Content
6. SOURCE OF MATERIAL	Quarry #085
7. TEST SPECIFICATION:	T-307
8. TEST DATE:	9-18-2013

PARAMETER	Chamber Confining Pressure	Nominal Maximum Axial Stress	Actual Applied Max. Axial Load	Actual Applied Cyclic Load	Actual Applied Contact Load	Actual Applied Max. Axial Stress	Actual Applied Cyclic Stress	Actual Applied Contact Stress	Average Recov Def. LVDT 1 and 2	Resilient Strain	Resilient Modulus
DESIGNATION	S_3	S_{cyclic}	P_{max}	P_{cyclic}	$P_{contact}$	S_{max}	S_{cyclic}	$S_{contact}$	H_{avg}	ε_r	M_r
UNIT	psi	psi	lbs	lbs	lbs	psi	psi	psi	in	in/in	psi
Sequence 1	3.0	3.0	87.8	78.0	9.8	3.2	2.8	0.4	0.00323	0.00027	10,406
Sequence 2	3.0	6.0	168.6	153.9	14.7	6.1	5.5	0.5	0.00584	0.00049	11,358
Sequence 3	3.0	9.0	258.2	235.4	22.8	9.3	8.4	0.8	0.00766	0.00064	13,231
Sequence 4	5.0	5.0	141.7	129.8	11.9	5.1	4.7	0.4	0.00398	0.00033	14,051
Sequence 5	5.0	10.0	282.4	257.5	24.9	10.1	9.2	0.9	0.00662	0.00055	16,749
Sequence 6	5.0	15.0	429.1	391.0	38.1	15.4	14.0	1.4	0.00893	0.00074	18,865
Sequence 7	10.0	10.0	285.1	260.2	24.9	10.2	9.3	0.9	0.00480	0.00040	23,360
Sequence 8	10.0	20.0	566.2	516.0	50.2	20.3	18.5	1.8	0.00837	0.00070	26,548
Sequence 9	10.0	30.0	845.0	768.1	77.0	30.3	27.6	2.8	0.01183	0.00099	27,953
Sequence 10	15.0	10.0	277.9	253.4	24.6	10.0	9.1	0.9	0.00400	0.00033	27,289
Sequence 11	15.0	15.0	420.3	382.5	37.7	15.1	13.7	1.4	0.00568	0.00047	28,988
Sequence 12	15.0	30.0	853.3	776.3	77.1	30.6	27.9	2.8	0.00997	0.00083	33,529
Sequence 13	20.0	15.0	421.2	383.4	37.7	15.1	13.8	1.4	0.00489	0.00041	33,798
Sequence 14	20.0	20.0	567.4	517.0	50.4	20.4	18.6	1.8	0.00625	0.00052	35,639
Sequence 15	20.0	40.0	1141.3	1036.9	104.4	41.0	37.2	3.7	0.01133	0.00094	39,414

TESTED BY Suriyati B S DATE 9-18-2013
REVIEWED BY DATE

Materials & Tests Unit

NCDOT

NORTH CAROLINA DEPARTMENT OF TRANSPORTATION
DIVISION OF HIGHWAY
MATERIALS & TESTS UNIT - SOILS LABORATORY
SUMMARY REPORT OF RESILIENT MODULUS TEST
Subgrade Soils and Untreated Base/Subgrade Materials

1. LAB NO.:	T-5650
2. PROJECT NO.:	5.952
3. SAMPLE NO.:	Q# 081
4. STATION NO.:	
5. SPECIMEN PROPERTIES:	100.0 % Maximum Dry Density at 6.0 % Moisture Content
6. SOURCE OF MATERIAL	Hendersonville Quarry
7. TEST SPECIFICATION:	T-307
8. TEST DATE:	6-25-2013

PARAMETER	Chamber Confining Pressure	Nominal Maximum Axial Stress	Actual Applied Max. Axial Load	Actual Applied Cyclic Load	Actual Applied Contact Load	Actual Applied Max. Axial Stress	Actual Applied Cyclic Stress	Actual Applied Contact Stress	Average Recov Def. LVDT 1 and 2	Resilient Strain	Resilient Modulus
DESIGNATION	S_3	S_{cyclic}	P_{max}	P_{cyclic}	$P_{contact}$	S_{max}	S_{cyclic}	$S_{contact}$	H_{avg}	ε_r	M_r
UNIT	psi	psi	lbs	lbs	lbs	psi	psi	psi	in	in/in	psi
Sequence 1	3.0	3.0	88.1	77.7	10.4	3.2	2.8	0.4	0.00377	0.00031	8,892
Sequence 2	3.0	6.0	169.5	154.6	14.9	6.1	5.6	0.5	0.00650	0.00054	10,268
Sequence 3	3.0	9.0	256.3	233.2	23.1	9.2	8.4	0.8	0.00854	0.00071	11,778
Sequence 4	5.0	5.0	140.5	127.9	12.6	5.1	4.6	0.5	0.00435	0.00036	12,692
Sequence 5	5.0	10.0	281.0	255.2	25.7	10.1	9.2	0.9	0.00742	0.00062	14,850
Sequence 6	5.0	15.0	423.1	384.3	38.8	15.2	13.8	1.4	0.00995	0.00083	16,666
Sequence 7	10.0	10.0	282.1	256.1	26.0	10.1	9.2	0.9	0.00519	0.00043	21,319
Sequence 8	10.0	20.0	565.9	514.0	51.9	20.4	18.5	1.9	0.00906	0.00075	24,497
Sequence 9	10.0	30.0	849.0	771.0	77.9	30.5	27.7	2.8	0.01233	0.00103	26,982
Sequence 10	15.0	10.0	278.7	253.0	25.8	10.0	9.1	0.9	0.00415	0.00035	26,324
Sequence 11	15.0	15.0	423.8	385.2	38.5	15.2	13.9	1.4	0.00599	0.00050	27,740
Sequence 12	15.0	30.0	842.9	765.3	77.6	30.3	27.5	2.8	0.01035	0.00086	31,904
Sequence 13	20.0	15.0	418.9	380.6	38.3	15.1	13.7	1.4	0.00510	0.00042	32,209
Sequence 14	20.0	20.0	565.2	514.1	51.1	20.3	18.5	1.8	0.00658	0.00055	33,739
Sequence 15	20.0	40.0	1125.2	1021.7	103.4	40.5	36.7	3.7	0.01157	0.00096	38,126

TESTED BY	Suriyati B S	DATE	6-25-2013
REVIEWED BY		DATE	

Materials & Tests Unit

NCDOT

NORTH CAROLINA DEPARTMENT OF TRANSPORTATION
DIVISION OF HIGHWAY
MATERIALS & TESTS UNIT - SOILS LABORATORY
SUMMARY REPORT OF RESILIENT MODULUS TEST
Subgrade Soils and Untreated Base/Subgrade Materials

1. LAB NO.: T-5649
2. PROJECT NO.: Jamestown Q#046
3. SAMPLE NO.: Q#046
4. STATION NO.:
5. SPECIMEN PROPERTIES: 101.0 % Maximum Dry Density at 5.0 % Moisture Content
6. SOURCE OF MATERIAL Quarry
7. TEST SPECIFICATION: T-307
8. TEST DATE: 7-3-2013

PARAMETER	Chamber Confining Pressure	Nominal Maximum Axial Stress	Actual Applied Max. Axial Load	Actual Applied Cyclic Load	Actual Applied Contact Load	Actual Applied Max. Axial Stress	Actual Applied Cyclic Stress	Actual Applied Contact Stress	Average Recov Def. LVDT 1 and 2	Resilient Strain	Resilient Modulus
DESIGNATION	S_3	S_{cyclic}	P_{max}	P_{cyclic}	$P_{contact}$	S_{max}	S_{cyclic}	$S_{contact}$	H_{avg}	ε_r	M_r
UNIT	psi	psi	lbs	lbs	lbs	psi	psi	psi	in	in/in	psi
Sequence 1	3.0	3.0	87.0	76.3	10.6	3.1	2.7	0.4	0.00299	0.00025	10,982
Sequence 2	3.0	6.0	169.4	153.4	15.9	6.1	5.5	0.6	0.00532	0.00044	12,417
Sequence 3	3.0	9.0	254.0	229.8	24.2	9.1	8.2	0.9	0.00685	0.00057	14,449
Sequence 4	5.0	5.0	141.6	128.5	13.1	5.1	4.6	0.5	0.00362	0.00030	15,266
Sequence 5	5.0	10.0	282.3	255.3	27.0	10.1	9.2	1.0	0.00604	0.00050	18,197
Sequence 6	5.0	15.0	422.9	382.0	40.8	15.2	13.7	1.5	0.00814	0.00068	20,217
Sequence 7	10.0	10.0	282.3	255.3	27.0	10.1	9.2	1.0	0.00440	0.00037	24,961
Sequence 8	10.0	20.0	563.5	508.9	54.6	20.2	18.3	2.0	0.00776	0.00065	28,254
Sequence 9	10.0	30.0	843.9	761.5	82.4	30.3	27.3	3.0	0.01089	0.00091	30,129
Sequence 10	15.0	10.0	282.2	255.2	27.0	10.1	9.2	1.0	0.00385	0.00032	28,532
Sequence 11	15.0	15.0	422.8	381.9	40.9	15.2	13.7	1.5	0.00544	0.00045	30,222
Sequence 12	15.0	30.0	843.9	761.4	82.5	30.3	27.3	3.0	0.00934	0.00078	35,122
Sequence 13	20.0	15.0	423.0	382.5	40.5	15.2	13.7	1.5	0.00476	0.00040	34,584
Sequence 14	20.0	20.0	563.3	508.8	54.5	20.2	18.3	2.0	0.00600	0.00050	36,546
Sequence 15	20.0	40.0	1123.4	1013.2	110.3	40.3	36.4	4.0	0.01051	0.00088	41,535

TESTED BY Suriyati B S DATE 7-3-2013
REVIEWED BY DATE

Materials & Tests Unit

NCDOT

NORTH CAROLINA DEPARTMENT OF TRANSPORTATION
DIVISION OF HIGHWAY
MATERIALS & TESTS UNIT - SOILS LABORATORY
SUMMARY REPORT OF RESILIENT MODULUS TEST
Subgrade Soils and Untreated Base/Subgrade Materials

1. LAB NO.:	T-5721
2. PROJECT NO.:	
3. SAMPLE NO.:	Q#097
4. STATION NO.:	
5. SPECIMEN PROPERTIES:	100.8 % Maximum Dry Density at 5.0 % Moisture Content
6. SOURCE OF MATERIAL	MM Lemon Springs Quarry
7. TEST SPECIFICATION:	T-307
8. TEST DATE:	7-31-2013

PARAMETER	Chamber Confining Pressure	Nominal Maximum Axial Stress	Actual Applied Max. Axial Load	Actual Applied Cyclic Load	Actual Applied Contact Load	Actual Applied Max. Axial Stress	Actual Applied Cyclic Stress	Actual Applied Contact Stress	Average Recov Def. LVDT 1 and 2	Resilient Strain	Resilient Modulus
DESIGNATION	S_3	S_{cyclic}	P_{max}	P_{cyclic}	$P_{contact}$	S_{max}	S_{cyclic}	$S_{contact}$	H_{avg}	ε_r	M_r
UNIT	psi	psi	lbs	lbs	lbs	psi	psi	psi	in	in/in	psi
Sequence 1	3.0	3.0	87.7	77.5	10.2	3.1	2.8	0.4	0.00321	0.00027	10,411
Sequence 2	3.0	6.0	170.5	155.3	15.2	6.1	5.6	0.5	0.00557	0.00046	12,010
Sequence 3	3.0	9.0	257.3	233.6	23.7	9.2	8.4	0.8	0.00713	0.00059	14,118
Sequence 4	5.0	5.0	140.6	128.2	12.4	5.0	4.6	0.4	0.00381	0.00032	14,491
Sequence 5	5.0	10.0	284.5	258.5	26.0	10.2	9.3	0.9	0.00632	0.00053	17,630
Sequence 6	5.0	15.0	426.1	386.0	40.2	15.3	13.9	1.4	0.00844	0.00070	19,692
Sequence 7	10.0	10.0	284.6	258.4	26.2	10.2	9.3	0.9	0.00465	0.00039	23,908
Sequence 8	10.0	20.0	568.3	514.5	53.8	20.4	18.5	1.9	0.00806	0.00067	27,500
Sequence 9	10.0	30.0	848.9	767.3	81.6	30.5	27.5	2.9	0.01120	0.00093	29,508
Sequence 10	15.0	10.0	284.3	258.4	25.9	10.2	9.3	0.9	0.00407	0.00034	27,346
Sequence 11	15.0	15.0	426.1	386.4	39.7	15.3	13.9	1.4	0.00569	0.00047	29,237
Sequence 12	15.0	30.0	850.1	768.4	81.7	30.5	27.6	2.9	0.00960	0.00080	34,480
Sequence 13	20.0	15.0	426.7	387.0	39.6	15.3	13.9	1.4	0.00496	0.00041	33,580
Sequence 14	20.0	20.0	568.5	515.0	53.5	20.4	18.5	1.9	0.00621	0.00052	35,737
Sequence 15	20.0	40.0	1131.8	1022.0	109.8	40.6	36.7	3.9	0.01073	0.00089	41,024

TESTED BY	Suriyati B S	DATE	7-31-2013
REVIEWED BY		DATE	

Materials & Tests Unit

NCDOT

NORTH CAROLINA DEPARTMENT OF TRANSPORTATION
DIVISION OF HIGHWAY
MATERIALS & TESTS UNIT - SOILS LABORATORY
SUMMARY REPORT OF RESILIENT MODULUS TEST
Subgrade Soils and Untreated Base/Subgrade Materials

1. LAB NO.: T-5693
2. PROJECT NO.: 5.542
3. SAMPLE NO.: Q#100
4. STATION NO.:
5. SPECIMEN PROPERTIES: 99.6% Maximum Dry Density at 6.0 % Moisture Content
6. SOURCE OF MATERIAL Moncure Quarry
7. TEST SPECIFICATION: T-307
8. TEST DATE: 6-25-2013

PARAMETER	Chamber Confining Pressure	Nominal Maximum Axial Stress	Actual Applied Max. Axial Load	Actual Applied Cyclic Load	Actual Applied Contact Load	Actual Applied Max. Axial Stress	Actual Applied Cyclic Stress	Actual Applied Contact Stress	Average Recov Def. LVDT 1 and 2	Resilient Strain	Resilient Modulus
DESIGNATION	S_3	S_{cyclic}	P_{max}	P_{cyclic}	$P_{contact}$	S_{max}	S_{cyclic}	$S_{contact}$	H_{avg}	ε_r	M_r
UNIT	psi	psi	lbs	lbs	lbs	psi	psi	psi	in	in/in	psi
Sequence 1	3.0	3.0	67.9	59.1	8.8	2.4	2.1	0.3	0.00230	0.00019	11,081
Sequence 2	3.0	6.0	138.0	124.8	13.3	5.0	4.5	0.5	0.00437	0.00036	12,322
Sequence 3	3.0	9.0	252.0	229.3	22.7	9.1	8.2	0.8	0.00645	0.00054	15,352
Sequence 4	5.0	5.0	139.2	127.4	11.7	5.0	4.6	0.4	0.00346	0.00029	15,880
Sequence 5	5.0	10.0	281.1	256.5	24.6	10.1	9.2	0.9	0.00580	0.00048	19,084
Sequence 6	5.0	15.0	420.3	382.9	37.4	15.1	13.8	1.3	0.00770	0.00064	21,473
Sequence 7	10.0	10.0	280.1	255.6	24.4	10.1	9.2	0.9	0.00433	0.00036	25,452
Sequence 8	10.0	20.0	566.8	516.1	50.7	20.4	18.6	1.8	0.00739	0.00062	30,157
Sequence 9	10.0	30.0	848.9	772.2	76.8	30.5	27.8	2.8	0.01000	0.00083	33,317
Sequence 10	15.0	10.0	273.2	249.2	24.0	9.8	9.0	0.9	0.00376	0.00031	28,576
Sequence 11	15.0	15.0	416.8	379.5	37.3	15.0	13.7	1.3	0.00523	0.00044	31,345
Sequence 12	15.0	30.0	840.2	764.4	75.9	30.2	27.5	2.7	0.00866	0.00072	38,073
Sequence 13	20.0	15.0	422.5	385.7	36.8	15.2	13.9	1.3	0.00473	0.00039	35,209
Sequence 14	20.0	20.0	563.2	513.8	49.4	20.3	18.5	1.8	0.00586	0.00049	37,852
Sequence 15	20.0	40.0	1124.5	1022.3	102.2	40.4	36.8	3.7	0.00969	0.00081	45,546

TESTED BY Suriyati B S DATE 6-25-2013
REVIEWED BY DATE

Materials & Tests Unit

NCDOT

NORTH CAROLINA DEPARTMENT OF TRANSPORTATION
DIVISION OF HIGHWAY
MATERIALS & TESTS UNIT - SOILS LABORATORY
SUMMARY REPORT OF RESILIENT MODULUS TEST
Subgrade Soils and Untreated Base/Subgrade Materials

1. LAB NO.:	T-5631_A1
2. PROJECT NO.:	Wake Stone Q223
3. SAMPLE NO.:	UW-10-12
4. STATION NO.:	
5. SPECIMEN PROPERTIES:	101.3 % Maximum Dry Density at 6.2 % Moisture Content
6. SOURCE OF MATERIAL	Stockpile
7. TEST SPECIFICATION:	T307
8. TEST DATE:	January 9, 2013

PARAMETER	Chamber Confining Pressure	Nominal Maximum Axial Stress	Actual Applied Max. Axial Load	Actual Applied Cyclic Load	Actual Applied Contact Load	Actual Applied Max. Axial Stress	Actual Applied Cyclic Stress	Actual Applied Contact Stress	Average Recov Def. LVDT 1 and 2	Resilient Strain	Resilient Modulus
DESIGNATION	S_3	S_{cyclic}	P_{max}	P_{cyclic}	$P_{contact}$	S_{max}	S_{cyclic}	$S_{contact}$	H_{avg}	ε_r	M_r
UNIT	psi	psi	lbs	lbs	lbs	psi	psi	psi	in	in/in	psi
Sequence 1	3.0	3.0	87.5	76.8	10.7	3.1	2.8	0.4	0.00486	0.00040	6,793
Sequence 2	3.0	6.0	170.1	154.2	15.9	6.1	5.5	0.6	0.00831	0.00069	7,978
Sequence 3	3.0	9.0	253.4	229.4	24.0	9.1	8.2	0.9	0.01055	0.00088	9,342
Sequence 4	5.0	5.0	142.4	129.3	13.1	5.1	4.6	0.5	0.00455	0.00038	12,210
Sequence 5	5.0	10.0	284.1	257.3	26.8	10.2	9.2	1.0	0.00741	0.00062	14,927
Sequence 6	5.0	15.0	423.3	382.9	40.4	15.2	13.7	1.4	0.00928	0.00077	17,722
Sequence 7	10.0	10.0	281.8	254.8	27.0	10.1	9.1	1.0	0.00406	0.00034	26,974
Sequence 8	10.0	20.0	566.3	511.9	54.5	20.3	18.3	2.0	0.00692	0.00058	31,773
Sequence 9	10.0	30.0	849.2	767.5	81.8	30.4	27.5	2.9	0.00964	0.00080	34,193
Sequence 10	15.0	10.0	282.5	255.6	26.9	10.1	9.2	1.0	0.00338	0.00028	32,509
Sequence 11	15.0	15.0	422.6	382.1	40.5	15.1	13.7	1.5	0.00471	0.00039	34,883
Sequence 12	15.0	30.0	846.4	764.8	81.6	30.3	27.4	2.9	0.00794	0.00066	41,405
Sequence 13	20.0	15.0	422.8	382.2	40.6	15.1	13.7	1.5	0.00396	0.00033	41,489
Sequence 14	20.0	20.0	566.2	511.8	54.3	20.3	18.3	1.9	0.00500	0.00042	43,969
Sequence 15	20.0	40.0	1022.3	924.8	97.6	36.6	33.1	3.5	0.00795	0.00066	49,999

TESTED BY	Suriyati B S	DATE	January 9, 2013
REVIEWED BY		DATE	

Materials & Tests Unit

NCDOT

NORTH CAROLINA DEPARTMENT OF TRANSPORTATION
DIVISION OF HIGHWAY
MATERIALS & TESTS UNIT - SOILS LABORATORY
SUMMARY REPORT OF RESILIENT MODULUS TEST
Subgrade Soils and Untreated Base/Subgrade Materials

1. LAB NO.:	T-5719
2. PROJECT NO.:	
3. SAMPLE NO.:	Q#079
4. STATION NO.:	
5. SPECIMEN PROPERTIES:	99.8 % Maximum Dry Density at 5.4 % Moisture Content
6. SOURCE OF MATERIAL	V M Quarry 115
7. TEST SPECIFICATION:	T-307
8. TEST DATE:	7-29-2013

PARAMETER	Chamber Confining Pressure	Nominal Maximum Axial Stress	Actual Applied Max. Axial Load	Actual Applied Cyclic Load	Actual Applied Contact Load	Actual Applied Max. Axial Stress	Actual Applied Cyclic Stress	Actual Applied Contact Stress	Average Recov Def. LVDT 1 and 2	Resilient Strain	Resilient Modulus
DESIGNATION	S_3	S_{cyclic}	P_{max}	P_{cyclic}	$P_{contact}$	S_{max}	S_{cyclic}	$S_{contact}$	H_{avg}	ε_r	M_r
UNIT	psi	psi	lbs	lbs	lbs	psi	psi	psi	in	in/in	psi
Sequence 1	3.0	3.0	86.6	77.7	8.9	3.1	2.8	0.3	0.00267	0.00022	12,547
Sequence 2	3.0	6.0	170.5	156.5	14.0	6.1	5.6	0.5	0.00492	0.00041	13,695
Sequence 3	3.0	9.0	255.1	233.3	21.8	9.2	8.4	0.8	0.00661	0.00055	15,210
Sequence 4	5.0	5.0	142.6	131.4	11.2	5.1	4.7	0.4	0.00337	0.00028	16,796
Sequence 5	5.0	10.0	284.3	260.4	23.9	10.2	9.3	0.9	0.00584	0.00049	19,205
Sequence 6	5.0	15.0	430.0	393.2	36.8	15.4	14.1	1.3	0.00809	0.00067	20,939
Sequence 7	10.0	10.0	284.1	260.4	23.7	10.2	9.3	0.9	0.00432	0.00036	25,938
Sequence 8	10.0	20.0	570.8	522.0	48.8	20.5	18.7	1.8	0.00777	0.00065	28,923
Sequence 9	10.0	30.0	859.8	784.9	74.8	30.9	28.2	2.7	0.01098	0.00092	30,780
Sequence 10	15.0	10.0	282.4	259.7	22.7	10.1	9.3	0.8	0.00369	0.00031	30,307
Sequence 11	15.0	15.0	426.8	390.2	36.5	15.3	14.0	1.3	0.00525	0.00044	32,024
Sequence 12	15.0	30.0	845.1	772.3	72.8	30.3	27.7	2.6	0.00925	0.00077	35,975
Sequence 13	20.0	15.0	417.6	382.0	35.6	15.0	13.7	1.3	0.00454	0.00038	36,247
Sequence 14	20.0	20.0	562.8	514.7	48.0	20.2	18.5	1.7	0.00584	0.00049	37,973
Sequence 15	20.0	40.0	1138.8	1039.2	99.6	40.9	37.3	3.6	0.01065	0.00089	42,022

TESTED BY	Suriyati B S	DATE	7-29-2013
REVIEWED BY		DATE	

Materials & Tests Unit

NCDOT

NORTH CAROLINA DEPARTMENT OF TRANSPORTATION
DIVISION OF HIGHWAY
MATERIALS & TESTS UNIT - SOILS LABORATORY
SUMMARY REPORT OF RESILIENT MODULUS TEST
Subgrade Soils and Untreated Base/Subgrade Materials

1. LAB NO.:	T-5726
2. PROJECT NO.:	Quarry Research
3. SAMPLE NO.:	Q#064
4. STATION NO.:	
5. SPECIMEN PROPERTIES:	99.6% Maximum Dry Density at 5.7 % Moisture Content
6. SOURCE OF MATERIAL	Hanson Quarry#064
7. TEST SPECIFICATION:	T-307
8. TEST DATE:	10-2-2013

PARAMETER	Chamber Confining Pressure	Nominal Maximum Axial Stress	Actual Applied Max. Axial Load	Actual Applied Cyclic Load	Actual Applied Contact Load	Actual Applied Max. Axial Stress	Actual Applied Cyclic Stress	Actual Applied Contact Stress	Average Recov Def. LVDT 1 and 2	Resilient Strain	Resilient Modulus
DESIGNATION	S_3	S_{cyclic}	P_{max}	P_{cyclic}	$P_{contact}$	S_{max}	S_{cyclic}	$S_{contact}$	H_{avg}	ε_r	M_r
UNIT	psi	psi	lbs	lbs	lbs	psi	psi	psi	in	in/in	psi
Sequence 1	3.0	3.0	87.6	77.0	10.6	3.1	2.8	0.4	0.00390	0.00033	8,492
Sequence 2	3.0	6.0	170.3	154.6	15.7	6.1	5.5	0.6	0.00647	0.00054	10,290
Sequence 3	3.0	9.0	256.9	233.1	23.8	9.2	8.4	0.9	0.00813	0.00068	12,351
Sequence 4	5.0	5.0	140.1	127.0	13.1	5.0	4.6	0.5	0.00417	0.00035	13,106
Sequence 5	5.0	10.0	286.0	259.3	26.7	10.3	9.3	1.0	0.00674	0.00056	16,566
Sequence 6	5.0	15.0	428.7	388.2	40.5	15.4	13.9	1.5	0.00888	0.00074	18,828
Sequence 7	10.0	10.0	284.2	257.4	26.8	10.2	9.2	1.0	0.00470	0.00039	23,582
Sequence 8	10.0	20.0	566.6	512.5	54.1	20.3	18.4	1.9	0.00808	0.00067	27,334
Sequence 9	10.0	30.0	843.1	762.1	81.0	30.3	27.4	2.9	0.01102	0.00092	29,790
Sequence 10	15.0	10.0	278.7	252.1	26.6	10.0	9.0	1.0	0.00398	0.00033	27,275
Sequence 11	15.0	15.0	422.4	382.0	40.4	15.2	13.7	1.5	0.00556	0.00046	29,582
Sequence 12	15.0	30.0	849.7	768.6	81.1	30.5	27.6	2.9	0.00944	0.00079	35,063
Sequence 13	20.0	15.0	420.5	380.1	40.4	15.1	13.6	1.5	0.00486	0.00041	33,676
Sequence 14	20.0	20.0	567.1	513.0	54.1	20.4	18.4	1.9	0.00615	0.00051	35,937
Sequence 15	20.0	40.0	1134.4	1025.7	108.7	40.7	36.8	3.9	0.01060	0.00088	41,662

TESTED BY	Suriyati B S	DATE	10-2-2013
REVIEWED BY		DATE	

Materials & Tests Unit

NCDOT

NORTH CAROLINA DEPARTMENT OF TRANSPORTATION
DIVISION OF HIGHWAY
MATERIALS & TESTS UNIT - SOILS LABORATORY

SUMMARY REPORT OF RESILIENT MODULUS TEST

Subgrade Soils and Untreated Base/Subgrade Materials

1. LAB NO.: T-5723
2. PROJECT NO.: Hanson Inc-Raleigh
3. SAMPLE NO.: Q#067
4. STATION NO.:
5. SPECIMEN PROPERTIES: 99.0 % Maximum Dry Density at 7.3 % Moisture Content
6. SOURCE OF MATERIAL Quarry #067
7. TEST SPECIFICATION: T-307
8. TEST DATE: 8-19-2013

PARAMETER	Chamber Confining Pressure	Nominal Maximum Axial Stress	Actual Applied Max. Axial Load	Actual Applied Cyclic Load	Actual Applied Contact Load	Actual Applied Max. Axial Stress	Actual Applied Cyclic Stress	Actual Applied Contact Stress	Average Recov Def. LVDT 1 and 2	Resilient Strain	Resilient Modulus
DESIGNATION	S_3	S_{cyclic}	P_{max}	P_{cyclic}	$P_{contact}$	S_{max}	S_{cyclic}	$S_{contact}$	H_{avg}	ε_r	M_r
UNIT	psi	psi	lbs	lbs	lbs	psi	psi	psi	in	in/in	psi
Sequence 1	3.0	3.0	88.2	78.6	9.6	3.2	2.8	0.3	0.00276	0.00023	12,256
Sequence 2	3.0	6.0	170.8	156.7	14.1	6.1	5.6	0.5	0.00503	0.00042	13,431
Sequence 3	3.0	9.0	258.1	236.1	22.1	9.3	8.5	0.8	0.00695	0.00058	14,634
Sequence 4	5.0	5.0	144.0	132.6	11.4	5.2	4.8	0.4	0.00339	0.00028	16,827
Sequence 5	5.0	10.0	282.4	258.5	23.9	10.1	9.3	0.9	0.00601	0.00050	18,525
Sequence 6	5.0	15.0	426.1	389.5	36.6	15.3	14.0	1.3	0.00864	0.00072	19,417
Sequence 7	10.0	10.0	286.3	263.0	23.3	10.3	9.4	0.8	0.00433	0.00036	26,169
Sequence 8	10.0	20.0	577.9	528.0	49.9	20.7	19.0	1.8	0.00803	0.00067	28,321
Sequence 9	10.0	30.0	858.8	783.6	75.3	30.8	28.1	2.7	0.01119	0.00093	30,147
Sequence 10	15.0	10.0	282.6	259.6	23.1	10.1	9.3	0.8	0.00354	0.00030	31,560
Sequence 11	15.0	15.0	425.9	389.8	36.0	15.3	14.0	1.3	0.00507	0.00042	33,140
Sequence 12	15.0	30.0	863.4	788.5	74.9	31.0	28.3	2.7	0.00922	0.00077	36,847
Sequence 13	20.0	15.0	427.6	391.7	35.9	15.3	14.1	1.3	0.00434	0.00036	38,870
Sequence 14	20.0	20.0	568.7	520.4	48.2	20.4	18.7	1.7	0.00558	0.00047	40,149
Sequence 15	20.0	40.0	1128.0	1029.3	98.7	40.5	36.9	3.5	0.01017	0.00085	43,596

TESTED BY Suriyati B S DATE 8-19-2013
REVIEWED BY DATE

Materials & Tests Unit

NCDOT

NORTH CAROLINA DEPARTMENT OF TRANSPORTATION
DIVISION OF HIGHWAY
MATERIALS & TESTS UNIT - SOILS LABORATORY
SUMMARY REPORT OF RESILIENT MODULUS TEST
Subgrade Soils and Untreated Base/Subgrade Materials

1. LAB NO.:	T-5708
2. PROJECT NO.:	Quarry Research
3. SAMPLE NO.:	Quarry #094
4. STATION NO.:	-
5. SPECIMEN PROPERTIES:	100.5 % Maximum Dry Density at 5.9 % Moisture Content
6. SOURCE OF MATERIAL	Rockingham Quarry #094
7. TEST SPECIFICATION:	T-307
8. TEST DATE:	7-3-2013

PARAMETER	Chamber Confining Pressure	Nominal Maximum Axial Stress	Actual Applied Max. Axial Load	Actual Applied Cyclic Load	Actual Applied Contact Load	Actual Applied Max. Axial Stress	Actual Applied Cyclic Stress	Actual Applied Contact Stress	Average Recov Def. LVDT 1 and 2	Resilient Strain	Resilient Modulus
DESIGNATION	S_3	S_{cyclic}	P_{max}	P_{cyclic}	$P_{contact}$	S_{max}	S_{cyclic}	$S_{contact}$	H_{avg}	ε_r	M_r
UNIT	psi	psi	lbs	lbs	lbs	psi	psi	psi	in	in/in	psi
Sequence 1	3.0	3.0	88.5	80.8	7.6	3.2	2.9	0.3	0.00331	0.00028	10,519
Sequence 2	3.0	6.0	170.4	160.0	10.4	6.1	5.7	0.4	0.00593	0.00049	11,622
Sequence 3	3.0	9.0	258.7	241.7	17.0	9.3	8.7	0.6	0.00794	0.00066	13,114
Sequence 4	5.0	5.0	139.7	131.6	8.1	5.0	4.7	0.3	0.00393	0.00033	14,420
Sequence 5	5.0	10.0	282.7	264.5	18.2	10.1	9.5	0.7	0.00684	0.00057	16,653
Sequence 6	5.0	15.0	419.6	392.4	27.3	15.1	14.1	1.0	0.00963	0.00080	17,553
Sequence 7	10.0	10.0	280.0	263.1	16.9	10.1	9.4	0.6	0.00486	0.00041	23,314
Sequence 8	10.0	20.0	569.9	533.5	36.3	20.5	19.2	1.3	0.00890	0.00074	25,828
Sequence 9	10.0	30.0	871.8	812.5	59.2	31.3	29.2	2.1	0.01270	0.00106	27,561
Sequence 10	15.0	10.0	282.2	265.3	16.9	10.1	9.5	0.6	0.00403	0.00034	28,379
Sequence 11	15.0	15.0	428.7	402.1	26.6	15.4	14.4	1.0	0.00578	0.00048	29,938
Sequence 12	15.0	30.0	871.6	814.4	57.2	31.3	29.2	2.1	0.01033	0.00086	33,969
Sequence 13	20.0	15.0	419.8	394.0	25.8	15.1	14.1	0.9	0.00485	0.00040	35,029
Sequence 14	20.0	20.0	569.4	533.8	35.6	20.4	19.2	1.3	0.00625	0.00052	36,759
Sequence 15	20.0	40.0	1141.3	1065.8	75.5	41.0	38.3	2.7	0.01123	0.00094	40,866

TESTED BY Suriyati B S DATE 7-3-2013
REVIEWED BY DATE

Materials & Tests Unit

NCDOT

NORTH CAROLINA DEPARTMENT OF TRANSPORTATION
DIVISION OF HIGHWAY
MATERIALS & TESTS UNIT - SOILS LABORATORY
SUMMARY REPORT OF RESILIENT MODULUS TEST
Subgrade Soils and Untreated Base/Subgrade Materials

1. LAB NO.:	T-5691
2. PROJECT NO.:	5.272
3. SAMPLE NO.:	Q#161
4. STATION NO.:	
5. SPECIMEN PROPERTIES:	100.0 % Maximum Dry Density at 5.9 % Moisture Content
6. SOURCE OF MATERIAL	Quarry Rocky Point
7. TEST SPECIFICATION:	T-307
8. TEST DATE:	6-18-2013

PARAMETER	Chamber Confining Pressure	Nominal Maximum Axial Stress	Actual Applied Max. Axial Load	Actual Applied Cyclic Load	Actual Applied Contact Load	Actual Applied Max. Axial Stress	Actual Applied Cyclic Stress	Actual Applied Contact Stress	Average Recov Def. LVDT 1 and 2	Resilient Strain	Resilient Modulus
DESIGNATION	S_3	S_{cyclic}	P_{max}	P_{cyclic}	$P_{contact}$	S_{max}	S_{cyclic}	$S_{contact}$	H_{avg}	ε_r	M_r
UNIT	psi	psi	lbs	lbs	lbs	psi	psi	psi	in	in/in	psi
Sequence 1	3.0	3.0	87.4	76.8	10.6	3.1	2.8	0.4	0.00309	0.00026	10,734
Sequence 2	3.0	6.0	169.9	154.3	15.6	6.1	5.5	0.6	0.00505	0.00042	13,198
Sequence 3	3.0	9.0	253.9	230.1	23.7	9.1	8.3	0.9	0.00633	0.00053	15,702
Sequence 4	5.0	5.0	139.7	126.8	12.9	5.0	4.6	0.5	0.00318	0.00026	17,228
Sequence 5	5.0	10.0	281.2	254.7	26.4	10.1	9.2	0.9	0.00524	0.00044	20,968
Sequence 6	5.0	15.0	424.6	384.9	39.7	15.3	13.8	1.4	0.00703	0.00059	23,639
Sequence 7	10.0	10.0	281.4	254.9	26.5	10.1	9.2	1.0	0.00372	0.00031	29,559
Sequence 8	10.0	20.0	567.8	514.5	53.3	20.4	18.5	1.9	0.00647	0.00054	34,311
Sequence 9	10.0	30.0	854.2	773.9	80.3	30.7	27.8	2.9	0.00900	0.00075	37,127
Sequence 10	15.0	10.0	279.7	253.6	26.1	10.1	9.1	0.9	0.00309	0.00026	35,435
Sequence 11	15.0	15.0	423.4	383.8	39.6	15.2	13.8	1.4	0.00440	0.00037	37,643
Sequence 12	15.0	30.0	837.4	758.5	78.8	30.1	27.3	2.8	0.00760	0.00063	43,101
Sequence 13	20.0	15.0	419.4	380.2	39.2	15.1	13.7	1.4	0.00376	0.00031	43,686
Sequence 14	20.0	20.0	564.2	511.7	52.6	20.3	18.4	1.9	0.00479	0.00040	46,061
Sequence 15	20.0	40.0	1118.0	1012.0	106.0	40.2	36.4	3.8	0.00842	0.00070	51,845

TESTED BY	Suriyati B S	DATE	6-18-2013
REVIEWED BY		DATE	

Materials & Tests Unit

NCDOT

NORTH CAROLINA DEPARTMENT OF TRANSPORTATION
DIVISION OF HIGHWAY
MATERIALS & TESTS UNIT - SOILS LABORATORY
SUMMARY REPORT OF RESILIENT MODULUS TEST
Subgrade Soils and Untreated Base/Subgrade Materials

1. LAB NO.:	T-5724
2. PROJECT NO.:	Hanson- Rougemont
3. SAMPLE NO.:	Q #217
4. STATION NO.:	
5. SPECIMEN PROPERTIES:	99.6% Maximum Dry Density at 6.8 % Moisture Content
6. SOURCE OF MATERIAL	Quarry #217
7. TEST SPECIFICATION:	T-307
8. TEST DATE:	9-18-2013

PARAMETER	Chamber Confining Pressure	Nominal Maximum Axial Stress	Actual Applied Max. Axial Load	Actual Applied Cyclic Load	Actual Applied Contact Load	Actual Applied Max. Axial Stress	Actual Applied Cyclic Stress	Actual Applied Contact Stress	Average Recov Def. LVDT 1 and 2	Resilient Strain	Resilient Modulus
DESIGNATION	S_3	S_{cyclic}	P_{max}	P_{cyclic}	$P_{contact}$	S_{max}	S_{cyclic}	$S_{contact}$	H_{avg}	ε_r	M_r
UNIT	psi	psi	lbs	lbs	lbs	psi	psi	psi	in	in/in	psi
Sequence 1	3.0	3.0	67.4	57.0	10.5	2.4	2.0	0.4	0.00367	0.00031	6,685
Sequence 2	3.0	6.0	169.7	154.0	15.6	6.1	5.5	0.6	0.00845	0.00070	7,851
Sequence 3	3.0	9.0	260.9	237.1	23.9	9.4	8.5	0.9	0.01108	0.00092	9,216
Sequence 4	5.0	5.0	141.7	128.7	13.0	5.1	4.6	0.5	0.00550	0.00046	10,076
Sequence 5	5.0	10.0	280.4	254.1	26.2	10.1	9.1	0.9	0.00875	0.00073	12,513
Sequence 6	5.0	15.0	428.5	388.2	40.2	15.4	13.9	1.4	0.01216	0.00101	13,754
Sequence 7	10.0	10.0	283.4	256.9	26.5	10.2	9.2	1.0	0.00589	0.00049	18,801
Sequence 8	10.0	20.0	572.3	518.5	53.8	20.5	18.6	1.9	0.01095	0.00091	20,390
Sequence 9	10.0	30.0	845.0	764.5	80.5	30.3	27.4	2.9	0.01512	0.00126	21,773
Sequence 10	15.0	10.0	282.2	256.0	26.2	10.1	9.2	0.9	0.00528	0.00044	20,880
Sequence 11	15.0	15.0	425.4	385.8	39.6	15.3	13.8	1.4	0.00744	0.00062	22,343
Sequence 12	15.0	30.0	857.4	776.5	80.9	30.8	27.9	2.9	0.01273	0.00106	26,283
Sequence 13	20.0	15.0	424.7	385.0	39.7	15.2	13.8	1.4	0.00628	0.00052	26,384
Sequence 14	20.0	20.0	570.3	517.1	53.2	20.5	18.6	1.9	0.00794	0.00066	28,053
Sequence 15	20.0	40.0	1140.7	1032.2	108.5	40.9	37.0	3.9	0.01404	0.00117	31,674

TESTED BY	Suriyati B S	DATE	9-18-2013
REVIEWED BY		DATE	

APPENDIX D MULTI-STAGE PERMANENT DEFORMATION TEST RESULTS

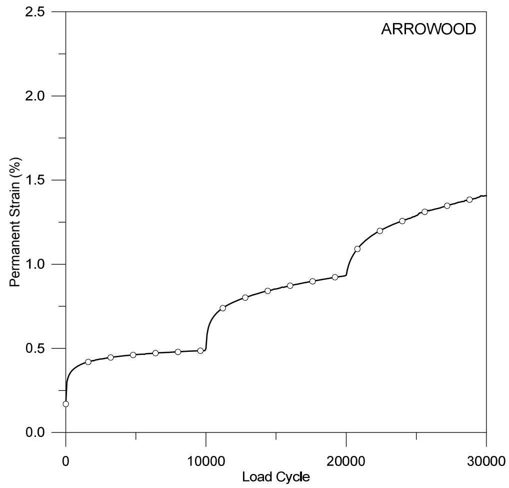

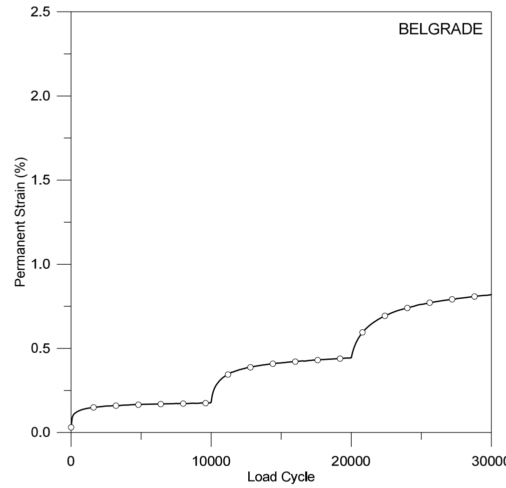

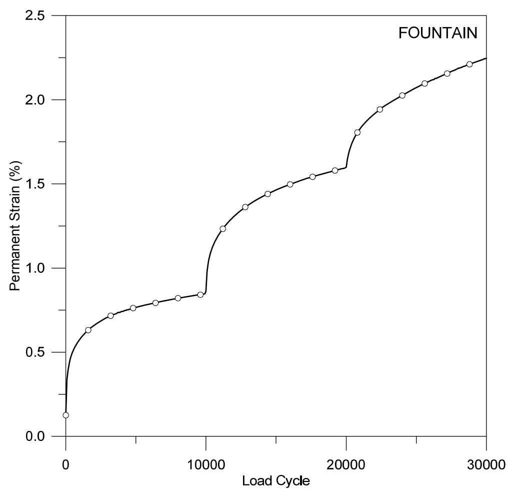

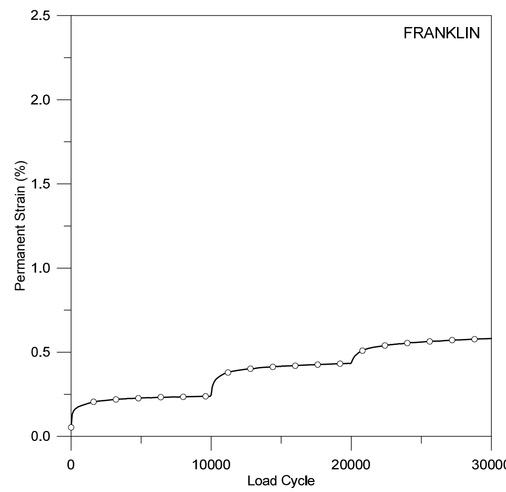

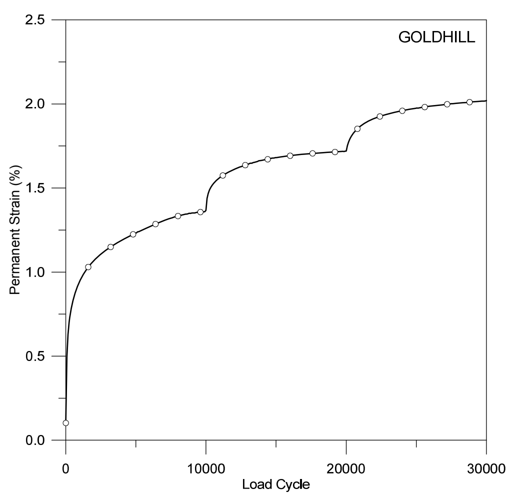

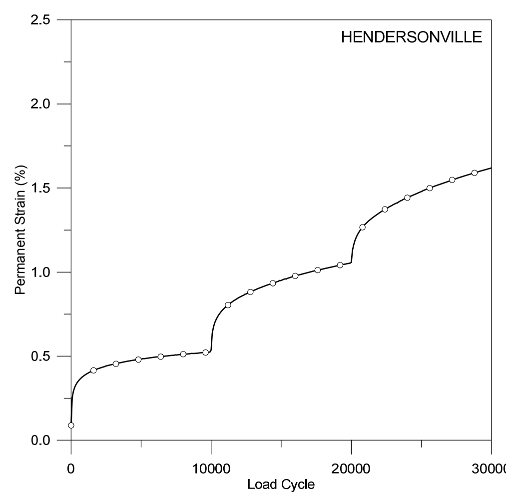

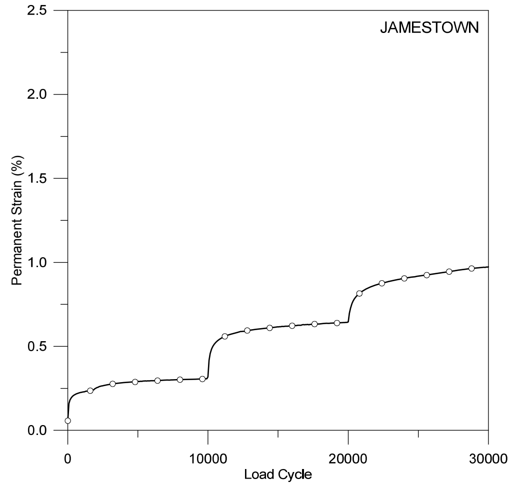
JAMESTOWN
Permanent Strain (%)
Load Cycle
0.0
0.5
1.0
1.5
2.0
2.5
0
10000
20000
30000

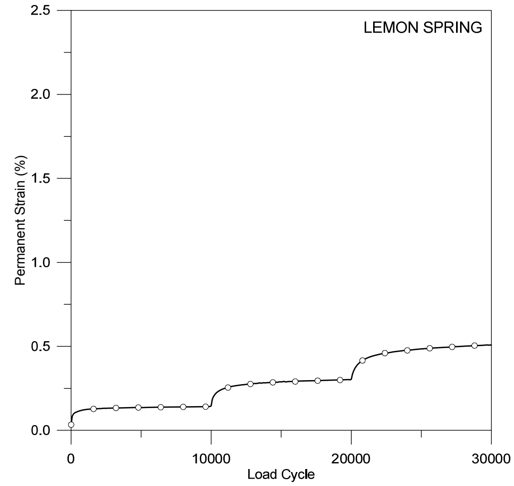
LEMON SPRING
Permanent Strain (%)
Load Cycle
0.0
0.5
1.0
1.5
2.0
2.5
0
10000
20000
30000

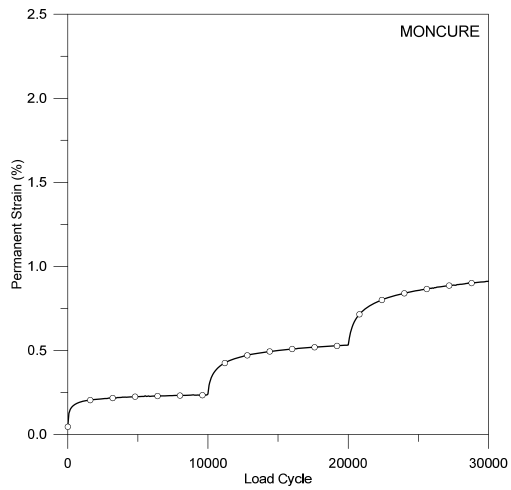
MONCURE
Permanent Strain (%)
Load Cycle
0.0
0.5
1.0
1.5
2.0
2.5
0
10000
20000
30000

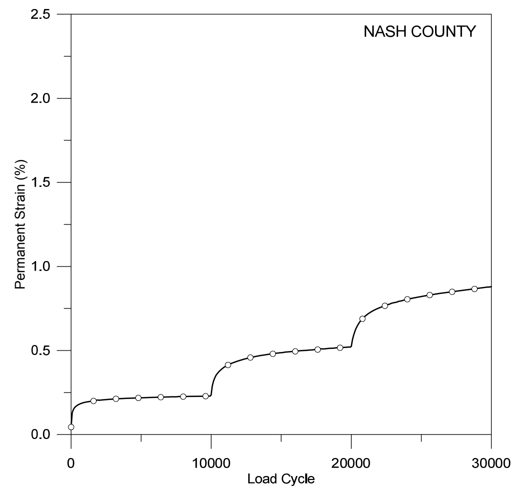
NASH COUNTY
Permanent Strain (%)
Load Cycle
0.0
0.5
1.0
1.5
2.0
2.5
0
10000
20000
30000

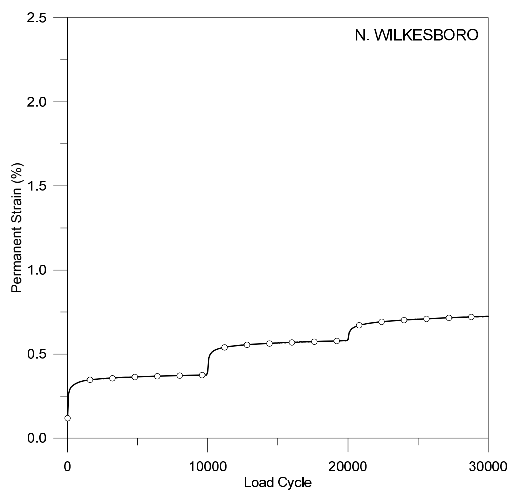
N. WILKESBORO
Permanent Strain (%)
Load Cycle
0.0
0.5
1.0
1.5
2.0
2.5
0
10000
20000
30000

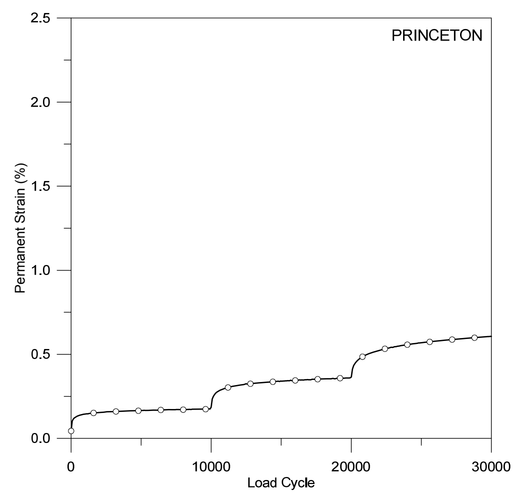
PRINCETON
Permanent Strain (%)
Load Cycle
0.0
0.5
1.0
1.5
2.0
2.5
0
10000
20000
30000

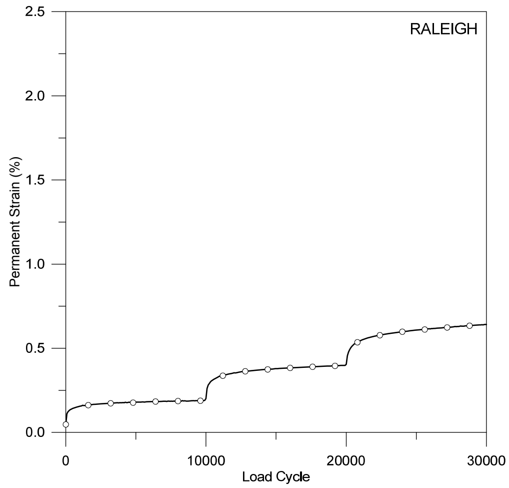
RALEIGH
Permanent Strain (%)
Load Cycle
0.0
0.5
1.0
1.5
2.0
2.5
0
10000
20000
30000

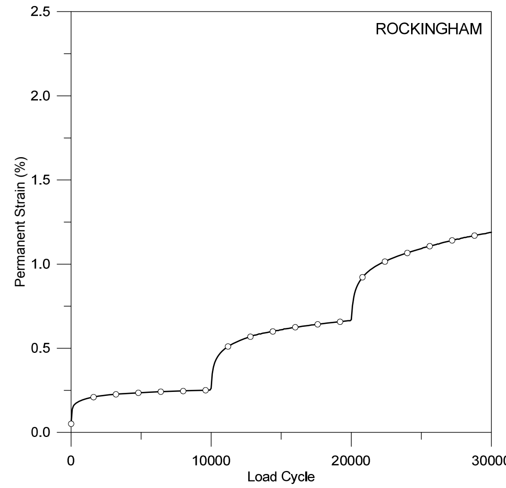
ROCKINGHAM
Permanent Strain (%)
Load Cycle
0.0
0.5
1.0
1.5
2.0
2.5
0
10000
20000
30000

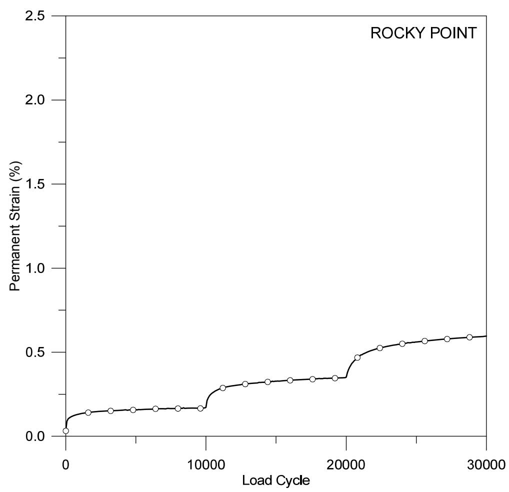
ROCKY POINT
Permanent Strain (%)
Load Cycle
0.0
0.5
1.0
1.5
2.0
2.5
0
10000
20000
30000

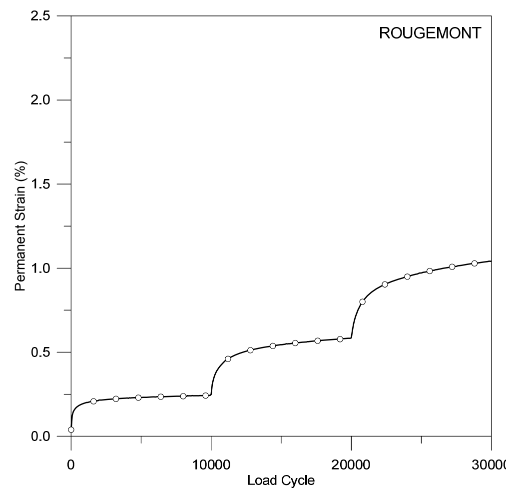
ROUGEMONT
Permanent Strain (%)
Load Cycle
0.0
0.5
1.0
1.5
2.0
2.5
0
10000
20000
30000

APPENDIX E SINGLE-STAGE PERMANENT DEFORMATION TEST RESULTS

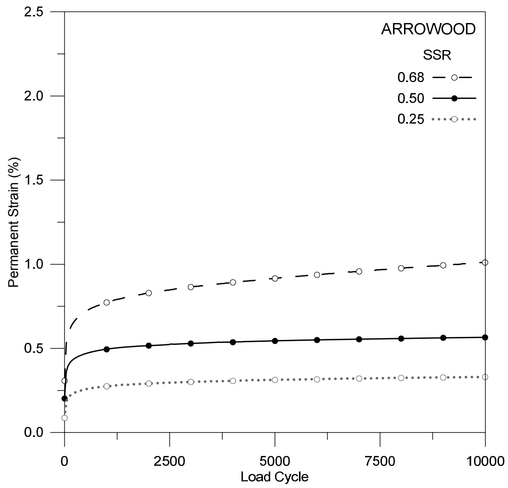

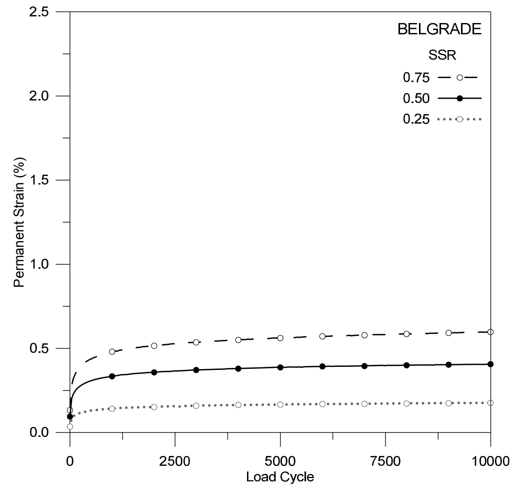

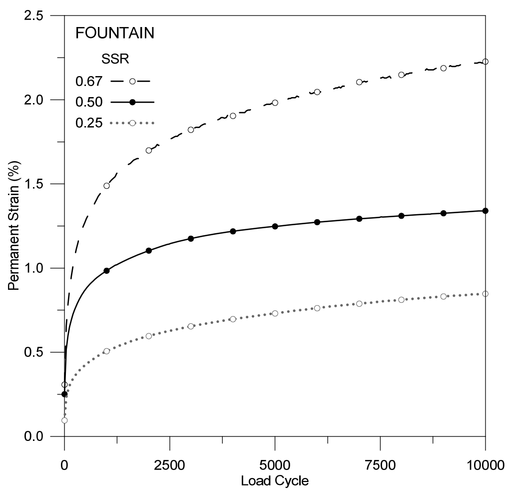

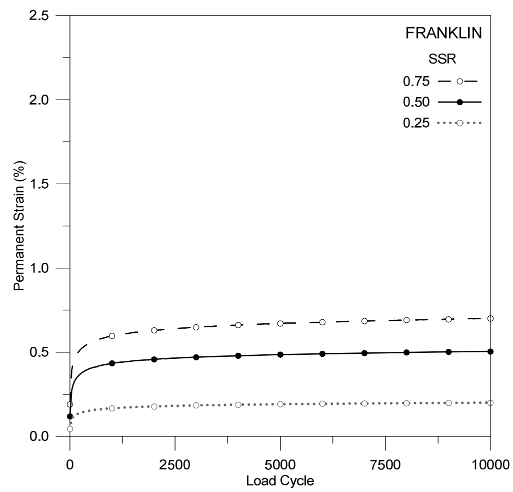

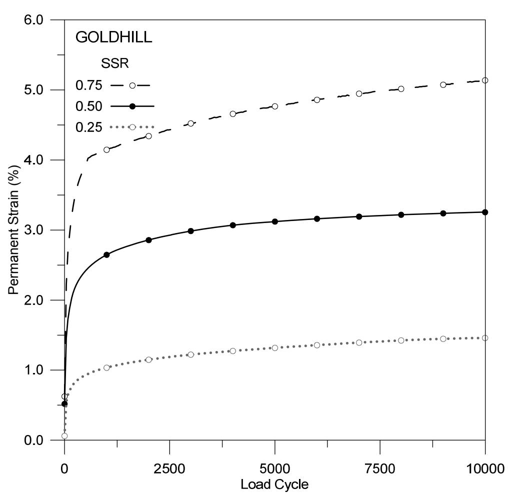

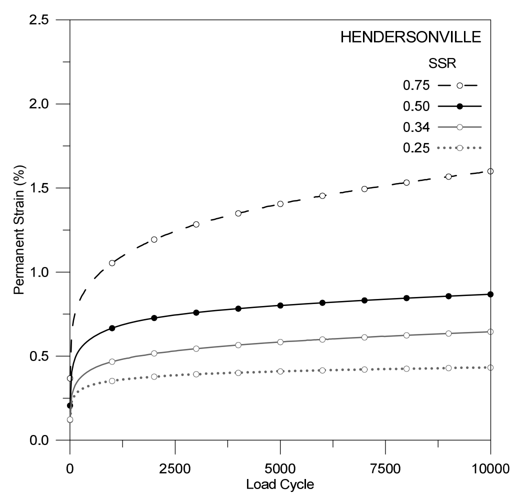

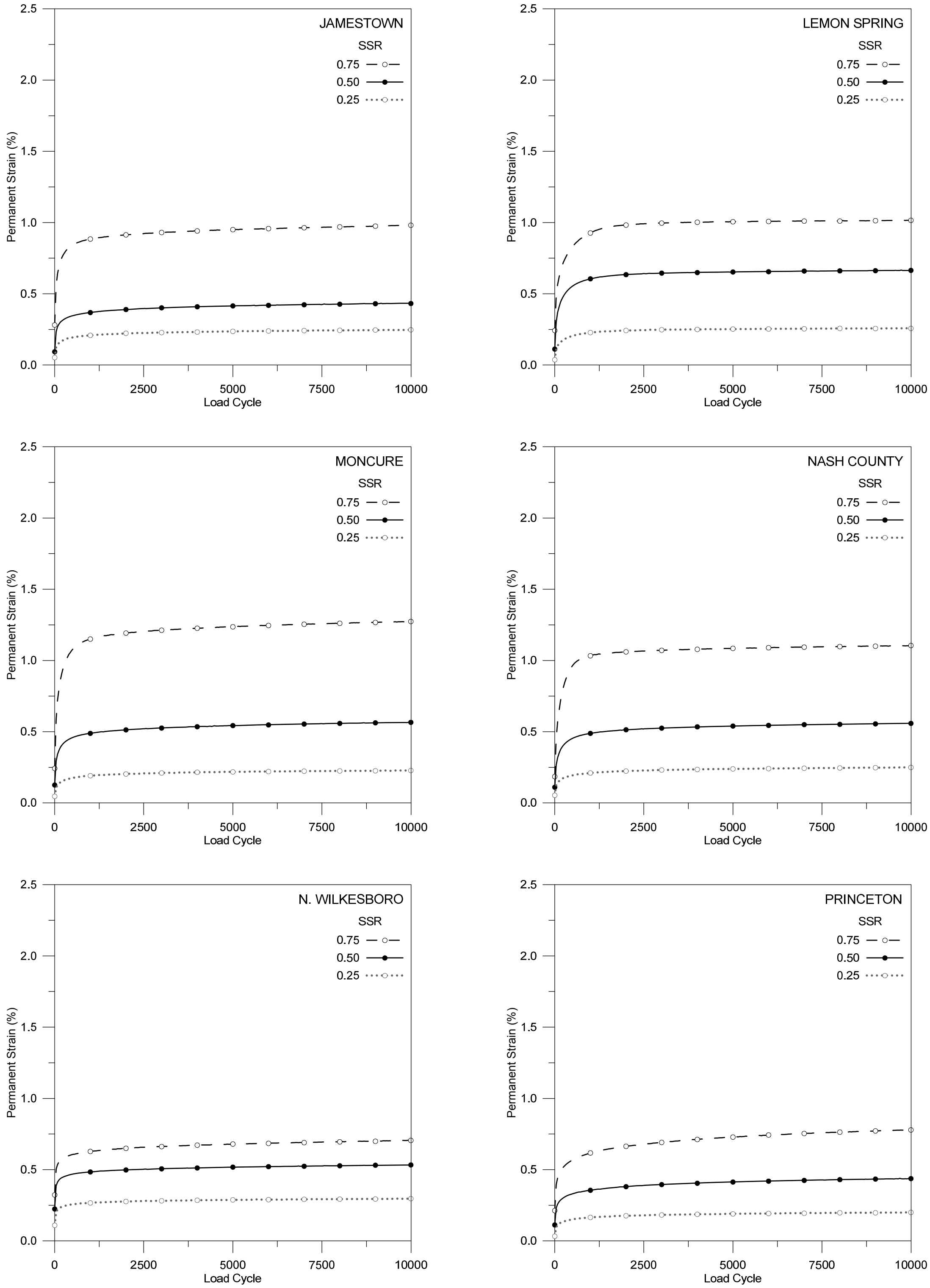
JAMESTOWN
LEMON SPRING
MONCURE
NASH COUNTY
N. WILKESBORO
PRINCETON
SSR
0.75
0.50
0.25
Permanent Strain (%)
Load Cycle
0.0
0.5
1.0
1.5
2.0
2.5
0
2500
5000
7500
10000

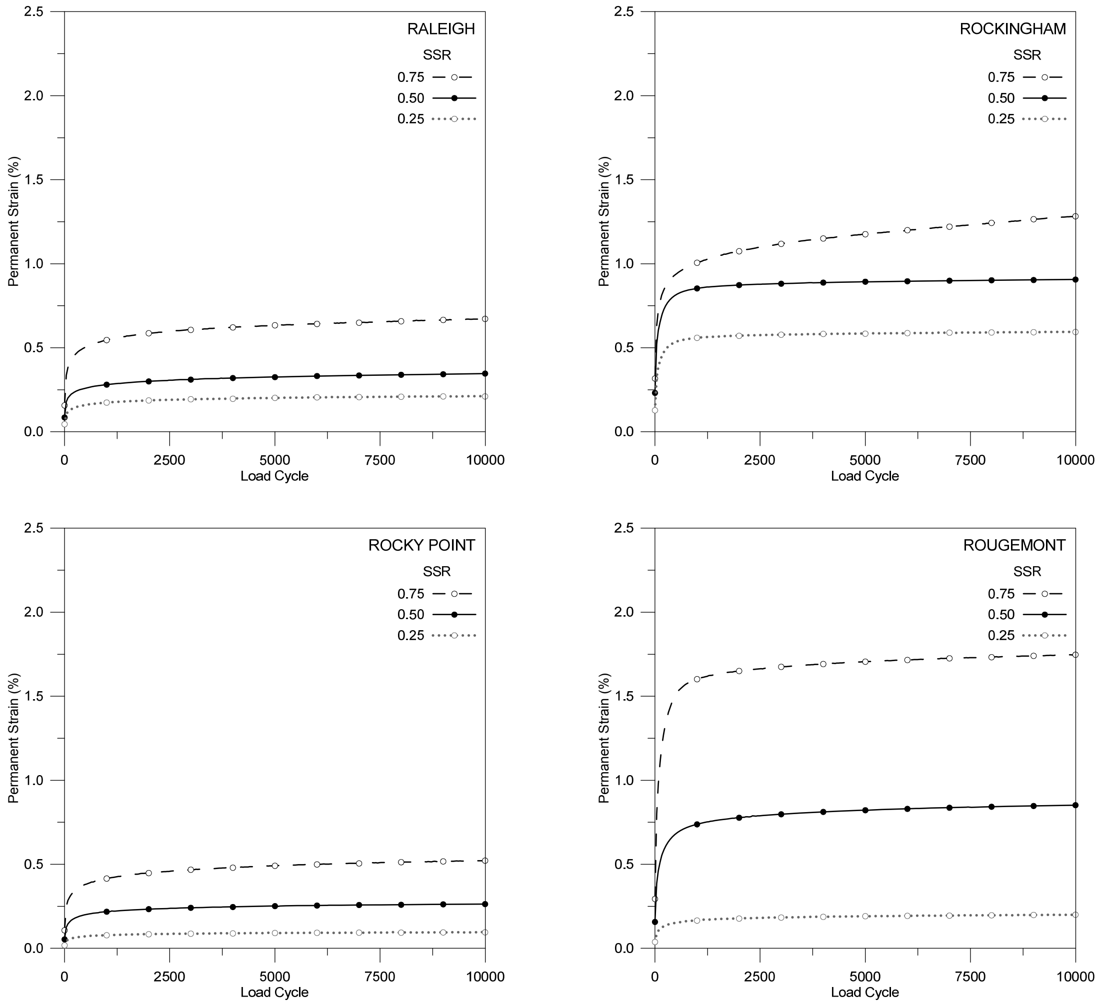
RALEIGH
SSR
0.75
0.50
0.25
Permanent Strain (%)
Load Cycle
ROCKINGHAM
SSR
0.75
0.50
0.25
Permanent Strain (%)
Load Cycle
ROCKY POINT
SSR
0.75
0.50
0.25
Permanent Strain (%)
Load Cycle
ROUGEMONT
SSR
0.75
0.50
0.25
Permanent Strain (%)
Load Cycle